Immobilization Of The Anti-Thrombin DNA Aptamer: Attachment, Optimal Packing Density And Kinetics

By
Douglas F. Holub

Submitted to the Department of Chemistry and the Faculty of the Graduate School of the University of Kansas in partial fulfillment of the requirement for the degree of Doctor of Philosophy

_____
George S. Wilson

_____
Craig Lunte

_____
Cindy Berrie

_____
Christian Schoeneich

_____
Peter A. Gegenheimer

Date Defended:_____

The Dissertation Committee for Douglas F. Holub certifies that this is the approved version of the following dissertation:

Immobilization Of The Anti-Thrombin DNA Aptamer: Attachment, Optimal Packing Density And Kinetics

Committee:

_____

George S. Wilson, Chairperson

Date Approved: _____

ABSTRACT

Douglas F. Holub, Ph.D. Department of Chemistry, December 2005
University of Kansas

Aptamers have been touted as viable complements to antibodies as molecular recognition elements in diagnostic assays. Several studies have demonstrated aptamer applicability in both homogeneous and heterogeneous assay formats. However, very few studies have been performed to investigate the parameters involving effect immobilization of aptamers, the analyte-binding kinetics of attached aptamers, and the optimal assay format for aptamers. These studies utilized the well-characterized anti-thrombin DNA aptamer. Investigations were conducted in order to ascertain effective methods of immobilization of the aptamer to silica and gold, the maximum packing density for which 100% of the aptamer activity is retained, and the binding kinetics of the immobilized aptamer. The attachment studies found that a short linker extending from the aptamer is essential for covalent attachment, the aptamer tertiary structure and cation dependence can influence the effectiveness of a covalent attachment, and affinity attachment methodologies are reliable for aptamer immobilization. In addition, the optimal packing density for active aptamers was determined to be similar to the reported optimal packing density of single-stranded oligonucleotides used for hybridization assays. The kinetic studies for the binding of the immobilized aptamer to its cognate ligand showed that the binding kinetics of the aptamer are unaffected by either covalent or affinity attachment to a substrate, the association and dissociation binding rates for this aptamer are very fast, and the association rate is diffusion-limited. These results indicate that aptamers may be well-suited to use in miniaturized, real-time, continuous-monitoring biosensors.

This dissertation is dedicated to my loving family. My sister, Diane M. Holub, whom could not have achieved this feat herself, but, through her existence, has taught our family many more important beauties of life. My son, Harley D. Holub, whom I know could achieve this if he desires, but must make his own course through life. My father, Fred H. Holub, who taught me patience and virtue in the best way possible- by example. My mother, Jeanette M. Holub, who bequest to me that good, German stubbornness and tolerated my life-long shenanigans. And my two brothers, Thomas R. and Gary L., whom I will always look up to (figuratively) and who have always been available to help and encourage me when my shenanigans have gotten me in trouble.

Acknowledgements

A vast array of people have assisted me in the completion of this work. My parents' nurturing and unconditional love, my brothers' encouragement and accolades, and my grandparents, aunts, uncles and cousins have all helped me to grow and realize my potential. My teachers in school, especially my early science teacher heroes: Mr. Fig and Mr. Plopylus, who modeled good teaching and learning. My son, Harley, who put up with many an hour spent in the dreary confines of Malott Hall and a summer spent at the Baldwin City pool with his father typing away at a laptop under the shelter. And even my ex-wife, Sherry L. Warren, who was and has been very supportive of my ambitions.

I would like to thank the people that encouraged me to attempt (and complete!) graduate school. My chemistry TA's and teachers during my undergraduate days at KU: Martha Morton, Luis Morales, Greg Harms, Craig Lunte, Dave Benson and Cary Johnson. Tim and Martha West who spent countless hours discussing biochemistry and biological processes with me and helped me to see that biology is cool and exciting!

The support I received (financial, psychological and academic) was immense. KU's chemistry department supported me financially through a teaching assistanceship, the chemistry-biology training grant, and a GK-12 fellowship. My advisor, George S. Wilson, provided research support, stimulating advice, and an environment that fostered independence and self-sufficiency. I am also grateful to Janet Bond-Robinson who believed in and supported me via the GK-12 fellowship. The chemistry staff, especially Sonja Payne, Jan Akers, Gary Harris, Bruce Johnston and Richard Fritz were always willing to help out. In addition, Rena Rouse was always a 'hoot' to borrow equipment from. The friendship and scientific discussions over just about any topic with Andrew Suddith were awesome! The camaraderie, softball and invaluable courier services from Roger 'fingon' MacKinnon will forever be engraved in my mind and heart.

I would like to thank Ottawa University for employing me for the past several years and believing in my ability to teach and complete my dissertation. In particular, I'd like to thank Tom Lewis who worked closely with me during my fledgling year at OU and has always been willing to help in any way that he can. Hank Tillinghast, Terry Malloy, Randy Weiss, Rich Menninger, Maurice Bryan, Barb Dinneen and the rest of the faculty, staff and students have always been supportive and encouraging.

Many people have provided assistance in my research endeavors. Mark Richter, Paul Hanson, Kevin Sprott, Andrew Harned, Donald Probst and Randall Robinson were always willing to offer advice. Boris Kornilaev, Cindy Berrie and Catherine Parrish provided insight and stimulating conversation with regard to the SPR experiments. I am indebted to Ken Mason and Nathan Parker for their graciousness in allowing a 'chemist' to invade their laboratory- I learned much about devising a research plan, working with RNA, radio-labeling, and the migration patterns of laboratory equipment from these two scientists. I will never forget the hours spent in the 'Gegenheimer zone' with Peter Gegenheimer- those discussions were invaluable to me.

The last group of people that I would like to thank (though there are many more!) are the members of the Wilson group that provided support, challenges and examples that helped me develop professionally as a scientist and researcher. The 'trial by fire' atmosphere of the group meetings, though intimidating at first, was the best kind of atmosphere for learning in graduate school. Giridharan Golkulrangan (aka- Giri-man) was a fantastic partner in the dark world of aptamers and I enjoyed many a time discussing research, basketball, cricket, good food and bird watching. I'll never forget the words we taught to Johanna Mora, nor the pronunciations she would provide for some words. However, Yoyo was not just an entertainment value, she provided immeasurable scientific insight and friendship throughout and it was an added benefit that her train ran on the same track as mine. Last, but certainly not least, Raeann Gifford has been an inspiration, a mentor and a wonderful companion to me. Her tenacity and focus taught me the true meaning of those words, her objective (and sometimes subjective) discussions about research, work and life helped me to grow and her strong allegiance to our relationship has helped me through these arduous years in grad. school.

Pura vida!

TABLE OF CONTENTS

LIST OF FIGURES AND TABLES

CHAPTER 1

CHAPTER 2

CHAPTER 3

CHAPTER 4

Chapter 1: Introduction

1.1 Aptamers In diagnostics

Aptamers rival antibodies for use in diagnostic assays[1-4] in part because they have equilibrium dissociation constants (K_D's) in the μM to pM range[4-6]. Their use as diagnostic reagents in homogeneous assays[7-10] and heterogeneous assays[11-20] has been demonstrated. In addition, they have been used as selective agents in affinity chromatography[11, 21-23] and as solid-phase modifiers for chiral[24-26] and non-chiral[25, 27] separations. Except for the homogeneous assays, the above techniques require immobilization of the aptamer to a solid support.

The immobilization of a recognition element (e.g. antibody, enzyme) can affect its function and may require considerable optimization steps for use in a heterogeneous assay format.[28] Aptamers have been immobilized via several different means,[11-18, 21-26, 29, 30] but there is only one report of a study that evaluated appropriate or viable attachment methodologies.[31] The selectivity of immobilized aptamers is reported to be unaltered by the attachment process.[11, 17, 21-23] However, immobilized aptamers may have altered affinities for their cognate ligand compared to solution-phase aptamers.

Investigations that determined the effect of immobilization on an aptamer's affinity have produced mixed results. Four studies of immobilized aptamers (two utilizing covalent attachment strategies[15, 17] and two utilizing biotin/streptavidin association[13, 21]) indicated that the aptamer-ligand affinity was comparable to solution-phase affinity values. In contrast, one study involving covalent immobilization[16] and two studies of aptamers immobilized via biotin/streptavidin interaction[21, 28] showed a decrease in affinity upon conjugation of the aptamer to a substrate. In addition, a study involving the DNA aptamer for IgE using a quartz crystal microbalance (QCM)[14] showed that direct immobilization of the aptamer (amide bond formation between an amine-appended aptamer and a three-carbon thiol-gold

linker) resulted in a lower sensitivity for IgE compared to the anti-IgE antibody. This same study showed that a biotin/streptavidin immobilized aptamer was as sensitive to IgE as an anti-IgE antibody. The sensitivity discrepancy between the two immobilization strategies for the aptamer was attributed to a fast dissociation of IgE molecules from the covalently attached aptamer compared to the affinity immobilized aptamer.

As we move from the initial curiosity of aptamer production, through proof-of-principle investigations of aptamer uses, and into feasible diagnostic applications for aptamers, further research into the specific parameters governing aptamer function is required. This work has concentrated on studying one well-characterized aptamer-ligand system (the anti-thrombin DNA aptamer) with regard to its use in heterogeneous-based diagnostic assays. Specifically, attachment parameters to two different substrates (silica and gold), the optimal packing density for the aptamer, and the effects of immobilization on the aptamer's kinetics are presented.

1.2 Aptamer Characteristics

Aptamers are short (15 – 100 bases), single-stranded pieces of RNA or DNA that can bind a ligand for which they have been selected. The selection process is known as SELEX: systematic evolution of ligands by exponential enrichment. The targets for which aptamers have been isolated against include nucleic acid-binding proteins, small molecules, peptides, non-nucleic acid-binding proteins and complex targets like anthrax spores.[32-39] The high affinity and specificity of the aptamer for its ligand is dependent on the aptamer tertiary structure: its unique structure allows for the necessary intermolecular interactions for binding.

There are essentially four different structural motifs exhibited by aptamers that allow for the specific intermolecular interactions involved in binding their cognate ligands: stem-loop/bulge, pseudo-knot, stacked G-quartet and hairpin.[40] Some of these structures are

very stable when the aptamer is free in solution and others are formed upon binding the ligand.[41-46] The folding and binding interactions of aptamers have been determined to be dependent upon the presence of cations- often times Mg^{2+} or K^{+}.[47-49]

All of the aptamer structures allow for multiple contact points between the aptamer and its ligand.[42] The intermolecular interaction that occurs at each contact point can vary from hydrogen-bonding, π-π stacking or electrostatic interactions.[40, 44, 50-53] The nature and strength of these interactions are what determine the specificity and affinity of the aptamer for its ligand.

1.3 Anti-thrombin DNA Aptamer – Thrombin Pair

The anti-thrombin DNA aptamer was chosen for these studies because it is a well-characterized aptamer – ligand system. Bock, *et. al.* isolated the aptamer in 1992[37] and numerous studies have been performed to study the aptamer structure,[41, 46, 54-57] binding characteristics and requirements,[48, 58-66] and its use in therapeutics and diagnostics.[16-18, 31, 60, 61, 63, 67-72]

Thrombin is a serine protease that is instrumental in blood clot formation. It has a pI of 7.5 and has two lysine- and arginine-rich binding sites: exosite I and exosite II.[73] Exosite I is the fibrinogen binding site and exosite II is the heparin binding site.[74]

The sequence of the single-stranded DNA (ssDNA) aptamer to thrombin that was isolated by *in vitro* selection (SELEX) is 5'- GGT TGG TGT GGT TGG -3'.[37] The sequence forms a stable, stacked, G-quartet structure in solution[41, 45, 54] in the presence of divalent and monovalent cations: Sr^{2+} > Ba^{2+} > K^{+} >> Rb^{+} > NH_4^{+} (listed in order of decreasing stabilizing effect).[46, 48] The stacked, G-quartet structure of the aptamer remains intact when it is immobilized on a substrate[75] and, unlike some aptamers, the aptamer structure is not significantly changed when it binds thrombin.[55] The melting temperature (T_m) of the stacked, G-quartet has been found to be ~45°C when K^{+} ions are present.[48]

Figure 1.1 shows a cartoon of the structure of the folded aptamer. The TT loops at the bottom of the structure purportedly insert into exosite I of thrombin for specific binding.[74, 75] The x-ray crystal structure of the DNA aptamer bound to thrombin indicated aptamer interactions with two different thrombin molecules: one interaction with the TT loops and the other interaction with the end containing the TGT loop.[46] However, Tsiang, *et. al.* found that there was no significant binding of the aptamer to thrombin outside of exosite I.[59]

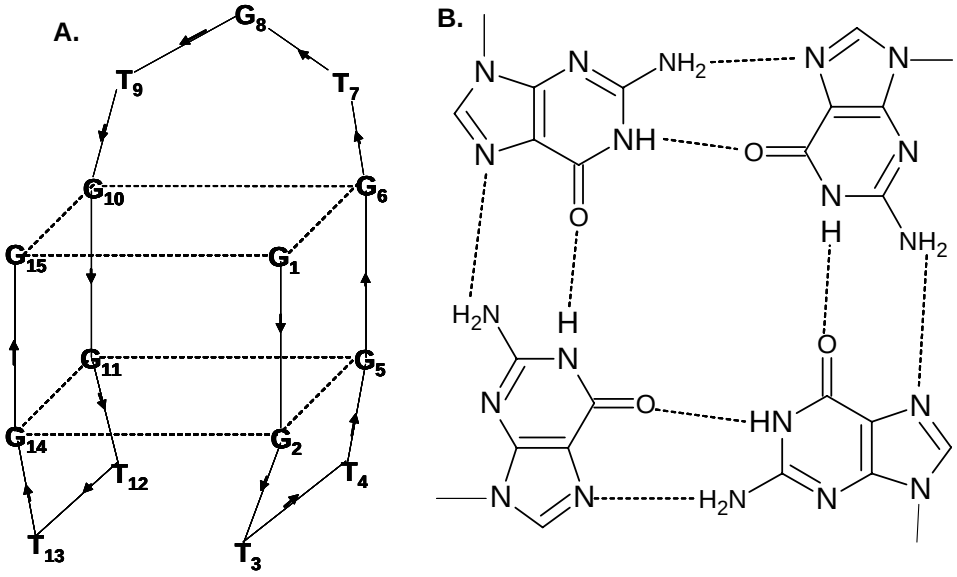

Figure 1.1: Anti-thrombin DNA aptamer. A: Cartoon of tertiary structure showing stacked, G-quartet. Nucleotide bases are numbered starting at the 5' end. Dashed lines emphasize the two G-quartet structures. Solid lines with arrows represent the phosphate backbone connections between bases. B: Schematic of hydrogen bond interactions between four guanine bases of one of the G-quartets in the aptamer structure. The deoxyribose-phosphate backbone is removed for clarity. Base connection to the deoxyribose is represented by a solid line extending from the N_8 atom. Figures adapted from Wang, *et. al.*[45]

The anti-thrombin DNA aptamer has been found to be selective for thrombin and binds thrombin with high affinity. Potyrailo, *et. al.* showed that the aptamer does not bind to porcine elastase,[17] Baldrich, *et. al.*, showed that the aptamer does not bind to gliadin,[31] and Rye and Nustad found that the aptamer was able to bind thrombin specifically even in the

presence of high concentrations of bovine serum albumin (BSA) and IgG.[76] A scrambled ssDNA sequence (5'- GGT GGT TGT TGT GGT -3') did not bind to thrombin.[17] The affinity of the aptamer for thrombin (K_D) has been found to be 100 nM by filter binding assay,[58] 25 nM by clotting time analysis, [37] 2.7 nM by competitive equilibrium binding[75] and between 1.4 and 6.2 nM when an aptamer solution was allowed to react with immobilized thrombin.[74]

1.4 Current Studies

An analytical assay has many requirements in order for it to be valid and practical. These figures of merit include: selectivity, linearity, accuracy, precision, sensitivity, range, limit of detection, limit of quantitation and robustness. All of these parameters can be affected by immobilization of the recognition element, especially if the attachment is not well controlled. The following studies investigated the method of attachment to two different substrates, the optimal packing density and the kinetics for the thrombin – DNA aptamer system.

Immobilization of a recognition element is essential for a continuous-monitoring, heterogeneous assay system. The requirements for the immobilization are strict: the attachment must be robust so that the material does not get washed away throughout the course of the assay, but it must also allow for retention of the active form of the recognition element. Too many attachment points, attachment at the wrong location and harsh chemistries during the immobilization process are all factors that can lead to inactive or compromised recognition elements.

Aptamers have inherent advantages over proteins and antibodies because they have natural attachment points through their 5' or 3' ends and they readily refold into their active conformation. This means that the point of attachment can be easily controlled and denaturing conditions during the immobilization should not be problematic as long as the nucleic acid sequence is not degraded nor the aptamer composition chemically modified. In

spite of this advantage, aptamers may present some unique characteristics that require consideration for optimal attachment to surfaces.

Assay linearity and operational range is dependent upon the number of active recognition elements available. The optimal packing density of the recognition element is the greatest loading density of the molecule per unit area that allows for 100% of the molecules to be fully active (bind the analyte specifically). The attachment method and the nature of the recognition element (its size, the analyte size and any binding requirements like conformational changes) can influence the optimal packing density for a particular recognition element – ligand pair.

Attachment of a molecular recognition element can alter the kinetics of the binding interaction with its cognate ligand. There may be no effects, there may be small effects like a slight change in the on- or off- rates, or the immobilization can lead to changes in the binding kinetics that render the recognition element ineffective in the assay. As previously mentioned, an aptamer's binding kinetics may be altered when immobilized compared to its solution-phase values.[14, 16, 21, 28] Investigations were conducted to determine the kinetics of the immobilized anti-thrombin aptamer when it was attached via covalent and affinity means to a gold-based substrate. These studies gave insight into the best suited assay format for this recognition element – ligand pair.

1.5 References

1 Hesselberth, J., Robertson, M.P., Jhaveri , S., Ellington, A.D *Reviews in Molecular Biotechnology* **2000,** *74*, 15-25.
2 Brody, E. N., Gold, L. *Reviews in Molecular biotechnology* **2000,** *74*, 5-13.
3 Osborne, S. E.; Matsumura, I.; Ellington, A. D. *Curr Opin Chem Biol* **1997,** *1*, 5-9.
4 Jayasena, S. D. *Clin. Chem. (Washington, D. C.)* **1999,** *45*, 1628-1650.
5 Ellington, A. D.; Conrad, R. *Biotechnol Annu Rev* **1995,** *1*, 185-214.
6 Bier, F. F.; Fuerste, J. P. *Exs* **1997,** *80*, 97-120.
7 Fang, X.; Cao, Z.; Beck, T.; Tan, W. *Anal. Chem.* **2001,** *73*, 5752-5757.
8 Jayasena, S.; Gold, L. In *U.S.*; (Gilead Sciences, Inc., USA).: US, 2001, pp 42 pp., Cont.-in-part of U.S. 5,989,823.
9 Li, J. J.; Fang, X.; Tan, W. *Biochem. Bioph. Res. Co.* **2002,** *292*, 31-40.
10 Perlette, J.; Li, J.; Fang, X.; Schuster, S.; Lou, J.; Tan, W. *Rev. Anal. Chem.* **2002,** *21*, 1-14.
11 Cho, S.; Lee, S.-H.; Kim, Y.-K.; Kim, B.-G. *Proc. Micro Tot. Anal. Sys.* **2001**, 601-602.
12 Nakamura, C.; Kobayashi, T.; Miyake, M.; Shirai, M.; Miyakea, J. *Mol. Cryst. Liq. Crys. A* **2001,** *371*, 369-374.
13 McCauley, T. G.; Hamaguchi, N.; Stanton, M. *Anal. Biochem.* **2003,** *319*, 244-250.
14 Liss, M.; Petersen, B.; Wolf, H.; Prohaska, E. *Anal. Chem.* **2002,** *74*, 4488-4495.
15 Smith, D.; Collins, B. D.; Heil, J.; Koch, T. H. *Mol. Cell. Proteomics* **2003,** *2*, 11-18.
16 Lee, M.; Walt, D. R. *Anal. Biochem.* **2000,** *282*, 142-146.
17 Potyrailo, R. A.; Conrad, R. C.; Ellington, A. D.; Hieftje, G. M. *Anal. Chem.* **1998,** *70*, 3419-3425.
18 Lin, Y.; Heil, J.; Jayasena, S. In *PCT Int. Appl.*; (Gilead Sciences, Inc., USA).: Wo, 2001, pp 47 pp.
19 Collett, J. R.; Cho, E. J.; Lee, J. F.; Levy, M.; Hood, A. J.; Wan, C.; Ellington, A. D. *Anal. Biochem.* **2005,** *338*, 113-123.
20 Savran, C.; Knudsen, S.; Ellington, A. D.; Manalis, S. *Anal. Chem.* **2004,** *76*, 3194-98.
21 Deng, Q.; German, I.; Buchanan, D.; Kennedy, R. T. *Anal. Chem.* **2001,** *73*, 5415-5421.
22 Romig, T. S.; Bell, C.; Drolet, D. W. *J. Chrom., B* **1999,** *731*, 275-284.
23 Clark, S. L.; Remcho, V. T. *J. Separ. Sci.* **2003,** *26*, 1451-1454.
24 Michaud, M.; Jourdan, E.; Villet, A.; Ravel, A.; Grosset, C.; Peyrin, E. *J. Am. Chem. Soc.* **2003,** *125*, 8672-8679.
25 Kotia, R. B.; Li, L.; McGown, L. B. *Anal. Chem.* **2000,** *72*, 827-831.
26 Michaud, M.; Jourdan, E.; Ravelet, C.; Villet, A.; Ravel, A.; Grosset, C.; Peyrin, E. *Anal. Chem.* **2004,** *76*, 1015-1020.
27 Rehder, M. A.; McGown, L. B. *Electrophoresis***,** *22*, 3759-64.
28 Kirby, R.; Cho, E. J.; Gehrke, B.; Bayer, T. S.; Park, Y. S.; Neikirk, D.; McDevitt, J.; Ellington, A. D. *Anal. Chem.* **2004,** *76*, 4066-75.
29 Schmid, B.; Hoffmann, D.; Wefing, S.; Schnaible, V.; Quandt, E.; Tewes, M.; Famulok, M. In *U.S. Pat. Appl. Publ.*; (Germany).: Us, 2002, pp 6 pp.
30 Kumar, P. K. R.; Yamamoto, R. In *Jpn. Kokai Tokkyo Koho*; Agency of Industrial Sciences and Technology: Jp, 2001, pp 19 pp.
31 Baldrich, E.; Restrepo, A.; O'Sullivan, C. *Anal. Chem.* **2004,** *76*, 7053-63.
32 Gold, L.; Polisky, B.; Uhlenbeck, O.; Yarus, M. *Annu Rev Biochem* **1995,** *64*, 763-97.
33 Wilson, C.; Nix, J.; Szostak, J. *Biochemistry-USA* **1998,** *37*, 14410-14419.
34 Burgstaller, P.; Famulok, M. *Angew Chem Int Ed* **1994,** *33*, 1084-1087.
35 Lorsch, J. R.; Szostak, J. W. *Biochemistry USA* **1994,** *33*, 973-982.
36 Burke, D. H.; Hoffman, D. C.; Brown, A.; Hansen, M.; Pardi, A.; Gold, L. *Chem Biol* **1997,** *4*, 833-843.

37 Bock, L. C.; Griffin, L. C.; Latham, J. A.; Vermaas, E. H.; Toole, J. J. *Nature* **1992,** *355*, 564-566.
38 Iwai, S. *Tanpakushitsu Kakusan Koso* **1995,** *40*, 1430-7.
39 Bruno, J. G.; Kiel, J. L. *Biosens. Bioelectron.* **1999,** *14*, 457-464.
40 Feigon, J.; Dieckmann, T.; Smith, F. W. *Chem Biol* **1996,** *3*, 611-617.
41 Macaya, R. F.; Schultze, P.; Smith, F. W.; Roe, J. A.; Feigon, J. *Proc Nat Acad Sci USA* **1993,** *90*, 3745-3749.
42 Hermann, T.; Patel, D. J. *Science (Washington, D. C.)* **2000,** *287*, 820-827.
43 Lin, C. H.; Wang, W.; Jones, R. A.; Patel, D. J. *Chemistry and Biology London* **1998,** *5*, 555-572.
44 Patel, D. J.; Suri, A. K.; Jiang, F.; Jiang, L. C.; Fan, P.; Kumar, R. A.; Nonin, S. *J Mol Biol* **1997,** *272*, 645-664.
45 Wang, K. Y.; McCurdy, S.; Shea, R. G.; Swaminathan, S.; Bolton, P. H. *Biochemistry USA* **1993,** *32*, 1899-1904.
46 Padmanabhan, K.; Padmanabhan, K. P.; Ferrara, J. D.; Sadler, J. E.; Tulinsky, A. *J. Biol. Chem.* **1993,** *268*, 17651-4.
47 Gebhardt, K.; Shokraei, A.; Babaie, E.; Lindqvist, B. H. *Biochemistry-US* **2000,** *39*, 7255-65.
48 Kankia, B. I.; Marky, L. A. *J. Am. Chem. Soc.* **2001,** *123*, 10799-10804.
49 Zimmermann, G. R.; Wick, C. L.; Shields, T. P.; Jenison, R. D.; Pardi, A. *RNA* **2000,** *6*, 659-667.
50 Chang, K. Y.; Varani, G. *Nature Structural Biology* **1997,** *4*, 854-858.
51 Famulok, M. *Curr Opin Struct Biol* **1999,** *9*, 324-9.
52 Patel, D. J. S., A.F. *Reviews in Molecular Biotechnology* **2000,** *74*, 39-60.
53 Westhof, E.; Patel, D. J. *Curr. Opin. Struct. Biol.* **1999,** *9*, 293-297.
54 Schultze, P.; Macaya, R. F.; Feigon, J. *J Mol Biol* **1994,** *235*, 1532-47.
55 Wang, K. Y.; Krawczyk, S. H.; Bischofberger, N.; Swaminathan, S.; Bolton, P. H. *Biochemistry USA* **1993,** *32*, 11285-11292.
56 Feigon, J.; Smith, F. W.; Macaya, R. F.; Schultz, P. *Struct. Biol. State of the Art, Proc. Conversation Discip. Biomol. Stereodyn., 8th* **1994,** *2*, 127-34, 4 plates.
57 Kelly, J. A.; Feigon, J.; Yeates, T. O. *J. Mol. Biol.* **1996,** *256*, 417-22.
58 Macaya, R. F.; Waldron, J. A.; Beutel, B. A.; Gao, H.; Joesten, M. E.; Yang, M.; Patel, R.; Bertelsen, A. H.; Cook, A. F. *Biochemistry-USA* **1995,** *34*, 4478-92.
59 Tsiang, M.; Gibbs, C. S.; Griffin, L. C.; Dunn, K. E.; Leung, L. L. *J Biol Chem* **1995,** *270*, 19370-6.
60 Callas, D.; Fareed, J. *Thromb Haemost* **1995,** *74*, 473-81.
61 Shaw, J. P.; Fishback, J. A.; Cundy, K. C.; Lee, W. A. *Pharm Res* **1995,** *12*, 1937-42.
62 Sumikura, K.; Yano, K.; Ikebukuro, K.; Karube, I. *Nucleic Acids Symp Ser* **1997,** *37*, 257-8.
63 Kubik, M. F.; Stephens, A. W.; Schneider, D.; Marlar, R. A.; Tasset, D. *Nucleic Acids Res.* **1994,** *22*, 2619-2626.
64 Tasset, D. M.; Kubik, M. F.; Steiner, W. *J. Mol. Biol.* **1997,** *272*, 688-698.
65 Griffin, L. C.; Toole, J. J.; Leung, L. L. K. *Gene* **1993,** *137*, 25-31.
66 Vairamani, M.; Gross, M. L. *J. Am. Chem. Soc.* **2003,** *125*, 42-43.
67 Xu, S.; Cai, X.; Tan, X.; Lu, B. *Proc. SPIE-Int. Soc. Opt. Eng.* **2001,** *4414*, 123-125.
68Yu, S.; Cai, X.; Tan, X.; Zhu, Y.; Lu, B. *Proc. SPIE-Int. Soc. Opt. Eng.* **2001,** *4414*, 35-37.
69 Hamaguchi, N.; Ellington, A.; Stanton, M. *Anal. Biochem.* **2001,** *294*, 126-131.
70 Charles, J. A. M.; McGown, L. B. *Electrophoresis* **2002,** *23*, 1599-1604.
71 Pavlov, V.; Xiao, Y.; Shlyahovsky, B.; Willner, I. *J. Am. Chem. Soc.* **2004,** *126*, 11768-11769.
72 Pavlov, V.; Shlyahovsky, B.; Willner, I. *J. Am. Chem. Soc.* **2005,** *127*, 6522-6523.
73 Giddings, J. C. *Thrombin, thrombomodulin and the control of hemostasis*; R.G. Landes: Austin, 1994.

74 Tsiang, M.; Jain, A. K.; Dunn, K. E.; Rojas, M. E.; Leung, L. L. K.; Gibbs, C. S. *J. Biol. Chem.* **1995,** *270*, 16854-16863.
75 Wu, Q.; Tsiang, M.; Sadler, J. E. *J. Biol. Chem.* **1992,** *267*, 24408-12.
76 Rye, P. D.; Nustad, K. *BioTechniques* **2001,** *30*, 290,292,294-295.

Chapter 2: Immobilization Investigations Of The Anti-Thrombin DNA Aptamer On Surfaces

2.1 Introduction

Investigations were conducted to determine the feasibility of attaching the thrombin single-stranded DNA aptamer to two different surfaces: silica and gold. In order to preserve the aptamer's function (specific thrombin binding), it was believed that a single attachment point at either the 5' or 3' end was desirable. In addition to aiding preservation of the thrombin aptamer function, end attachment of single-stranded DNA is a standard technique for creating DNA hybridization arrays; therefore, several attachment chemistries are readily available.

The two substrates that were used in these investigations were chosen because of their application for diagnostic assays. Silica is a common substrate used in micrototal analytical systems (μTAS), also known as microfluidic devices. Gold is the substrate of choice for surface plasmon resonance (SPR) and quartz crystal microbalance (QCM) detection schemes. The attachment of aptamers to these two surfaces could prove to be valuable in diagnostics; hence, investigation of the parameters regulating their efficient and stable attachment is relevant.

There are basically two different techniques that have been utilized for immobilization of aptamers to solid supports: covalent attachment and affinity attachment. All of the covalent attachment strategies involve a rather long tether: a six-carbon amine appended to either the 5' or 3' end of the aptamer and then linked through an additional carbon chain (e.g. polyethylene glycol-NH_2 or polythylenemine)[1-5] or a twelve-carbon thiol appended aptamer that is attached via a self-assembled monolayer (SAM).[6] All of the affinity attachments utilize the biotin/streptavidin system where biotin is appended to either the 3' or

5' end of the aptamer using a linker with up to sixteen carbons[7-16] and streptavidin is covalently immobilized to the substrate.

In order to ascertain the feasibility of attachment of aptamers to surfaces for diagnostic testing, these studies concentrated on the attachment of the thrombin DNA aptamer to two different surfaces: silica and gold. Covalent attachment strategies were attempted for attachment of the aptamer to the silica; while both covalent and affinity attachment methodologies were attempted for the attachment to gold. The covalent attachment attempts to the gold substrate supported some of the results obtained from the silica attachment attempts.

2.2 Attachment To Silica

2.2.1 Introduction

One method of attaching DNA (aptamers and single-stranded DNA for hybridization assays) to silica has been to modify the silica with a silanizing reagent that has an amine or carboxyl functional group extending away from the silica (attachment functional group). The DNA is covalently attached to the modified silica via an amide or phosphoramide bond. It is possible to modify the silica so that a thiol group is extending away from the silica, but there was concern that the necessary covalent attachment method (formation of a disulfide bond) would not be stable either to the washings that would be necessary in order to remove adsorbed DNA and/or the storage of the modified silica. The silanization of the silica can result in either a monolayer coverage of the silica by the attachment functional group or an extended, three-dimensional coverage of the silica by the attachment functional group. Monolayer or three-dimensional coverage is determined by whether the silanizing reagent is a monosiloxy siloxane or a trisiloxy siloxane, respectively. A monolayer forming silanizing reagent with an amine functional group (on a three-carbon linker) available for the aptamer attachment was pursued for two reasons: 1) the monolayer structure would allow for

accurate aptamer packing density data and 2) the amine functional group would give the outermost boundary of the modified silica a net positive charge. Determination of the aptamer packing density is crucial in optimal activity and response linearity studies. The net positive charge on the modified silica will allow for the approach of the predominantly negatively charged aptamer (due to its phosphate backbone).

Attachment of the aptamer to the amine-modified silica was attempted by utilizing two different chemistries: 1) phosphoramide bond formation and 2) thioamide bond formation. The phosphoramide bond attachment strategy required a phosphate group appended to the aptamer and the use of N-ethyl-N'-(dimethylaminopropyl)carbodiimide (EDC)[17]. The thioamide bond attachment method required an end-appended amine to the aptamer and the use of 1,4-phenylene diisothiocyanate (PDC).[18] These two reactions are illustrated in figures 2.2 and 2.3, respectively.

2.2.2 Materials And Methods

2.2.2.1 Materials

Non-porous, silica beads were chosen for the attempts at attaching the thrombin DNA aptamer to silica because of their perceived ease of manipulation and their consistent surface area. Sunsphere NP-100 (AGA Chemicals, Inc., Charlotte, NC) were chosen for the experiments. They are non-porous, spherical silica beads with a 10 micrometer diameter and a surface area of 80 m^2/gram; this surface area corresponds to 304 cm^2 per 5 μL of bead suspension (as used in the following experiments).

3-Aminopropyldimethylethoxysilane (3-APdMES) was purchased from Gelest, Inc. (Morrisville, PA). 1-methylimidazole and the Type IV porcine pancreas elastase (elastase) were purchased from Sigma (St. Louis, MO). 3-Aminopropyldiisopropylethoxysilane (3-APdIES) was purchased from United Chemical Technologies, Inc. (Bristol, PA). p-Phenylene diisothiocyanate (PDC) was purchased from Fisher Scientific (St. Louis, MO). The T4 polynucleotide kinase was purchased from New England Biolabs (Ipswich, MA).

2.2.2.2 Methods

2.2.2.2.1 Cleaning Of The Silica Beads

The beads were sonicated for ten minutes in a piranha solution (4:1 concentrated sulfuric acid: 30% hydrogen peroxide).[19] After sonication in the piranha solution, the beads were rinsed 10 times with water: each time with a volume of water equal to the volume of piranha solution used during the sonication.

2.2.2.2.2 Modification Of The Silica Beads

The cleaned silica beads were modified with the same protocol for both aminosiloxanes (3-APdMES and 3-APdIES). The structures for these two compounds are provided in Figure 2.1. Reaction A in Figure 2.3 shows the linking for the 3-APdIES modifier to the silica surface. Briefly, the cleaned silica beads were incubated at 37°C for 4 hours with slow rotation in a solution of 10% aminosilioxane in 95% EtOH. After the 4 hour incubation, the supernatant was removed, the beads were rinsed with a small amount of 95% EtOH and then dried in a vacuum oven set at 105°C for 24 hours.

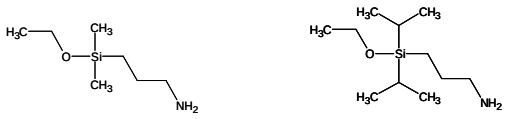

3-APdMES **3-APdIES**

Figure 2.1: 3-aminopropyldimethylethoxysilane (3-APdMES) and 3-aminopropyldiisopropylethoxysilane (3-APdIES).

2.2.2.2.3 Silica Bead Storage

All modified beads were stored at -20°C at a bead density of 7.6 X 10^{-2} mg/μL in potassium phosphate buffer, pH 7.4.

2.2.2.2.4 Aptamer Immobilization Chemistries

2.2.2.2.4.1 EDC-mediated Phosphoramide Bond

The single-stranded DNA was phosphorylated on the 5' end using T4 Polynucleotide Kinase (PNK) (Promega, Madison, WI) according to the supplier's protocol. The DNA was radiolabeled during the PNK reaction by spiking the reaction with ^{32}P γ-ATP (5000 Ci/mmol, BLU502Z, Perkin Elmer (NEN), Boston, MA). After phosphorylation, the DNA was purified on a 20% polyacrylamide gel, the bands were visualized and excised utilizing UV shadowing and phospho-imaging, and the DNA was eluted in water, ethanol precipitated and then resuspended in water at the desired concentration.

Three strategies for immobilizing the DNA to the silica beads utilizing the EDC-mediated phosphoramide bond reaction were performed as follows: 1) One was to form the bond by mixing 5'-phosphorylated DNA with the amine-modified beads in the presence of EDC (shown in figure 2.2); 2) another was to expose the amine-modified beads to double-stranded salmon sperm DNA prior to the reaction of the 5'-phosphorylated DNA utilizing EDC; 3) the last attempt was to attach the 5'-phosphorylated DNA to the 3-APdIES via EDC and then expose the cleaned beads to the DNA-modified 3-APdIES. Reaction conditions for all procedures were: 13 mg of EDC, 5 μL of silica bead suspension, 5 μL of 0.5 M N-methylimidazole buffer (pH 6) and 747 pmol of DNA were combined in a microcentrifuge tube. The total volume of the reaction mixture was adjusted to 20 μL by the addition of purified water and then incubated at 50°C for 5 hours with slow rotation.

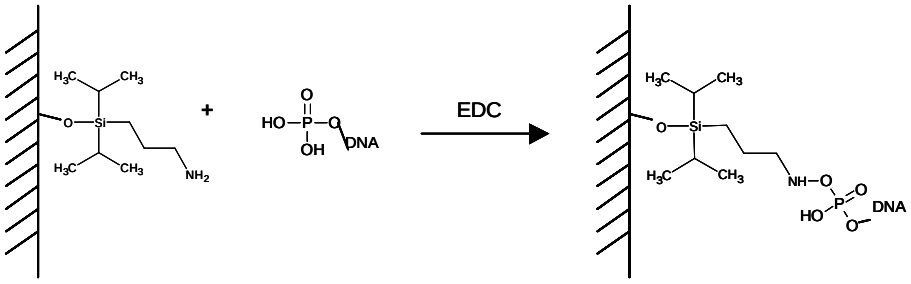

Figure 2.2: EDC-mediated phosphoramide coupling of 3-APdIES-modified silica with phosphorylated DNA.

2.2.2.2.4.2 PDC-mediated Thioamide Bond Formation

The single-stranded DNA was first phosphorylated, as per above, and then a 5' amine appended by the use of ethylenediamine and EDC (same as above except 3 M ethylenediamine was added to a final concentration of 0.3 M). EDC adducts on the DNA were eliminated by a 10 hour incubation at 45 °C in 0.2 M sodium carbonate buffer, pH 10.5.[20, 21] Additional experiments utilized commercially available DNA that had a 3' amine attached via a seven carbon linker (Integrated DNA Technologies, Inc., Coralville, IA). This 3' amine-modified DNA was also 5' phosphorylated (as per above) for tracking and quantitation purposes. All DNA was stored in 100 mM sodium borate buffer, pH 8.5 at -20°C until used for immobilization to the PDC-activated silica beads.

The PDC-activated silica beads were produced by removing all of the water from an aliquot of 3-APdIES-modified beads, rinsing the beads five times with 1 mL of dimethylformamide (DMF), removing the excess DMF, and then adding 1 mL of a 0.2% PDC in 10% pyridine/DMF solution and rotating the tube at room temperature for 2 hours. The reaction solution was removed after the 2 hour incubation, the activated beads washed three times with 1 mL of methanol, followed with three washings of acetone (1 mL each) and then allowed to dry via evaporation. The dry, activated beads were then stored until use in the appropriate amount of 100 mM sodium borate buffer, pH 8.5 such that the bead suspension was at a bead density of 7.6 X 10^{-2} mg/μL. Reaction B of Figure 2.3 shows the activation of the 3-APdIES-modifies beads with PDC.

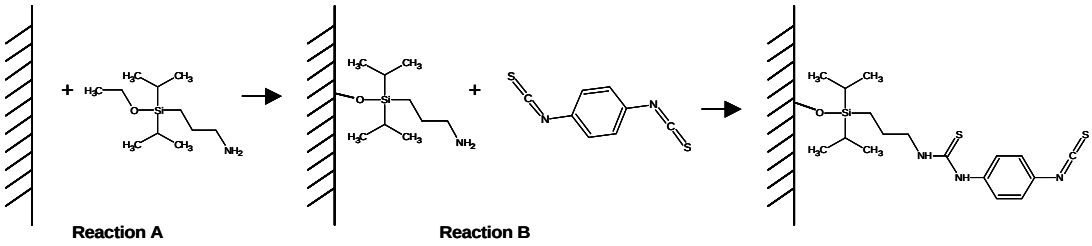

Figure 2.3: Reaction A: silanization of silica surface with 3-APdIES. Reaction B: reaction of 3-APdIES-modified silica surface with PDC, leaving a reactive isothiocyanate extending into solution.

The immobilization of the amine-modified DNA (5' and 3') to the PDC-activated silica beads was accomplished by combining the DNA and beads in a tube and rotating the tube at room temperature for 24 hours. Remaining reactive thiocyanate moieties were blocked by the addition of 0.1 M ethanolamine in 100 mM sodium borate buffer, pH 8.5 and incubation at room temperature for an additional 8 hours. Figure 2.4 depicts this procedure. The reactions were stopped by separating the beads from the reaction mixture and rinsing the beads with 50°C 0.4 M NaOH (see below: removal of adsorbed DNA).

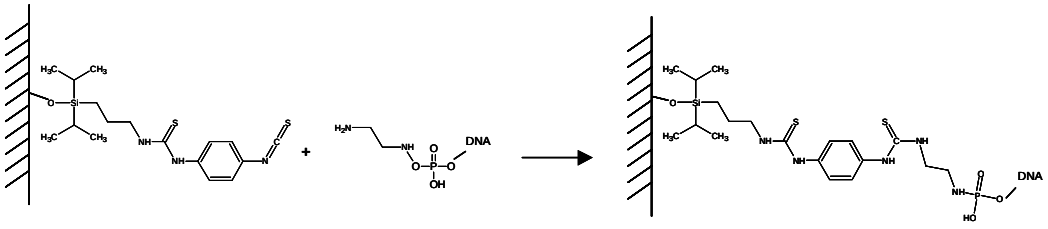

Figure 2.4: Reaction scheme for the attachment of amine-appended DNA to PDC-activated silica.

2.2.2.2.5 Removal Of Adsorbed DNA

In order to remove any non-specifically adsorbed DNA that was not covalently linked to the silica beads, the beads (which had been subjected to the above immobilization chemistries) were washed two times with 200 μL of 50°C 0.4 M NaOH followed by five consecutive washes with 200 mL of 50°C 100 mM Phosphate Buffered Saline, pH 7.4 (PBS).[17, 22]

2.2.2.2.6 Evaluation

2.2.2.2.6.1 DNA Quantitation

The quantity of single-stranded DNA in solution was determined by reading the absorbance of an aliquot dissolved in water at 260 nm on a Cary 50 UV/Vis spectrophotometer. The concentration of the original ssDNA solution was back-calculated using the relationship that 1 absorbance unit at 260 nm ≡ 33 mg/mL of ssDNA.[23]

2.2.2.2.6.2 Verification Of Amine Modification And Test Of Stability After Washing

A ninhydrin test based on the protocol provided in L. Henke, *et. al.*[19] was used to ascertain the quantity of amine attached via silanization to the silica beads. Briefly: 5 μL of the suspended bead sample was combined with 50 μL of .2 mM KCN in ammonia-free pyridine, 50 μL of 80% phenol and 50 μL of 4% ninhydrin in 50% EtOH. The solution was heated at 95°C for 5 minutes and then allowed to cool slowly to room temperature. The cooled solution was then diluted ten-fold in 50% EtOH and the absorbance at 570 nm read using a Cary 50 UV/Vis spectrophotometer. A calibration curve using the appropriate 3-aminopropyl siloxane was created in order to estimate the surface coverage of the amine-modifier on the beads.

2.2.2.2.6.3 Quantifying The Amount Of DNA Associated With The Silica Beads

Phosphorous-32 (^{32}P) (a β particle-emitter) was incorporated into all of the ssDNA used in the attachment investigations. The specific activity of the radiolabeled ssDNA was established by determining the disintegration counts per unit volume with a Tri-Carb 2100TR Liquid Scintillation Analyzer (Packard Instruments Company, Meriden, CT) and integrating this information with the DNA concentration as determined via the A_{260} readings outlined above. Knowledge of the half-life of ^{32}P and scintillation counts of the bead suspensions allowed for the determination of the amount of DNA associated with the beads.

2.2.3 Results And Discussion For Silica

2.2.3.1 Amine-modification Of Silica Beads

2.2.3.1.1 3-APdMES

Several trials involving modification of the silica beads with 3-APdMES were attempted. Beads modified with a 10% solution of 3-APdMES in 95% EtOH gave the best results. The ninhydrin test showed that there were 40.06 $\pm$ 8.12 nmol of available amine per 5 μL of bead suspension (representative data shown in figure 2.5). This corresponds to a packing density of ~132 pmol/cm^2, which is in agreement with the expected maximum packing density for small molecules (~166 pmol/cm^2).[24] Obviously, there was significant variability in the absorbance values for the modified beads, but additional trials of bead modification with 3-APdMES produced similar results (data not shown).

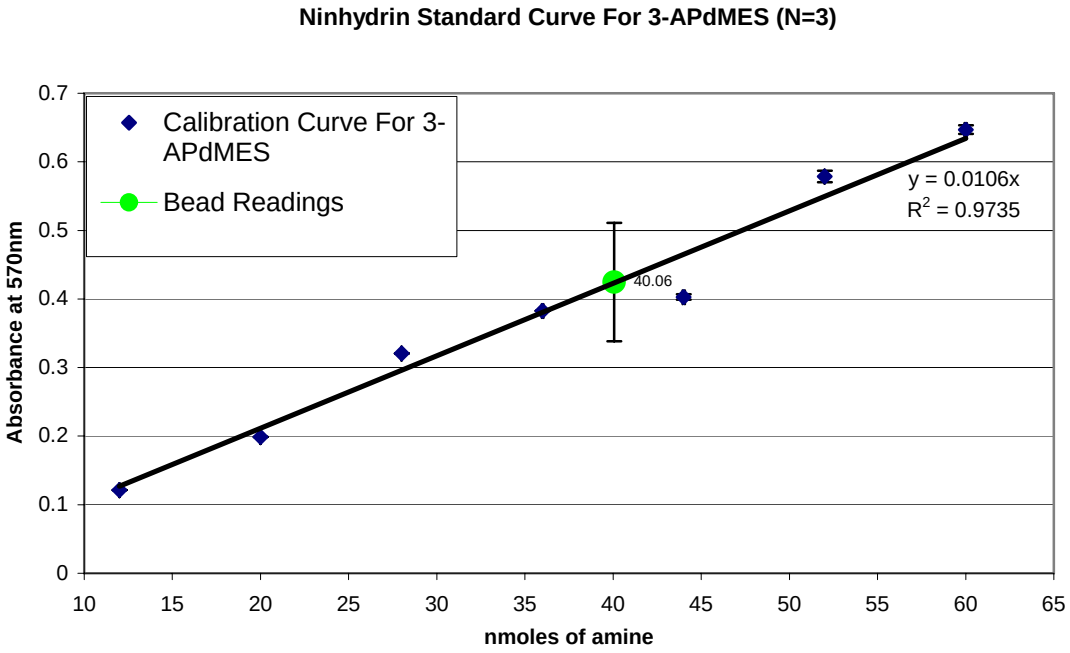

Figure 2.5: Representative ninhydrin standard curve for 3-APdMES modified beads.

3-APdMES modification of silica will result in a monolayer of amino-siloxane; however, the 3-APdMES-modified beads were not stable to the 50°C 0.4 M NaOH washes (needed for the DNA attachment trials to remove any adsorbed DNA). Figure 2.6 illustrates this instability with the results of the ninhydrin test for two trials. Each trial consisted of a washing of one set of 3-APdMES modified beads with 50°C PBS and another set of 3-APdMES modified beads with 50°C 0.4 M NaOH. N = 3 for each set and every set came from the same stock of 3-APdMES modified beads. For each trial the beads washed with the NaOH solution had a significantly lower absorbance reading (corresponding to lower amount of amine) than the beads washed with the PBS solution. An amine calibration curve was not performed for these trials, so the A_{570} absorbance does not correlate to a specific amount of amine available. However, it is obvious that the amount of available amine decreased significantly upon washing with the NaOH solution. This loss of amine

correlates with a loss of amino-siloxane by base-catalyzed hydrolysis. Therefore, 3-APdMES was not used as a silica modifier for the DNA attachment experiments.

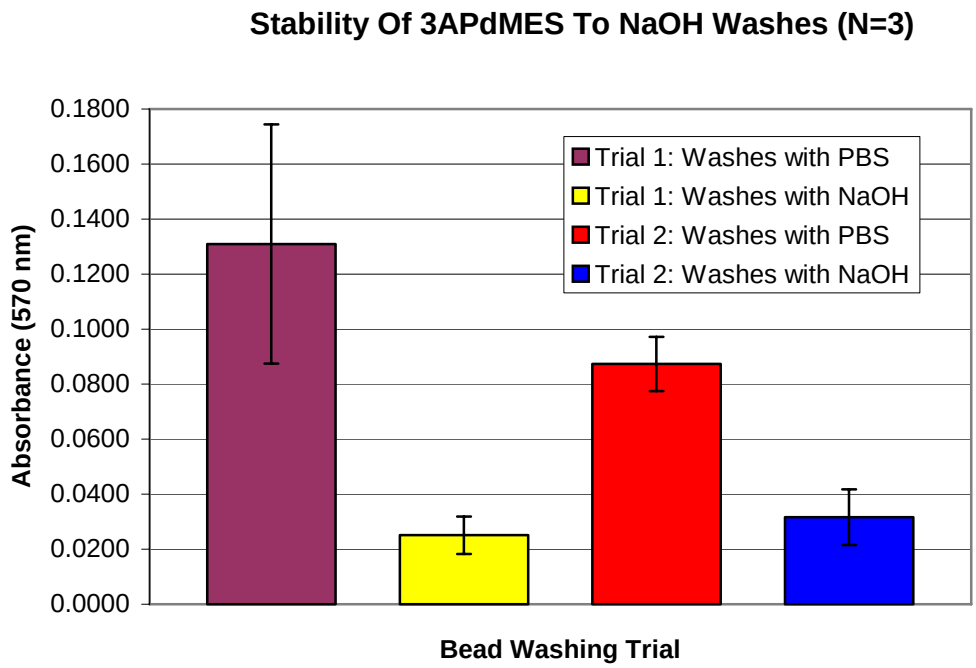

Figure 2.6: Stability test of 3-APdMES modified silica beads

2.2.3.1.2 3-APdIES

Silanization of the silica beads with 3-APdIES will also result in mono-layer coverage. The amine coverage of the 3-APdIES modified beads was determined to be 50.1 ± 4.9 nmol of amine per 5 μL of bead suspension via the ninhydrin test (figure 2.7).

The stability of the 3-APdIES modified beads to base-catalyzed hydrolysis was tested in the same manner as the 3-APdMES modified beads. Again, there was no calibration curve established for these trials so determination of the amount of amine on the beads is relative. Figure 2.8 shows that there is no loss of amine due to washing the modified beads with 0.4 M NaOH. **Therefore, the 3-APdIES modified beads were used in the anti-thrombin DNA aptamer immobilization experiments.**

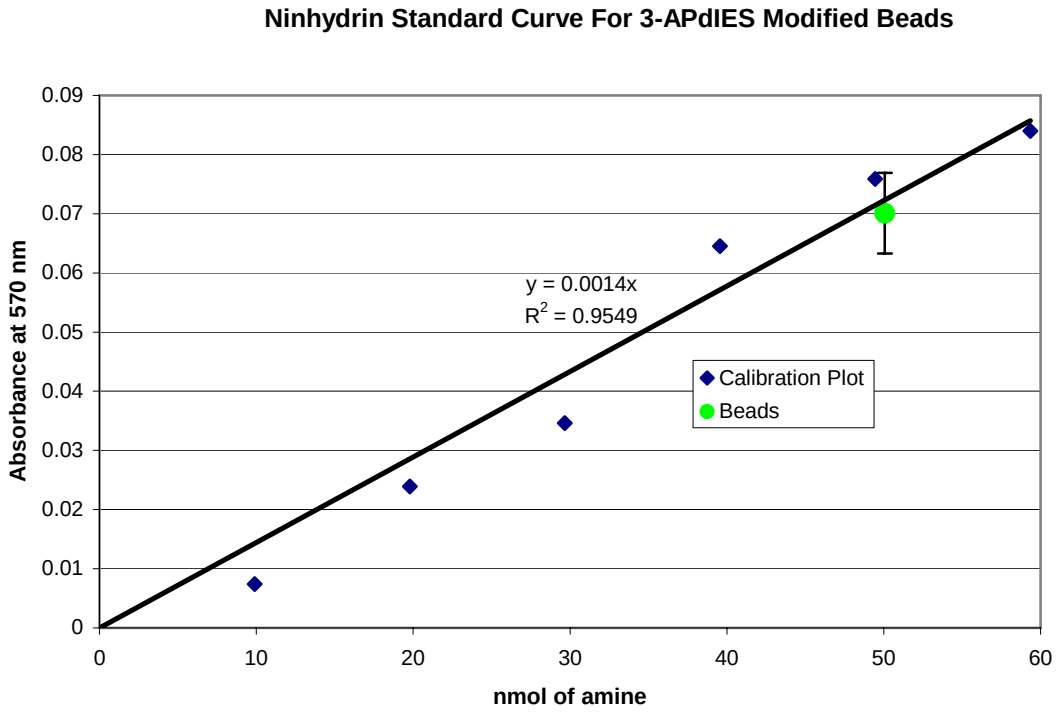

Figure 2.7: Ninhydrin standard curve for 3-APdIES modified beads.

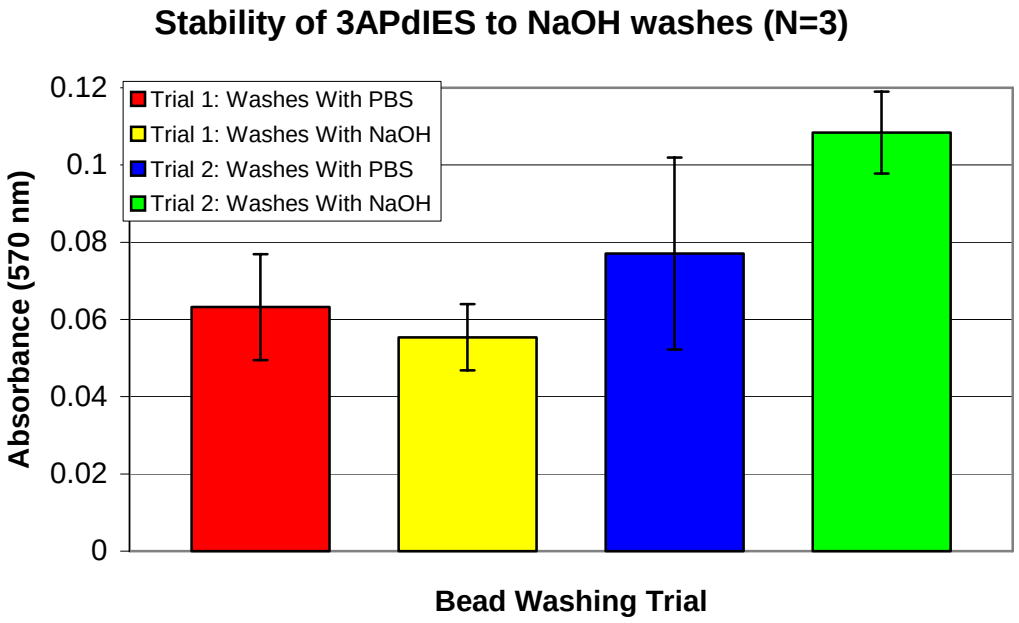

Figure 2.8: Stability test of 3-APdIES modified silica beads

2.2.3.2 Removal Of Adsorbed DNA From Amine-modified Beads

Trials were conducted to verify that NaOH washing is an effective technique for removing any DNA that may be electrostatically adsorbed to the amine-modified beads. ^{32}P-labeled aptamer was incubated with the modified beads under immobilization conditions in the absence of EDC. After this incubation, the beads were first washed 5 times with 200 μL of 50°C PBS and an aliquot was removed for scintillation counting. The second washing involved 2 washes of 200 μL of 50°C 0.4 M NaOH followed by 5 washings of 200 μL of 50°C PBS. Figure 2.9 illustrates the effective removal of the adsorbed DNA from the amine-modified beads.

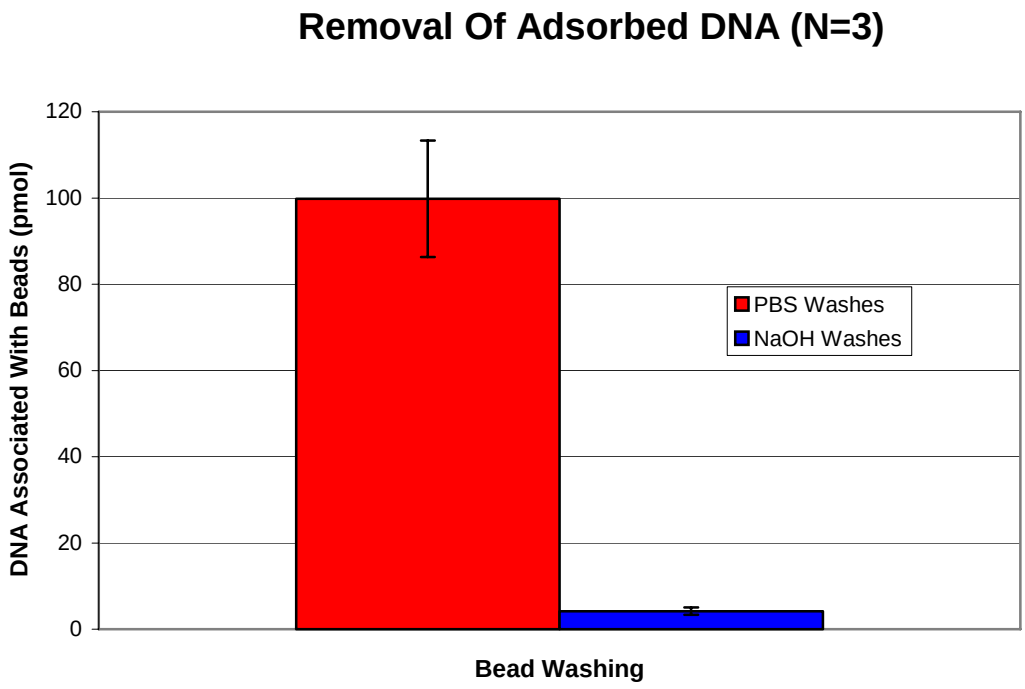

Figure 2.9: Removal of adsorbed DNA via 50°C NaOH washings.

2.2.3.3 DNA Immobilization To Silica Beads

2.2.3.3.1 EDC-mediated Attachment

Attempts to immobilize the DNA (Aptamer and Scrambled sequences) on the silica beads via the EDC-mediated reaction met with limited success. The results illustrated in figure 2.10 are typical for the attempts that involved the mixing of 5'-phosphorylated DNA sequence with the 3-APdIES-modified silica in the presence of EDC: initial indications after washing the beads with 50°C PBS showed small amounts of DNA associated with the beads; however, consecutive washes with 50°C NaOH/PBS displayed a continual decrease in DNA associated with the beads. The DNA that was removed from the beads by the NaOH washings was not covalently attached: Rasmussen, *et. al*. has shown that the phosphoramide bond linkage to DNA is stable to 0.4 M NaOH washing.[22] Trials showed that the maximum amount of DNA immobilized to the 3-APdIES-modified beads via the EDC-mediated reaction was 45.3 fmol/cm^2. There was no apparent difference between attachment of the aptamer sequence and the scrambled sequence.

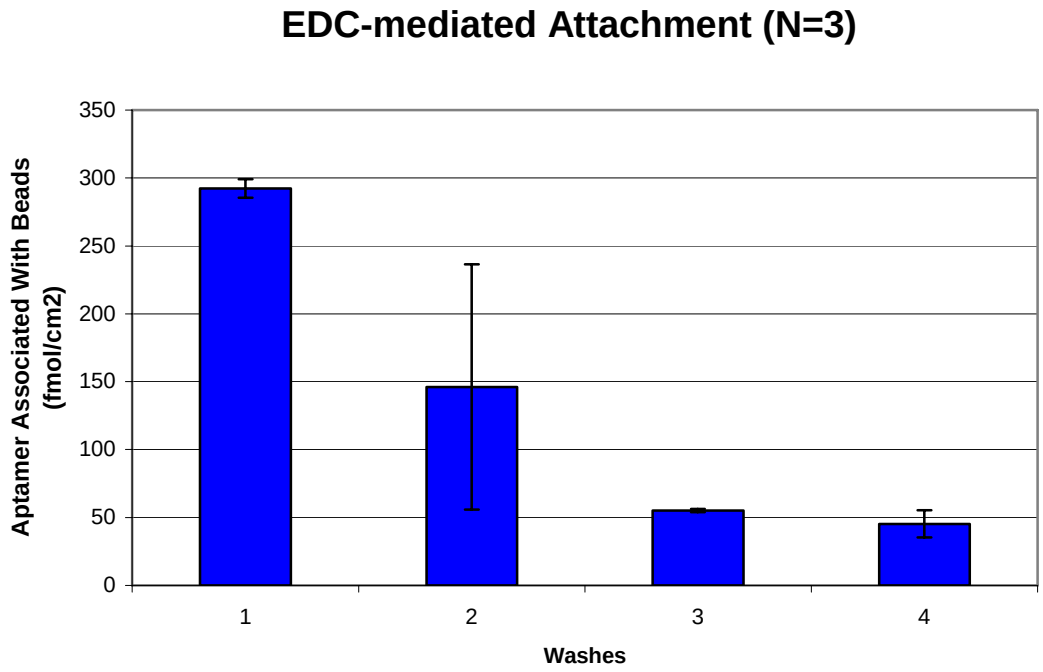

Figure 2.10: EDC-mediated attachment of 5'-phosphorylated aptamer to 3-APdIES-modified silica beads. Wash 1 is with PBS only. Washes 2-4 are each with NaOH followed by PBS.

Two variations were attempted to increase the packing density of the DNA onto the silica beads via the EDC-mediated reaction: 1) coating the amine-modified beads with salmon sperm DNA prior to attempting the attachment to 5'-phosphorylated DNA; 2) attaching the 3-APdIES to the 5'-phosphorylated DNA and then modifying the surface of the silica beads with this chimera. Ghosh and Musso have shown that attachment efficiency is increased when controlled pore glass was first coated with salmon sperm DNA.[17] That was not the case in this situation: there was no improvement in the packing density when the attachment was tried with silica beads that had first been coated with salmon sperm DNA. These results indicated that the attachment level was being limited by the formation of the phosphoramide bond reaction. Therefore, the phosphoramide bond was formed between the 3-APdIES and the 5'-PO_4DNA prior to the silica bead modification. Even though the

phosphoramide linkage was successful for this solution reaction, the attachment of the chimera to the silica beads was unsuccessful- there was no DNA attached to the beads.

The limiting factor for the attachment of the 5'-PO_4DNA to the amine-modified silica appears to have been the formation of the phosphoramide bond. This bond is readily formed in solution[19, 25] and has been shown to work between surface-immobilized amines and 5'-PO_4DNA.[19, 22, 25] However, the results of this investigation showed limited attachment success. The combination of 1) limited access to the activated phosphate because of its close proximity to the DNA (no linker) and 2) a relatively short linker attaching the reactive amine to the silica may have reduced the ability of the two reactive moieties (the EDC-activated phosphate and the silica-tethered amine) to get close enough for the reaction to occur. Therefore, a different linkage strategy was tried that gave both reactive moieties longer linker arms.

2.2.3.3.2 PDC-mediated Attachment

The PDC-mediated chemistry was attempted for attaching the DNA to the amine-modified beads in order to try to increase the packing density of the DNA on the silica beads. This method was chosen because it had been used successfully with the thrombin aptamer for attachment to an amine-modified silica[5] and it extends both reactive moieties into solution by means of a linker arm. In order to perform this chemistry, an amine needed to be appended to one of the ends of the DNA. This was effected by utilizing the EDC-mediated phosphoramide bond between an end phosphate group on the DNA and ethylenediamine.

Both 5' amine-modified (3-carbon linker) DNA (aptamer and scrambled sequence) and 3' amine-modified (7-carbon linker) DNA were attached to the PDC-activated amine-modified silica beads. Figure 2.11 shows the attachment results for both the 5' amine-modified aptamer and the 5' amine-modified scrambled DNA. Figure 2.12 shows the attachment results for both the 3' amine-modified aptamer and the 3' amine-modified

scrambled DNA. These results show that there is no difference in the level of attachment of DNA due to: 1) which end the DNA is amine-modified (5' or 3' end); 2) the sequence of the DNA (aptamer or scrambled); or 3) the length of the linker attaching the amine to the DNA (3-carbon for the 5'-attached and 7-carbon for the 3'-attached). The level of DNA attachment appears to increase as the amount of DNA applied to the beads increases (for low values of DNA applied) and then levels off to a maximum packing density of 325 fmol/cm^2.

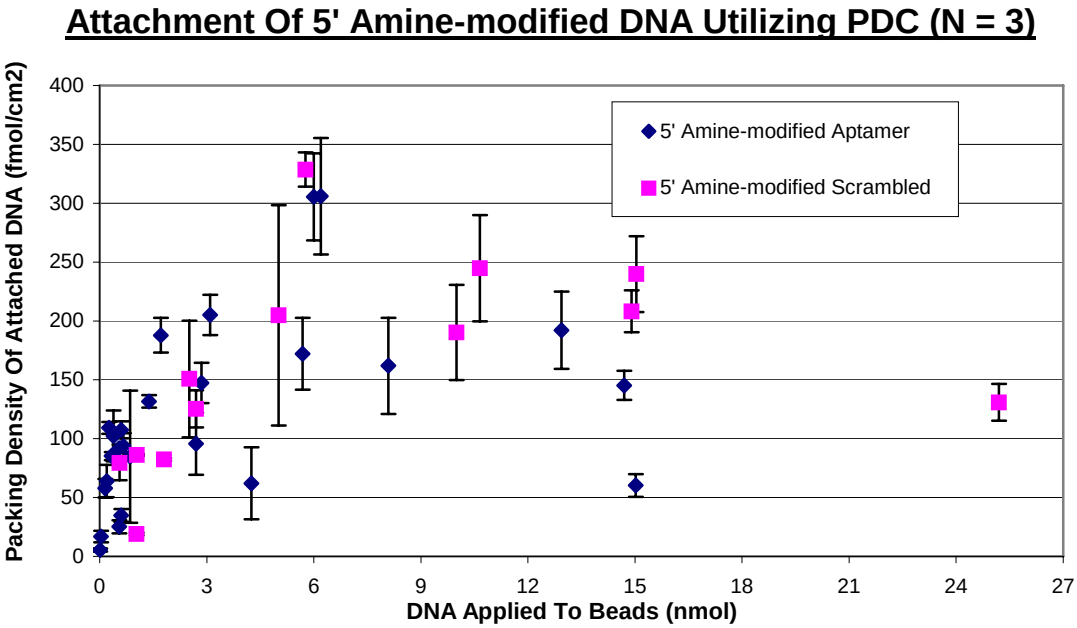

Figure 2.11: Attachment of 5' amine-modified DNA utilizing PDC.

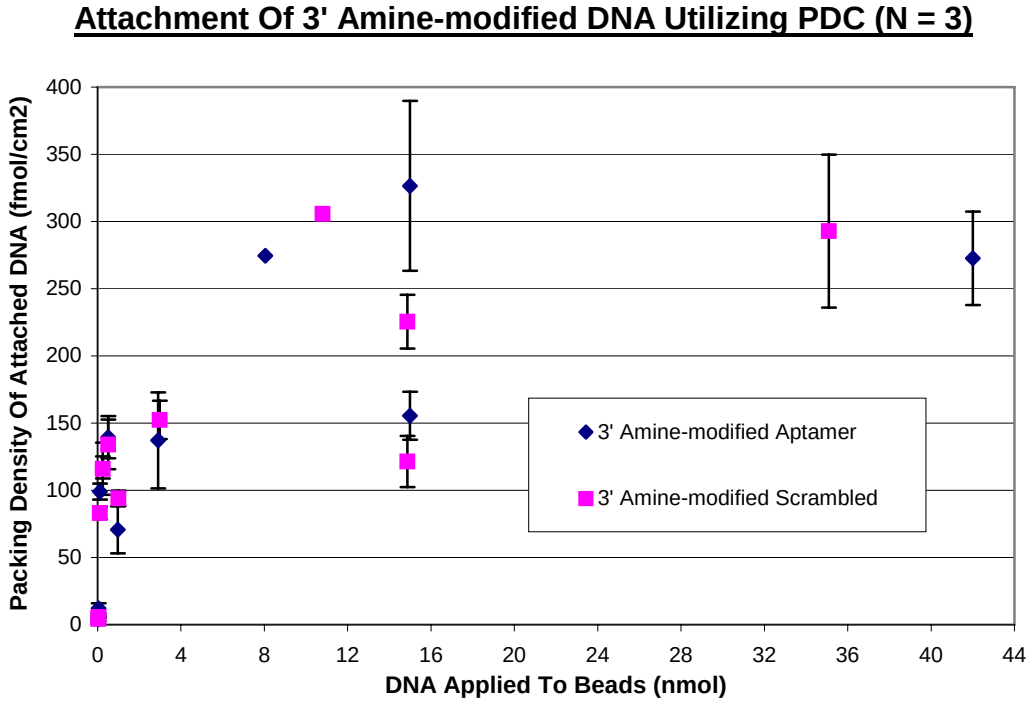

Figure 2.12: Attachment of 3' amine-modified DNA utilizing PDC.

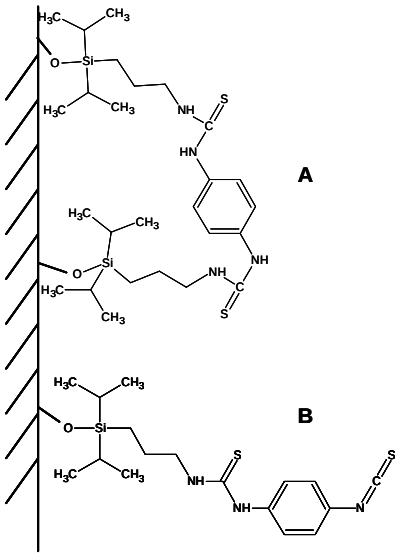

Figure 2.13: Two possible attachment arrangements for the PDC molecule to the amine-modified silica. A: Both of the isothiocyanates on one molecule of PDC react with surface amine groups. B: Only one isothiocyanate moiety on the PDC molecule reacts with the surface amine, leaving a reactive isothiocyanate group for amine-appended DNA attachment.

The low maximum attachment levels achieved for the DNA attachment to the silica may have been due to a limited number of reactive isothiocyanate on the silica surface. If both of the isothiocyanate moieties on some of the PDC molecules reacted with surface amines on the surface (illustrated in figure 2.13), then a reduced level of reactive isothiocyanates would be available for amine-appended DNA attachment. This scenario was deemed unlikely because of the high ratio of PDC molecules to available amines during the activation reaction. However, no test was performed to assay the level of reactive isothiocyanates available on the silica beads.

2.2.4 Conclusions For Silica Attachment

For the trials involving the attachment of the ssDNA (aptamer and scrambled sequence) to silica, an amino-siloxane modifier was chosen in order to utilize standard attachment chemistries. The results of these studies indicate that 3-APdIES is an appropriate amino-siloxane modifier because it is stable to washing procedures that are necessary to remove non-specifically adsorbed DNA; 3-APdMES is inappropriate as an amino-siloxane modifier due to its instability to the washing procedure. 3-APdIES showed a sufficient amount of available amine (50.1 ± 5.9 nmol) as determined by the ninhydrin test. The theoretical maximum amount of amine that should be available (assuming monolayer coverage) for the aliquot of silica beads is 51 nmol (based on a modifier packing density of 10^{14} molecules/cm^2). 3-aminopropyltriethoxy silane (3-APtES) is probably the best choice as a modifier because of its resistance to hydrolysis and its potentially greater number of available reactive amine groups (both due to the extended three-dimensional structure that it forms); however, for these studies 3-APdIES was chosen because a monolayer coverage of the silica beads was desired in order to determine an accurate value for the DNA packing density.

The maximum DNA packing density values differed according to the immobilization chemistry. The EDC-mediated phosphoramidate bond to the 3-APdIES modified beads resulted in a maximum DNA packing density of 45.3 fmol/cm^2 (independent of sequence/conformation). The PDC-mediated thioamide immobilization to the 3-APdIES modified beads resulted in a maximum DNA packing density of about 325 fmol/cm^2 (independent of sequence, conformation, attachment end, and linker length). Both of these values are low compared to the reported literature values for covalent attachment of ssDNA (not aptamers) to silica (various immobilization techniques): $\leq$ 50 pmol/cm^2.[26-32] There are no reported packing density values for covalent attachment of aptamers to silica. The only covalent attachment of an aptamer for which a packing density was determined was for the anti-thrombin DNA aptamer immobilized to a nylon membrane. The values were between 0.5 and 1 nmol/cm^2.[11]

One commonality for all of the literature reports of immobilized DNA aptamers is that there is a significantly long linker arm between the DNA and the silica surface (12 carbons or more). In addition, the DNA had at least a 6-carbon linker between the end of the DNA and the reactive moiety for attachment.[1-5, 7-16, 33] In the experiments presented here, the EDC-mediated phosphoramide linkage resulted in a 3-carbon linker between the substrate and the DNA, while the PDC-mediated thioamide attachment resulted in a 15-carbon linker. The reactive moiety (a phosphate group and an amine group, respectively) appended to the DNA varied from zero carbons for the phosphate, 3 carbons for the 5' amine and 7 carbons for the 3' amine. The lack of any linker between the DNA and the reactive moiety may have contributed to the low attachment levels for the phosphoramide bond immobilization; however, the reactive amine distance from the DNA did not make a difference in the attachment level for the amide bond immobilization strategy. Apparently, the reactive moiety needs to be extended some distance away from the DNA by a linker in order for the covalent chemistry to work, but the length of the linker may not be crucial to the attachment level.

Another difference between the two immobilization techniques was the distance the reactive end of the linker extended away from the surface of the silica. For the phosphoramidate reaction, the amine from the 3-APdIES extended approximately four carbons away from the silica surface. Even though the PDC-mediated reaction used the same amino-siloxane linker on the silica, the reactive moiety extending away from the silica surface was significantly farther (approximately 7 more carbons) than the EDC-mediated reactive moiety because of the PDC activator. The DNA may be able to approach the reactive moiety closer when it extends further away from the silica because the DNA will not be as strongly influenced (repelled) by the negative surface charge of the silica.

2.3 Attachment To Gold

2.3.1 Introduction

Covalent and affinity immobilization strategies were used to attach ssDNA (aptamer and scrambled) to the surface of a modified gold substrate. Several different Biacore SPR chips (Biacore, Uppsala, Sweden) were used as the modified gold substrate in these experiments because the analytical tool for assessing the level of attachment utilized the Biacore 3000 SPR instrument. A hybridization assay between the attached ssDNA and its complementary ssDNA strand was used to determine the level of attachment. The packing density for the attached ssDNA on a specific chip flow cell was estimated using the following relationship: 1 resonance unit (RU) of change in the SPR signal is equivalent to 20 fmol/cm^2 of single-stranded 15-mer DNA attached (see Materials and Methods, section 2.3.2.2.3).

Two different covalent attachment strategies were tried: 1) a phosphoramide bond linked the 5'-phosphorylated DNA to an amine-modified surface, and 2) an amide bond was formed between 5' amine-modified DNA and a carboxyl-modified substrate. Figures 2.14 and 2.15 show the attachment schemes for 1 and 2 above, respectively. The

phosphoramide bond linkage strategy was performed in order to compare the results from the silica attachment to the gold attachment. PDC mediated attachment was not attempted due to the incompatibility of the reagents with the SPR system; specifically, the integrated microfluidic cartridge (IFC). The amide bond strategy for covalent attachment was pursued because of its similarity to the PDC-mediated strategy used for silica (both utilized an amine linker on the end of the ssDNA) and the reported success for attachment of ssDNA to the carboxyl-modified Biacore chips.[34, 35]

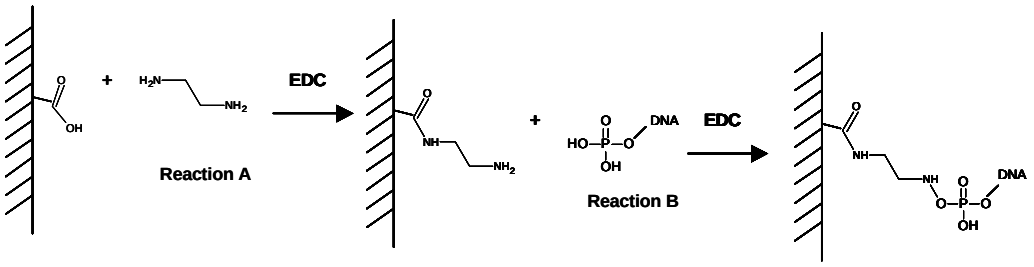

Figure 2.14: Covalent attachment strategy #1 for ssDNA to modified gold surface. Reaction A: amine modification of the carboxylated gold surface utilizing EDC chemistry. Reaction B: phosphoramide bond linking the 5'-phosphorylated DNA to the amine-modified gold surface.

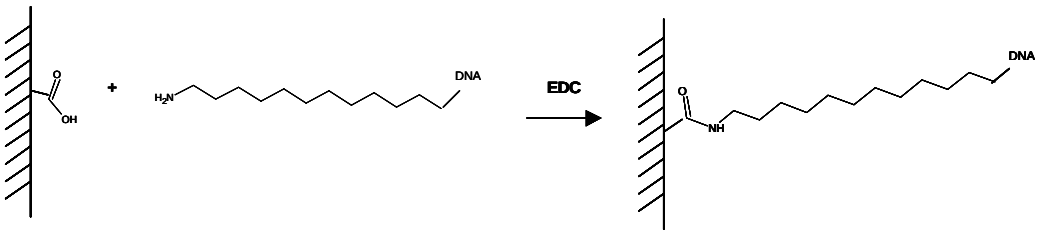

Figure 2.15: Covalent attachment strategy #2 for ssDNA to modified gold surface.

The affinity attachment method utilized the well-established streptavidin-biotin interaction. A streptavidin-modified gold Biacore chip was the substrate and the ssDNA was appended at the 5' end with a biotin molecule (via a 12-carbon linker).

Three different types of Biacore sensor chips were used in these studies (cartoons of chips shown in figure 2.16). All of the sensor chips are composed of a glass support with a thin gold layer. Two of them were used in the covalent attachment studies and one was used in the affinity attachment studies. Both of the sensor chips used in the covalent attachment studies come modified with carboxymethyl groups appended to the gold substrate through an alkyl-thiol linker. The difference between the two is that one chip (CM3) has a dextran sub-layer that is 40-50 nm thick between the gold surface and the reactive carboxyl groups; thus, giving the attached carboxyl groups 'solution phase-like' characteristics (providing solution conditions that are more like a homogeneous assay than a heterogeneous assay). The other chip (C1) does not have a dextran sub-layer; hence, it is more similar to immobilization on a surface (making the conditions more like a heterogeneous assay). A Biacore SA chip was used for the affinity attachment studies; it is a CM3 chip with streptavidin immobilized through the carboxyl groups. These three chips were specifically selected because they would allow for studies that investigated differences in immobilization, activity and kinetics between: 1) heterogeneous assay conditions and homogeneous assay conditions of covalently immobilized aptamers (C1 versus CM3 chips) and, 2) covalently and affinity immobilized aptamers (CM3 versus SA chips).

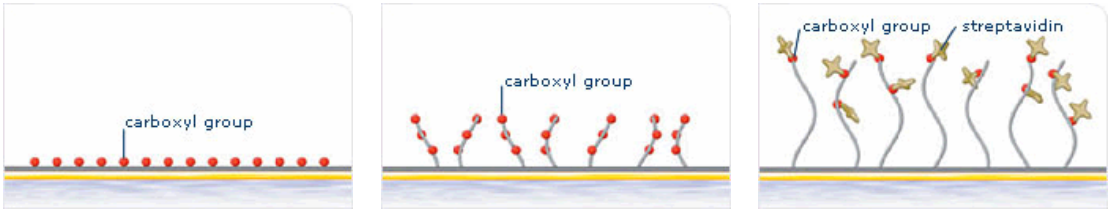

A: CM1 Chip B: CM3 Chip C: SA Chip

Figure 2.16: Cartoons of the three different Biacore chips used in the gold attachment experiments. www.biacore.com/lifescience/products/sensor_chips

2.3.2 Materials And Methods

2.3.2.1 Materials

The 1 M ethanolamine-HCl, N-hydroxysuccinimide (NHS) and EDC were purchased from Biacore (Uppsala, Sweden). The ethylenediamine and the hexadecyltrimethyl ammonium bromide (CTAB) were from Sigma (St. Louis, MO).

All solutions, containing 0.005% surfactant P20 (Biacore, Piscataway, NJ), were passed through a 0.22 μm filter and deaerated under partial vacuum prior to injection into the Biacore 3000 instrument.

All of the ssDNA was purchased from Integrated DNA Technologies, Inc (Coralville, IA). 5' biotin-appended DNA (5'-biotinDNA) and 5' amine-appended DNA (5'-NH_2DNA) utlized a 12 carbon linker. DNA used in the phosphoramide bond experiments were phosphorylated on the 5' end (5'-PO_4DNA). The sequences for the complementary DNA strand to the aptamer (AptComp) and the complementary DNA strand to the scrambled sequence (ScramComp) were 5'- CCA ACC ACA CCA ACC –3' and 5'- ACC ACA ACA ACC ACC –3', respectively. All of the DNA was purified via high-performance liquid chromatography (HPLC) by the vendor.

The three different gold substrates (sensor chips) were all purchased from Biacore (Piscataway, NJ). To review, the three chips were: 1) the C1 chip, which is a gold surface with a carboxymethyl modification (no dextran sub-layer) and provides a heterogeneous assay format; 2) the CM3 chip, a carboxymethyl surface with a dextran sub-layer that is attached to the gold substrate, considered to be similar to homogeneous assay conditions; 3) the SA chip, a CM3 chip with streptavidin immobilized to the surface carboxyl groups. All of the chips are constructed with four identical flow cells (FC) per chip that have a surface area of approximately 1.2 mm^2 per flow cell.

2.3.2.2 Methods

2.3.2.2.1 Covalent Attachment

Covalent attachment via phosphoramide bond formation between a substrate-immobilized amine group and a 5' phosphate group on the ssDNA was performed on the Biacore 3000 instrument with a flow rate of 5 μL/min of 100 mM sodium borate buffer, pH 8.5 (borate buffer). The injections over the flow cell surface are as follows:

1. 50 μL injection of a 1:1 mixture of NHS:EDC (activation of the surface carboxyl groups).
2. 1:1 mixture of 8 μM 5'-PO_4DNA in borate buffer containing 0.6 μM CTAB with EDC/NHS mix created (activation of the DNA 5'-phosphate group).
3. Injection of 50 μL of 0.1 M ethylenediamine in borate buffer (amine modification of the surface).
4. Injection of 50 μL of the 5' PO_4DNA:EDC/NHS mixture (formation of the phosphoramide bond).
5. Injection of 30 μL of ethanolamine (blocking of unmodified, EDC-activated carboxyl groups).

The amide bond reaction between the surface carboxyl groups and the 5'-NH_2DNA utilized the same flow rate and buffer composition as the phosphoramidate reaction (above). The injection routine is as follows:

1. 50 μL injection of a 1:1 mixture of NHS:EDC (activation of the surface carboxyl groups).
2. Injection of 50 μL of 5'-NH_2DNA in borate buffer containing 0.6 μM CTAB (formation of the amide bond).
3. Injection of 30 μL of ethanolamine (blocking of unmodified, EDC-activated carboxyl groups).

Attempts to covalently attach the DNA included the use of duplexed DNA. The purpose of duplexing the DNA was to eliminate the native aptamer 3D structure. The dsDNA was created by hybridizing the ssDNA (aptamer or scrambled) with its complement. This was accomplished by combining (at a ratio of 1:2) ssDNA with its complement in 100 mM sodium borate, pH 8.5, heating the solution at 70°C for 5 minutes, and then allowing the solution to cool slowly to room temperature. CTAB was added to a concentration of 0.6 μM after the duplexed DNA solution had cooled.

Preconcentration experiments were performed in order to evaluate the potential success of a particular immobilization strategy (additives to the buffer or use of duplexed DNA). For these experiments a plug of the DNA solution (3.6 μM aptamer or 4.4 μM scrambled) was injected (50 μL at a flow rate of 5 μL/min) over the flow cell and the RU change measured by the SPR instrument.

2.3.2.2.2 Affinity Attachment

SA chips used for the affinity attachment of ssDNA were preconditioned in order to remove any adsorbed streptavidin as per the procedure outlined in Biacore Application Note 16.[36] Briefly, the new chips were docked in the Biacore 3000 and then washed with three consecutive 100 μL injections of 1M NaCl, 50 mM NaOH, each followed by a five minute injection of 100 mM potassium phosphate buffer, pH 7.4 (phosphate buffer) at a flow rate of 50 μL/min.

5'-biotinDNA was immobilized to the appropriate flow cell on a chip by injecting the appropriate volume of the 5'-biotinDNA in phosphate buffer at a flow rate of 10 μL/min.

2.3.2.2.3 Evaluation

The effectiveness of the various immobilization procedures was determined by standard hybridization assays on the Biacore 3000 instrument. The procedure involved an injection of 60 μL of a solution of the complementary DNA strand (7.07 μM AptComp or 6.44

μM ScramComp) at a flow rate of 30 μL/min in the phosphate buffer. Complementary binding is visualized by an increase in the post-injection baseline RU compared to the pre-injection baseline RU for the flow cell to which the appropriate ssDNA is immobilized. It is important to recognize that the SPR signal **during the complementary strand injection** is not indicative of any immobilized DNA; any signal change during the complementary strand injection can be due to a bulk refractive index change (change in bulk solution composition) and/or surface association effects. Complementary binding is signaled **only** by a stable post-injection baseline (due to surface association) that is greater than the pre-injection baseline.[37]

The immobilization density of the ssDNA was calculated based on the relationship that a change of 1 RU corresponds to a change in the association of 1 pg of material/mm^2 at the surface of the sensor[38] and that the ssDNA used in these experiments has a molecular mass of ~5000 g/mol. Therefore, 1 RU change corresponds to a change in 20 fmol/cm^2 of associated ssDNA.

After an injection of a complementary strand (AptComp or ScramComp) into a flow cell, regeneration of the flow cell surface was accomplished by an injection of 10 μL of 1 M NaCl, 50 mM NaOH at a flow rate of 5 μL/min. This solution removed all of the DNA that was not covalently attached in the flow cell (as signaled by a return in the SPR baseline signal back to the pre-injection level).

2.3.3 Results For Attachment To Gold

2.3.3.1 Covalent Attachment

2.3.3.1.1 Phosphoramide Bond

No measurable amount of DNA (aptamer or scrambled) was immobilized via the phosphoramide bond to either the C1 or the CM3 chip. Immobilization trials were unsuccessful even with extremely high concentrations of aptamer and scrambled

sequences (65.88 μM and 48 μM, respectively). It is possible that some ssDNA was immobilized, but that the immobilization level was below the detection threshold for the SPR instrument of 1 RU (or 20 fmol/cm^2). If there was immobilization of the 5'PO_4DNA via phosphoramide bond formation to the C1 and/or CM3 chip, the level is exceedingly low and, therefore, of little analytical use.

Figure 2.17 shows representative sensorgrams for a hybridization trial on a CM3 chip with a flow cell that does not have any DNA immobilized (blue trace) and one that does (green trace). The flow cell that has no DNA immobilized had previously been subjected to an immobilization attempt using phosphoramide bond chemistry with an injection of 65.88 μM 5'-PO_4Apt. The 5'-PO_4Apt trace (blue trace) shows a rapid increase in the response (~65 RU) upon injection of the aptamer complementary strand (AptComp). This response slowly decreases until it abruptly drops below the pre-injection baseline at the end of the AptComp injection. The baseline steadily increases back to the previous level prior to the AptComp injection, at which point a plug of 1 M NaCl, 10 mM NaOH (regeneration solution) is injected across the flow cell to remove any complementary DNA hybridized to the immobilized DNA. The response during the injection is due to changes in the bulk solution composition, not specific interactions between the surface and a solution component. A specific interaction would have resulted in a post-injection baseline greater than the pre-injection baseline. Therefore, the 5'-PO_4Apt trace is representative of a flow cell that has no DNA immobilized to it (aptamer or scrambled).

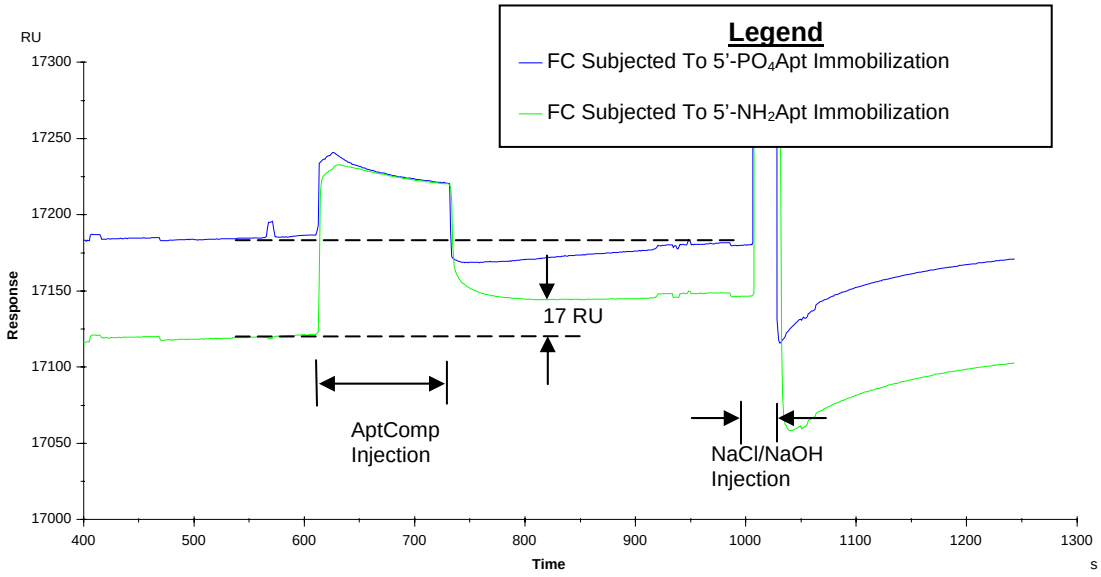

Figure 2.17: Sensorgram for a hybridization trial for two flow cells on a CM3 chip with aptamer potentially attached: one subjected to immobilization of 5'-PO_4Apt using phosphoramide bond chemistry and the other subjected to 5'-NH_2Apt using amide bond chemistry. The complementary DNA strand is the AptComp sequence at a concentration of 7.07 μM.

In contrast, the 5'-NH_2Apt trace (green trace in figure 2.17) is illustrative of a hybridization trial sensorgram for a flow cell that has the exact complement to the injected DNA immobilized on it. This flow cell had previously been subjected to an immobilization attempt via amide bond chemistry with an injection of 3.6 μM 5'-NH_2Apt. The trace parallels the 5'-PO_4Apt sensorgram **except that it never declines to the pre-injection baseline level until after the regeneration solution injection.** The increase in the baseline signal post-AptComp injection (compared to the baseline signal prior to the AptComp injection) is due to the duplex that is formed during the hybridization of the two complementary strands. Because one of the DNA strands is immobilized to the sensor surface (the aptamer sequence, in this case), the signal remains constant while the complementary strand is hybridized to the immobilized strand. The regeneration solution disrupts the hydrogen bond interactions between the attached aptamer and its complementary strand. Therefore, the complementary strand dissociates from the immobilized DNA with a concomitant decrease

in the SPR signal. In this sensorgram, the baseline difference between the post-AptComp injection and the pre-AptComp injection is indicative of 17 RU (or 344 fmol/cm^2) of aptamer immobilized in the flow cell.

2.3.3.1.2 Amide Bond

Hexadecyltrimethylammonium bromide (CTAB) was utilized in all of the DNA solutions for covalent attachment via amide bond formation (see figure 2.18 for CTAB structure). CTAB is a cationic surfactant that will form micelles in aqueous solutions.[39] Initial attempts at immobilization did not include CTAB in the DNA solutions and resulted in no DNA attachment. It has been proposed that CTAB micelles facilitate the approach of the negatively charged amine-modified DNA (due to the phosphate backbone) to the negatively charged carboxymethyl-modified gold substrate (due to the carboxyl groups) by serving as counter ions to the DNA.[35] This 'chaperone effect' allows the negatively charged DNA to approach the negatively charged surface; thereby allowing for amide bond formation.

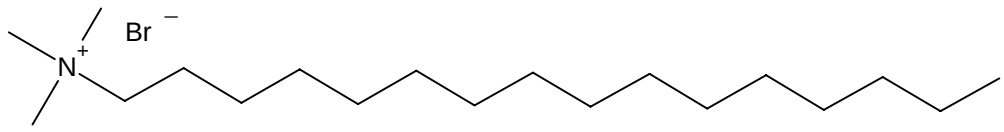

Figure 2.18: Hexadecyltrimethylammonium bromide (CTAB) structure.

Amide bond formation between the carboxymethyl-modified gold sensor chips (C1 and CM3) and the 5' amine-modified DNA (5'-NH_2DNA) was accomplished with the addition of CTAB to the 5'-NH_2DNA solution. However, there was a significant difference in the amount of immobilized DNA between the aptamer and scrambled sequences for both the C1 and CM3 chips. It was possible to immobilize the scrambled sequence at a higher packing density than the aptamer sequence for both the C1 and the CM3 chips. In addition,

the packing density of both sequences (aptamer and scrambled) was consistently higher on the CM3 chip than on the C1 chip. Data illustrating these results are presented below.

Greater packing density resulted for the scrambled DNA sequence immobilization than the aptamer DNA sequence immobilization when similar concentrations of 5'-NH_2DNA were injected during the immobilization procedure. Figure 2.19 shows the sensorgrams for a hybridization test on a CM3 chip. FC3 (green trace) was exposed to 4.4 μM of 5'-NH_2Scram during the immobilization procedure. FC4 (light blue trace) was exposed to 3.6 μM of 5'-NH_2Apt during the immobilization procedure. The sensorgrams in figure 2.19 show the typical responses to complementary and non-complementary injections of DNA. The first injection for these sensorgrams was of 6.44 μM ScramComp DNA: the FC3 trace shows a rapid decline in the RU level post-injection and stabilizes at 65 RUs above the pre-injection baseline; the FC4 trace shows a fairly rapid decline back to the pre-injection baseline level at the end of the ScramComp injection. After the surfaces of both flow cells were regenerated with an injection of 1 M NaCl/ 0.4 M NaOH, a 7.07 μM AptComp solution was injected. The FC3 trace shows a typical post-injection response curve for a flow cell with non-complementary DNA immobilized: a relatively fast dissociation curve that will eventually reach the pre-injection baseline level (however, it is preempted by the NaCl/NaOH injection). The difference between the post-injection baseline and the pre-injection baseline for the FC4 trace shows that there is 8 RU of Apt immobilized to the surface.

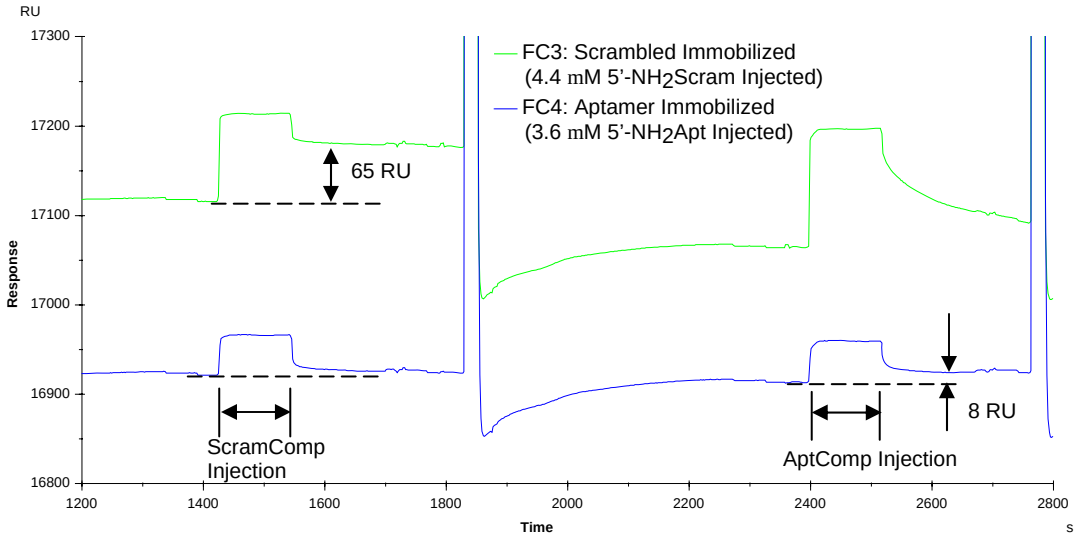

Figure 2.19: Sensorgrams of hybridization analysis for aptamer and scrambled DNA immobilized to a CM3 SPR sensor chip.

Table 2.1 summarizes the immobilization level (packing density) for the aptamer and the scrambled DNA sequences to the C1 chip based on hybridization assays. Rows 1 and 2 illustrate the difference in the attachment success between the aptamer sequence and the scrambled sequence for the C1 chip: immobilization of the aptamer sequence to the C1 chip was not achieved. The third and fifth rows were aptamer immobilization attempts with 3 and 10 times, respectively, the aptamer concentration during the initial immobilization attempts (row 1). Since none of these attempts succeeded, another strategy was employed.

Two attempts were made to immobilize the aptamer while it was hybridized to its complementary strand during the immobilization procedure. The reason for trying this procedure was to test a hypothesis: compared to the unstructured scrambled sequence, the aptamer sequence will have a much higher negative charge density due to its stacked, G-quartet structure. This greater charge density will make it harder for the aptamer to approach the negatively charged surface (due to the carboxyl groups) of the chip. Hybridization of the aptamer sequence to its complementary sequence will disrupt the

native aptamer structure. Hence, the hybridized aptamer should have a reduced negative charge density and be able to approach the surface for attachment. ssDNA has been attached to modified gold via an amide bond while the DNA was hybridized to its complementary strand.[40, 41] The results listed in row six show that this procedure did not work for attachment of the aptamer sequence to the C1 chip.

Row	DNA	Attempts	Immobilization Trial DNA Concentration (μM)	Baseline Difference (RU)	Packing Density (fmol/cm^2)
1	Aptamer	2	3.6	0	0
2	Scrambled	2	4.4	21 ± 0.57	410 ± 11
3	Aptamer	1	10.8	0	0
4	Scrambled	1	13.2	31	620
5	Aptamer	1	36	0	0
6	Aptamer	2	3.6 (Hybridized)	0	0

Table 2.1: Summary of the immobilization level (packing density) for the aptamer and the scrambled DNA to the C1 chip as determined by hybridization assays. Column 2: DNA sequence for the immobilization attempt. Column 3: number of immobilization attempts. Column 4: the concentration of the DNA injected during the immobilization attempt (all injection volumes were equal). Column 5: Difference in the baselines post-complement injection and pre-complement injection (in resonance units) for the hybridization assay. Column 6: the packing density of the immobilized DNA based on the baseline difference during the hybridization assay and the relationship that 1 RU = 20 fmol/cm^2.

Immobilization of the scrambled sequence to the C1 chip was successful. Rows 2 and 4 show the results for two different concentrations of injected scrambled sequence during the immobilization: 4.4 μM and 13.2 μM, respectively. The lower concentration of 4.4 μM resulted in approximately 400 fmol of scrambled sequence immobilized per cm^2 of sensor surface. The higher concentration of 13.2 μM resulted in a scrambled sequence packing density of approximately 600 fmol/cm^2. The increase in the packing density is not linear with the increase in the concentration injected during the immobilization step. It is possible that these experiments were approaching the maximum achievable packing density for these immobilization parameters; however, no further experiments were pursued regarding

the packing density of the scrambled sequence to the C1 chip because the focus of the study was on attachment of aptamers (not ssDNA, in general).

Immobilization attempts to the CM3 chip resulted in attachment of both the aptamer and scrambled sequences; but, as indicated in the results shown in figure 2.11, it was possible to immobilize the scrambled sequence at a greater packing density than the aptamer sequence. Table 2.2 shows the summary for the results for immobilization of the aptamer and scrambled sequences to the CM3 chip.

Rows 1 and 2 of table 2.2 show the results for immobilization attempts of 0.05 μM aptamer and scrambled sequence, respectively. There was no aptamer immobilized and a low amount of scrambled sequence (150 fmol/cm^2). Rows 3 and 4 of table 2.2 compare the attachment levels between aptamer and scrambled when the concentration of the injected DNA was increased almost 100-fold over the previous trials (3.6 and 4.4 μM, respectively). This trial resulted in a low amount of aptamer immobilized (160 fmol/cm^2) and an increase in the amount of scrambled sequence immobilized (1.7 ± 0.47 pmol/cm^2). As expected, the amount of scrambled sequence attached corresponds with the concentration of the ssDNA injected during the immobilization procedure. In addition, it is possible to attach the aptamer to the CM3 surface utilizing an EDC-mediated amide bond; albeit, at a significantly lower level than for similar concentrations of scrambled DNA.

There were several attempts at increasing the level of aptamer attachment by changing the buffer composition or the structure of the aptamer. The rationale for each of the modifications is given below in the section describing the preconcentration trials. Briefly, row 5 of table 2.2 shows the result when 50 mM $MgCl_2$ was added to the aptamer solution, the solution was heated, cooled slowly and then injected onto the flow cell. A moderate increase in aptamer immobilization resulted from this procedure (discussed in further detail below). Row 6 shows the results for two immobilization trials of aptamer sequence that was hybridized to its complementary strand prior to injection over the

activated flow cell. Another modification attempted was the denaturing of the aptamer's 3D structure by the addition of DMSO to the aptamer solution (row 7). Neither the hybridized aptamer attempts nor the attempt with DMSO resulted in attachment of the aptamer to the CM3 flow cell surface.

Row	DNA	Attempts	Immobilization Trial DNA Concentration (μM)	Baseline Difference (RU)	Packing Density (pmol/cm^2)
1	Aptamer	1	0.05	0	0
2	Scrambled	1	0.05	8	0.16
3	Aptamer	1	3.6	8	0.16
4	Scrambled	2	4.4	82 ± 24	1.7 ± 0.47
5	Aptamer	1	3.6 (with $MgCl_2$)	17	0.34
6	Aptamer	2	3.6 (Hybridized)	0	0
7	Aptamer	1	3.6 (in 50% DMSO)	0	0

Table 2.2: Summary of the immobilization level (packing density) for the aptamer and the scrambled DNA to the CM3 chip as determined by hybridization assays.

These CM3 attachment results indicate that immobilization of the aptamer sequence is more difficult than immobilization of the scrambled sequence using amide bond chemistry. Taken together with the results from the C1 chip (above), it appears that the difficulty in immobilization levels between the aptamer and the scrambled sequence is due to the difference in the chemistries of these two molecules and not the immobilization strategy or the difference in the substrates. Investigations were pursued in an attempt to elucidate the nature of this difference.

There is a slight difference in composition between the aptamer and the scrambled sequence (the scrambled sequence has a T substituted for a G) and the sequence order, but the main difference between the two sequences is their three-dimensional (3D) structure. As previously mentioned, the aptamer forms a very stable, stacked, G-quartet in solution[42-44] and the scrambled sequence has a random, undefined structure[45] that is typical

of most DNA probes used in hybridization assays. The unusually compact aptamer solution structure will have a significantly higher negative charge density and concomitant larger hydration sphere than the scrambled DNA. This high negative charge density/large hydration sphere will inhibit the approach of the aptamer towards the negatively charged carboxyl surface. Another possible result of the aptamer's unique compact structure is that a structural arrangement conducive to interactions between the appended amine and the aptamer's DNA bases may exist that are not available with the scrambled sequence. In either case, the likelihood for the close association of the appended amine with the activated, surface carboxyl groups necessary for nucleophilic attack by the appended amine would be reduced. Several experiments were conducted in an attempt to increase the aptamer immobilization level by eliminating the aptamer's structural effect on attachment.

One set of experiments attempted to increase the attachment of the aptamer by disrupting the 3D structure of the aptamer. Two techniques were tried: 1) forming double-stranded DNA (dsDNA) by reacting the aptamer with its complementary sequence and 2) adding dimethylsulfoxide (DMSO) to the immobilization buffer. dsDNA will have a 3D structure that is more compact than ssDNA, but it should not be as compact (nor have as high a charge density) as the aptamer structure. In addition, the non-Watson-Crick base pairings between guanines in the G-quartet will be replaced by stronger Watson-Crick base pairings between complementary bases. However, an interior structure of bases with conjugated ring systems (available for cation-π interactions) will still be available. DMSO was added to the immobilization buffer to disrupt hydrogen bond interactions between base pairs,[23] thereby denaturing the aptamer's G-quartet structure.

Another set of experiments employed the addition of a cationic species to the immobilization buffer in order to minimize any electrostatic interactions interfering with the immobilization reaction. A common method of reducing electrostatic interactions between molecules is the addition of a quaternary ammonium salt. Tetramethylammonium chloride (TMAC) was added to the immobilization buffer as a general method of minimizing any

inhibitory electrostatic interactions. Even though π-systems (including those of DNA bases) are known to interact with the methyl groups of the tetramethylammonium cation, these interactions are quite weak and do not perturb the DNA's native structure.[46] A second type of cationic species was employed because of its strong interactions with DNA.

Divalent cations, especially magnesium, are known to 1) form strong cation-lone pair bonds with phosphate oxygens that are part of the DNA backbone and 2) form cation-π bonding interactions with imidazole rings on purine bases.[46] Since it is known that ammonium ions will stabilize intramolecular G-quadraplexes by coordinating with O6 guanine carbonyl groups within the interior of the aptamer structure,[47] $MgCl_2$ was added to the immobilization buffer in an attempt to disrupt any amine-aptamer interactions. The liberated aptamer-appended amine would then be available to react with the activated carboxyl group on the substrate.

Preconcentration experiments were used to estimate the effectiveness of the experimental modifications for the aptamer attachment. This type of experiment can give an indication of the immobilization conditions that will be successful without using up precious flow cells. Preconcentration experiments involved the injection of the amine-modified aptamer over a CM3 flow cell that had not been activated by EDC. The principle is based on the assumption that if the moiety being immobilized (the aptamer, in this case) shows an increase in surface interactions (signaled by a steady increase in the sensor response **during** the injection), then there is an increased likelihood of immobilization under those specific conditions. Numerous preconcentration trials can be run over the same flow cell surface without compromising the flow cell's potential for future attachment.

Figure 2.20 shows a sample sensorgram for a preconcentration experiment with 3.6 μM NH_2Apt + 500 mM $MgCl_2$ in borate buffer (pH 8.5) containing 0.6 mM CTAB over a CM3 flow cell. When the injection of the sample plug commences (at about 630 seconds) the baseline rises dramatically due to the bulk change in refractive index. After this initial

change, the baseline will level out at a new value unless there are interactions between the surface and some component of the injection matrix that leads to a build-up of material on the sensor surface. An accumulation of material on the sensor surface is signaled by a steady rise in the resonance units during the course of the injection. The difference between the maximum RU signal during injection (often right before the end of the injection) and the plateau after the initial rise due to the bulk refractive index change is known as the preconcentration level and correlates to the amount of material built up on the sensor surface during the sample injection (589 RU for this example). Even though the technique is insensitive to the identity of the material causing the increase in resonance units during the injection, this procedure gives a reasonable indication of the likelihood for successful immobilization using the sample conditions.

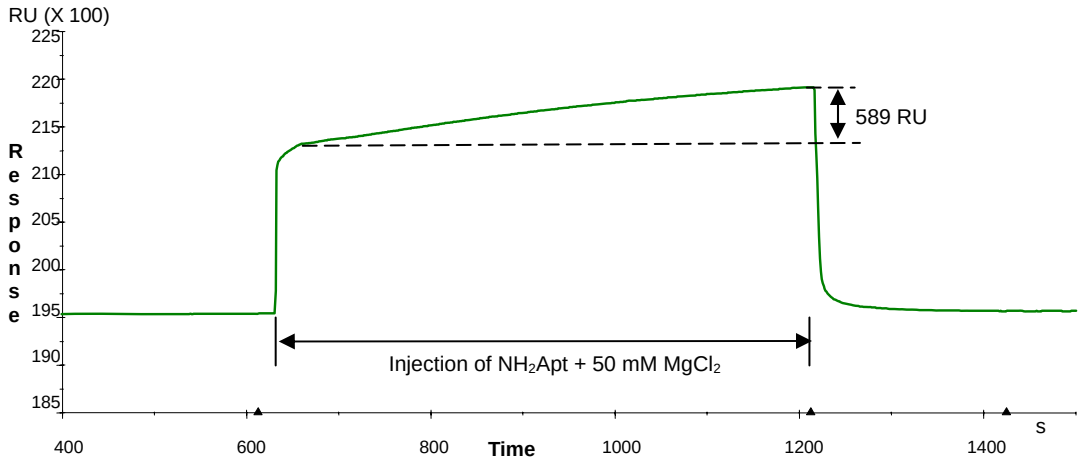

Figure 2.20: Sensorgram of a preconcentration trial for 3.6 μM NH_2Apt + 500 mM $MgCl_2$ in borate buffer (pH 8.5) containing 0.6 mM CTAB. The flow cell was an unmodified CM3 chip.

Table 2.3 summarizes the results of the preconcentration experiments with the exception of the $MgCl_2$ preconcentration experiments, which are summarized in table 2.4. The first two rows are the results for preconcentration (column 4) and immobilization

(column 5) trials for a 3.6 μM aptamer and 4.4 μM scrambled solution, respectively, in borate buffer (pH 8.5) containing 0.6 mM CTAB. The difference in the preconcentration level between the aptamer and the scrambled DNA is reflected in the immobilization level: the significantly higher preconcentration level for the scrambled sequence (344 RU) is correlated to a significantly higher immobilization level (1.65 ± 0.474 pmol/cm^2) for the scrambled sequence. The remaining preconcentration trials (rows 3-8) were all with DNA concentrations identical to the ones for rows one and two, and the DNA was dissolved in borate buffer containing 0.6 mM CTAB for rows 5-8. Rows 3 and 4 show that the preconcentration level increases significantly with a doubling of the CTAB concentration for the scrambled sequence, but the aptamer's preconcentration level is unaffected by this change. This result indicates that an increase in the CTAB concentration in the immobilization buffer would not affect the immobilization success for the aptamer and points to something other than simple electrostatic repulsions as the cause for the aptamer's lower attachment levels. Therefore, immobilization was not attempted for the aptamer with 1.2 mM CTAB (2X) in the buffer.

Preconcentration trials were performed for DNA solutions composed of 50% DMSO: one with the aptamer sequence (row 5) and one with the scrambled sequence (row 6). Again, the DMSO was added in order to denature the aptamer's 3D structure. The results show a significant increase in the preconcentration level (2581 RU and 2858 RU, respectively) for both DNA sequences but no DNA attachment. The increased preconcentration levels for both sequences are likely due to the association of the DMSO molecules with the sensor surface and not association of the DNA molecules with the sensor surface. Injections of a 5% DMSO solution and a 10% DMSO solution (identical composition to the immobilization buffer, without the DNA) resulted in a preconcentration level increase of 90.2 RU and 159.2 RU, respectively. Injections of the buffer with other modifiers (TMAC and $MgCl_2$) gave no increase in the preconcentration level. These results

indicate that the DMSO builds up on the sensor surface. This build-up gives a huge preconcentration level and may effectively block the sensor surface and prevent immobilization of the amine-appended DNA.

Row #	DNA	Modification	Preconc. Level (RU)	Immob. Level ($pmol/cm^2$)
1	Apt	None	50	0.16
2	Scram	None	344	1.65 ± 0.474
3	Apt	2X CTAB	45 ± 25	N/A
4	Scram	2X CTAB	1160 ± 256	N/A
5	Apt	50% DMSO	2581	0
6	Scram	50% DMSO	2858	0
7	Apt	Hybridized	387	0 (2 trials)
8	Apt	TMAC	0 (2 trials)	N/A

Table 2.3: Summary of preconcentration experimental results for a CM3 chip flow cell. The second column indicates the type of NH_2DNA. The third column gives any modifications in the immobilization buffer conditions or the DNA structure. All of the DNA concentrations were 3.6 μM or 4.4 μM (aptamer or scrambled, respectively) and the buffer composition was 100 mM borate buffer (pH 8.5) with 0.6 mM CTAB. The fourth column shows the change in the SPR signal during the injection (the preconcentration level). The fifth column indicates the amount of DNA immobilized (determined via hybridization assay), if it was attempted.

In another attempt to see if denaturing the aptamer would result in an increased level of immobilization, the aptamer was reacted with its complementary strand to form a hybridized (or duplexed) DNA. The preconcentration trial showed promise for this technique with an injection increase (above the bulk increase) of 387 RU (row 7). However, both immobilization attempts with this hybridized aptamer resulted in zero immobilization. These results indicate that the dsDNA was able to interact strongly with the carboxyl-modified gold surface, but something prevented the amide bond formation. It is likely that the appended amine was still able to interact with the O6 carbonyl groups of the guanine residues[47] and/or participate in cation-π interactions with base residues[46]; thereby remaining buried in the interior of the DNA's 3D structure and inaccessible for nucleophilic attack on

the activated, surface carboxyl groups. In retrospect, the addition of a magnesium-containing salt (like $MgCl_2$) to the dsDNA aptamer solution should have increased the attachment level because Mg^{2+} is known to distort the dsDNA helical structure by interacting strongly with the lone pair electrons on phosphate oxygens and the π systems of imidazole rings. The distortion of the dsDNA helical structure should cause a decrease in the amine interactions with the interior bases, freeing up the appended amine for reaction with the surface carboxyl groups.

The addition of a cationic species in the immobilization buffer met with limited success in attachment, but provided insight into the cause for the disparity between the attachment levels of the aptamer and scrambled sequences. The addition of the quaternary ammonium salt TMAC gave no increase in the baseline during the injection of the aptamer solution (after the initial increase due to the bulk refractive index change). This indicates that the quaternary ammonium cation does not sufficiently reduce any inhibitory electrostatic interactions nor can it stabilize the aptamer's stacked, G-quartet structure; therefore, the appended amine is not available for covalent attachment.

The addition of $MgCl_2$ to the immobilization buffer showed a markedly different result depending on the handling of the solutions. Table 2.4 shows a summary of the results for preconcentration experiments of DNA solutions containing $MgCl_2$. Rows 1 and 2 are the results for solutions of aptamer and scrambled sequence, respectively, that contain 500 mM $MgCl_2$ but no CTAB. The solution was mixed and allowed to incubate at room temperature for 3 hours prior to injection over the flow cell for preconcentration measurement. These trials were performed to determine if the addition of $MgCl_2$ alone (no CTAB) to the DNA solution caused an increase in DNA-surface interactions (signaled by a preconcentration level increase). The resulting preconcentration levels (91 and 139 RU, respectively) indicate that the $MgCl_2$ may increase the level of aptamer preconcentration compared to the addition of CTAB, but does not have the same ability to allow for equivalent preconcentration levels achieved for the scrambled sequence using CTAB (rows 1 and 2,

table 2.3, respectively). Immobilization experiments were not performed for DNA with this solution composition because of the low preconcentration levels. The remaining experiments listed in table 2.4 included 0.6 mM CTAB in the DNA solution in order to facilitate the DNA's approach to the flow cell surface.

Row	DNA	[$MgCl_2$] (mM)	Mixing Conditions	Preconc. Level (RU)	Immob. Level (pmol/cm^2)
1	Apt	500	No CTAB. Mixed 3 hrs. prior to injection.	91	N/A
2	Scram	500	No CTAB. Mixed 3 hrs. prior to injection.	139	N/A
3	Apt	500	Mixed 1 hr. prior to injection	83	N/A
4	Scram	500	Mixed 1 hr. prior to injection	85	N/A
5	Apt	500	Mixed 3 hrs. prior to injection	589	N/A
6	Scram	500	Mixed 3 hrs. prior to injection	133	N/A
7	Apt	50	Mixed 3 hr. prior to injection	99	N/A
8	Apt	50	Mixed, 95°C for 3 min. and then cooled slowly to room temp. prior to injection.	306 ± 101	0.34

Table 2.4: CM3 preconcentration results for $MgCl_2$ addition to the DNA solution. All of the DNA concentrations were 3.6 μM or 4.4 μM (aptamer or scrambled, respectively) and the buffer composition was 100 mM borate buffer (pH 8.5) with 0.6 mM CTAB (except rows 1 and 2). The second column indicates the type of NH_2DNA. The third column gives the concentration of the added $MgCl_2$. The fourth column describes the mixing conditions for combining the DNA with $MgCl_2$. The fifth column shows the change in the SPR signal during the injection (the preconcentration level). The sixth column indicates the amount of DNA immobilized, if it was attempted (N/A indicates that immobilization was not attempted).

Rows 3 and 4 show the results for aptamer and scramble sequence solutions, respectively, that were mixed with 500 mM $MgCl_2$ and allowed to incubate at room temperature for 1 hour prior to injection over the flow cell surface. Oddly, the preconcentration levels for both solutions were equivalent and close to the same value

achieved for the aptamer solution mixed with 500 mM $MgCl_2$ with no CTAB (row 1). In contrast, if the same aptamer solution was allowed to incubate at room temperature for 3 hours instead of 1 hour, a significant increase in the preconcentration level for the aptamer sequence resulted (row 5). Similar treatment of the scrambled sequence resulted in no improvement in the preconcentration level compared to the trial of scrambled sequence with $MgCl_2$ but without CTAB (row 2).

Row 7 shows the result of a preconcentration trial using 50 mM $MgCl_2$ instead of 500 mM $MgCl_2$. The solution was mixed and allowed to sit for 3 hours prior to injection over the flow cell. The result of this 10-fold decrease in $MgCl_2$ concentration (99 RU preconcentration level versus 589 RU preconcentration level for the 500 mM $MgCl_2$) indicates that the phenomenon responsible for the increase in the preconcentration level is dependent upon the Mg^{2+} ion concentration. Taken together with the results for the 500 mM $MgCl_2$ additions (specifically, the extended incubation time required for an increased preconcentration level), it appears that the action of the Mg^{2+} ions on the aptamer structure has very slow kinetics. An experiment was conducted to try to speed up the effect of the Mg^{2+} ions on the aptamer preconcentration level.

Row 8 shows the preconcentration and immobilization results for an aptamer mixture containing 50 mM $MgCl_2$ that was heated at 95°C for 3 minutes and then allowed to cool slowly to room temperature prior to injection onto the flow cell. The preconcentration results show an increase in the association of the DNA with the surface that approaches the level obtained for the scrambled sequence in borate buffer and 0.6 mM CTAB (row 2, table 2.3). In light of these results, an immobilization trial was attempted. The resulting attachment level was greater than two times the previous level attained for the aptamer: 0.34 pmol/cm^2 versus 0.16 pmol/cm^2. This result indicates that the denaturing of the aptamer's 3D structure (by heating at 95°C) accelerates the Mg^{2+}-aptamer interactions that free the appended amine for nucleophilic attack of the activated carboxyl groups. The combined

results for the $MgCl_2$ addition trials support the theory that kinetically slow but thermodynamically favorable interactions between the Mg^{2+} ions and the aptamer structure allow for the availability of the appended amine for an EDC-mediated reaction with surface carboxyl groups. A discussion about the plausible interactions that influenced the attachment of the aptamer to the gold substrate follows.

Cations are known to stabilize the 3D structure of aptamers and are often included in the selection buffer during the SELEX process for that specific purpose. An investigation into the stabilization of the anti-thrombin DNA aptamer's stacked, G-quartet structure by cations has shown that the order of stabilization is $Sr^{2+} > Ba^{2+} > K^{+} >> Rb^{+} > NH^{+}$. Na^{+}, Li^{+}, Mg^{2+} and Ca^{2+} ions also complex the aptamer structure, but the interactions are significantly weaker and the structures are only stable at very low temperatures (< 20°C). The specificity of the strongly stabilizing cations (Sr^{2+}, Ba^{2+}, K^{+}, Rb^{+} and NH^{+}) is attributed to an ionic radius that is optimal for sandwiching between the two stacked, G-quartets (1.3-1.5 Å) and coordinating with guanine O6 carbonyl groups. Other cations are either too big or too small to fit into the space and coordinate with the guanine bases.[47]

In the studies for attaching the aptamer and scrambled sequences to the carboxy-modified gold via an EDC-mediated amide bond the buffer composition was 100 mM sodium borate, pH 8.5 and the temperature during immobilization was ~25°C (room temp.). Under these conditions, the appended amine will be protonated (pK_a ~ 10 for primary alkyl amines) and is the strongest stabilizing cation available for the stacked, G-quartet structure of the aptamer. The long tether attaching the amine to the aptamer (12 carbons) may facilitate this interaction by allowing enough flexibility for the amine to assume the proper orientation for maximum interactions with the guanine bases. **The low attachment values obtained for the aptamer trials with borate buffer and CTAB (no other additives) are most likely due to the inability of most of the appended amines to attack the activated**

carboxyl groups because they were already involved in strong interactions with the guanine bases inside the aptamer's stacked, G-quartet structure.

The addition of the $MgCl_2$ to the DNA solutions (aptamer and scrambled) will result in similar cation-π and cation-lone pair electron interactions[46] for both of the DNA sequences but with diametrical consequences. The scrambled sequence showed a significant decrease in the preconcentration level when $MgCl_2$ was added to the DNA solution. This result is most likely due to the Mg^{2+} cation forming stabilizing interactions between the DNA bases and the phosphate backbone oxygens that create a more compact and structured 3D DNA configuration.[46] A well defined and stable scrambled DNA structure may facilitate amine-DNA interactions that inhibit surface-amine interactions. On the other hand, the Mg^{2+} cation destabilized the aptamer's 3D structure by the same type of interactions with the DNA phosphate oxygens and base π systems. These interactions will disrupt the aptamer's stacked, G-quartet structure in the same way that a double-stranded DNA's structure will be disrupted: by pulling the bases out of the interior region of the 3D DNA structure.[46] In doing so, the strength of the amine's stabilizing interactions with the aptamer will decrease and the amine will be free to interact with the surface carboxyl groups. The increase in the amine's interactions with the carboxyl groups do not approach the level that the scrambled sequence experiences because only a small percentage of the aptamer structures are perturbed enough to release the otherwise trapped amine. A simple solution to this dilemma should be the addition of potassium ions to the DNA solution. The aptamer's stacked, G-quartet will be stabilized preferentially by the K^+ ions, thereby releasing the amine to react with the surface carboxyl groups.

2.3.3.2 Affinity Attachment

The results for the affinity attachment of the 5' biotin-appended ssDNA to the SA chip (CM3 chip with streptavidin attached) showed that the levels of aptamer and scrambled

sequence immobilized were comparable and that this attachment strategy allowed for a greater amount of DNA attachment than the covalent strategies. Figure 2.21 is a plot of the immobilization level versus the amount of 5' biotin DNA injected for the aptamer and scrambled sequences. The data indicate that the amount of aptamer immobilized is proportional to the amount of 5' biotin aptamer injected; this appears to also be true for the scrambled sequence, but a limited number of data points were acquired since the focus of the study was on the immobilization of the aptamer sequence. Oddly, the immobilization level appears to be higher for the aptamer sequence than the scrambled sequence when equal amounts of 5' biotin DNA were injected. The cause of this result was not investigated because it was deemed to be outside the scope of the investigations since it was possible to achieve immobilization levels of the aptamer that were comparable to previously reported ssDNA attachment values ($\leq$ 30 pmol/cm^2).[10, 34, 48-53]

Some comments regarding the affinity attachment of the ssDNA are appropriate at this time. The maximum level of aptamer sequence attached was 13.8 pmol/cm^2 for 1.49 picomoles of 5' biotin aptamer applied. The maximum level of scrambled sequence attached was 18.6 pmol/cm^2 for 35.1 picomoles of 5' biotin scrambled applied. Investigations were not conducted in order to determine the maximum loading for either sequence since the optimal loading capacity (the aptamer loading level at which full activity is retained) was determined to be at a significantly lower attachment level (~ 4.5 - 6 pmol/cm^2, see chapter III). It was possible to increase the amount of ssDNA attached to a flow cell multiple times after an initial immobilization event; however, the attachment level was significantly reduced after about 3 or 4 immobilization trials and after numerous injections of complementary DNA and thrombin over the flow cell surface.

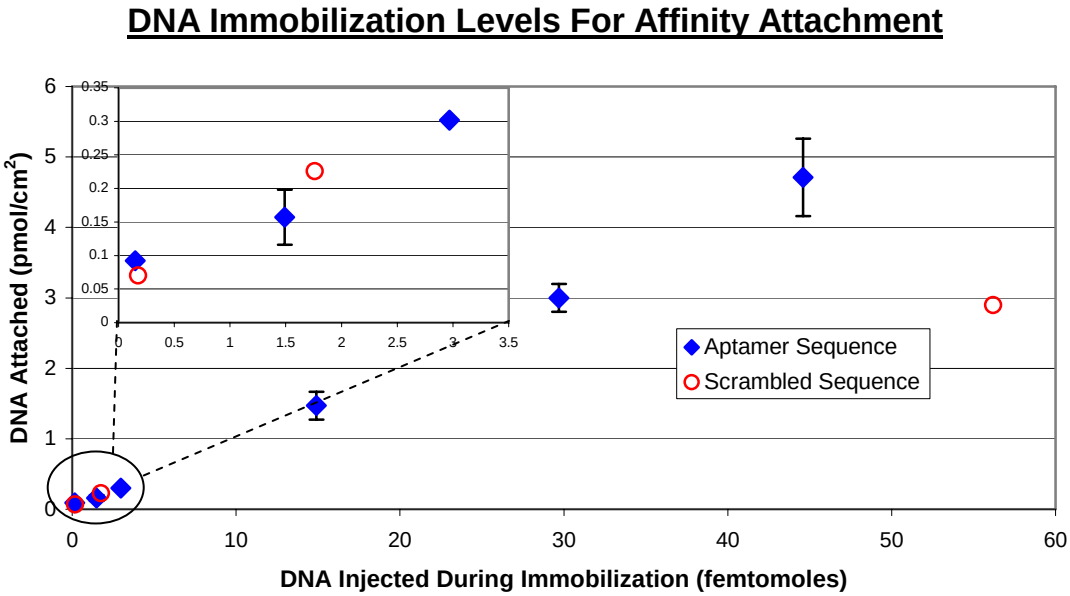

Figure 2.21: DNA immobilization levels for affinity attachment to the SA sensor chip. The lower values are shown in an expanded view in the inset chart.

2.3.4 Conclusions For Gold Attachment

The covalent attachment strategies for the gold substrate produced mixed results. Neither the aptamer nor the scrambled sequence were immobilized to the C1 or CM3 chip by an EDC-mediated phosphoramide bond between a surface-appended amine and a 5' phosphate on the DNA. The detection limit of the SPR instrument (20 fmol/cm^2) may have prevented the detection of low amounts of immobilized DNA; however, if any DNA was immobilized to these sensor chips via the phosphoramide bond, it is too low to be analytically useful. The amide bond method of immobilization, on the other hand, did result in immobilized DNA that could be used in a detection system.

The amide bond immobilization strategy resulted in attached DNA on both the C1 and the CM3 chips. However, there was a significant difference between the level of aptamer sequence and scrambled sequence immobilized on a particular substrate. In fact, attempts were unsuccessful for immobilization of the aptamer on the C1 surface and resulted in

significantly reduced levels for the CM3 chip (160 fmol/cm^2 compared to 1.31 pmol/cm^2 for the scrambled sequence). It was possible to increase the aptamer attachment level to 340 fmol/cm^2 on the CM3 chip through the addition of Mg^{2+} ions to the aptamer injection solution.

The $MgCl_2$ addition to the aptamer solution helped to increase the level of aptamer immobilization by destabilizing the amine-DNA interactions, thereby freeing up the appended amine to react with the activated carboxyl group. Investigations into the difference in attachment levels between the aptamer sequence and the scrambled sequence suggest that the 5'-appended amine interacts strongly with the bases of the aptamer. These amine/aptamer interactions are favored because of their stabilizing effect on the aptamer stacked, G-quartet structure (especially in the absence of any other strongly stabilizing ions). The amine is unavailable for nucleophilic attack on the activated surface carboxyl groups because it is buried inside the aptamer's structure between the two G-quartets. NMR and/or X-ray crystallography studies could potentially confirm this theory.

Charge repulsion between the negatively-charged carboxylated surface and the phosphate backbone of the ssDNA is a significant factor in the immobilization process. These repulsive forces inhibited the immobilization process for the amide bond attachment strategy by not allowing the reactive moieties to achieve the necessary proximity for nucleophilic attack of the activated carboxyl groups by the DNA-appended amine. This limitation was overcome by the addition of the cationic surfactant CTAB; which has been shown to form positively charged micelles in solution[39] that aid in the attachment of ssDNA to a negatively-charged surface.[35] It was unnecessary to add CTAB to the phosphoramide bond attachment trials since the oppositely charged reactive species (positively charged amine on the sensor surface and negatively charged phosphate on the DNA) allowed for the close approach of the DNA to the sensor surface. CTAB was also not needed in the affinity attachment method.

Both the aptamer sequence and the scrambled sequence were readily attached to the gold substrate via affinity interactions: streptavidin/biotin. The biotin was appended to the DNA with a 12 carbon linker through the 5' end; the streptavidin was covalently immobilized to the solution-like CM3 sensor chip via standard amide bond chemistry. The streptavidin-modified CM3 chip has a relatively neutral charge; thus, the negatively charged biotin-appended DNA can approach the surface close enough for establishment of the strong biotin/streptavidin affinity interaction. This immobilization strategy was the best suited to attachment of the anti-thrombin DNA aptamer because the level of attachment was controllable and the packing density for the aptamer was similar to literature values for immobilization of ssDNA (13.8 pmol/cm^2 versus $\leq$ 30 pmol/cm^2).[10, 34, 48-53]

2.4 Conclusions For Attachment Of Aptamers To Surfaces

As with the attachment of any moiety to a surface, aptamers have certain properties governing their efficient and effective attachment. The attachment of ssDNA for use in hybridization assays has been studied extensively and there are a multitude of methods available for their immobilization.[17, 19, 26, 28, 29, 32, 40, 54-64] Even though DNA aptamers are similar to ssDNA used for hybridization assays, they can differ significantly in one aspect: their 3D structure. Aptamers' somewhat unique 3D structures may be a prominent factor to consider when trying to effectively attach DNA aptamers to surfaces.

This structural influence was obvious from the results of the attachment experiments of the DNA to gold via amide bond formation: the scrambled sequence's attachment level was about 5 times as great as the aptamer sequence's attachment level (CM3 results). There was no difference for the EDC-mediated phosphoramide bond to silica, nor was there any distinction for the PDC-mediated attachment to silica. The amine linker used for the PDC-mediated attachment to silica did not interact strongly with the aptamer bases (as evidenced by the equivalent attachment levels for the aptamer and scrambled sequences),

but it was an influential factor in the EDC-mediated amide bond attachment to gold. The primary reason for the difference in the appended amine's interaction with the aptamer lies in the cations present in the DNA buffer solution: the presence of stacked, G-quartet-stabilizing K^+ ions decreased the amine-aptamer interactions (silica attachment trials); Na^+ ions aren't good G-quadraplex-stabilizing ions so the amine interacted strongly with the aptamer (gold attachment trials)- stabilizing the aptamer's compact structure but also inhibiting the amines ability to form an amide bond with the surface carboxyl groups. The linker length appending the amine to the DNA may play a role in the level of interactions between the amine moiety and the aptamer- a short linker (e.g.- 3-carbon) may diminish or eliminate any 3D-stabilizing interactions because the amine won't be able to extend into the aptamer's interior.

Several different linker lengths may have influenced the attachment efficacy for the ssDNA to the two substrates. There was little to no DNA attached for the phosphoramide bond experiments (silica and gold, respectively) and they had identical linker characteristics: the phosphate on the 5' end of the DNA was directly attached to the DNA (no linker) and the reactive amine moiety was attached to the substrate through a 3-carbon linker. When a linker separated the reactive moiety from the DNA (as in the thioamide bond attachment to silica and the amide bond attachment to gold), the level of attachment increased significantly. The sum of these results points to the need for a reactive moiety that is extended out into the solution away from the DNA in order to facilitate bond formation. However, once the reactive moiety is separated from the DNA by a linker, the attachment levels are governed by a different factor: the availability of reactive moieties on the substrate and the DNA.

2.5 References

1 Smith, D.; Collins, B. D.; Heil, J.; Koch, T. H. *Mol. Cell. Proteomics* **2003,** *2*, 11-18.
2 Lee, M.; Walt, D. R. *Anal. Biochem.* **2000,** *282*, 142-146.
3 Potyrailo, R. A.; Conrad, R. C.; Ellington, A. D.; Hieftje, G. M. *Anal. Chem.* **1998,** *70*, 3419-3425.
4 Clark, S. L.; Remcho, V. T. *J. Separ. Sci.* **2003,** *26*, 1451-1454.
5 Kotia, R. B.; Li, L.; McGown, L. B. *Anal. Chem.* **2000,** *72*, 827-831.
6 Schmid, B.; Hoffmann, D.; Wefing, S.; Schnaible, V.; Quandt, E.; Tewes, M.; Famulok, M. In *U.S. Pat. Appl. Publ.*; (Germany).: Us, 2002, pp 6 pp.
7 Cho, S.; Lee, S.-H.; Kim, Y.-K.; Kim, B.-G. *Proc. Micro Tot. Anal. Sys.* **2001**, 601-602.
8 Nakamura, C.; Kobayashi, T.; Miyake, M.; Shirai, M.; Miyakea, J. *Mol. Cryst. Liq. Crys. A* **2001,** *371*, 369-374.
9 McCauley, T. G.; Hamaguchi, N.; Stanton, M. *Anal. Biochem.* **2003,** *319*, 244-250.
10 Liss, M.; Petersen, B.; Wolf, H.; Prohaska, E. *Anal. Chem.* **2002,** *74*, 4488-4495.
11 Lin, Y.; Heil, J.; Jayasena, S. In *PCT Int. Appl.*; (Gilead Sciences, Inc., USA).: Wo, 2001, pp 47 pp.
12 Deng, Q.; German, I.; Buchanan, D.; Kennedy, R. T. *Anal. Chem.* **2001,** *73*, 5415-5421.
13 Romig, T. S.; Bell, C.; Drolet, D. W. *J. Chrom., B* **1999,** *731*, 275-284.
14 Michaud, M.; Jourdan, E.; Villet, A.; Ravel, A.; Grosset, C.; Peyrin, E. *J. Am. Chem. Soc.* **2003,** *125*, 8672-8679.
15 Michaud, M.; Jourdan, E.; Ravelet, C.; Villet, A.; Ravel, A.; Grosset, C.; Peyrin, E. *Anal. Chem.* **2004,** *76*, 1015-1020.
16 Kumar, P. K. R.; Yamamoto, R. In *Jpn. Kokai Tokkyo Koho*; Agency of Industrial Sciences and Technology: Jp, 2001, pp 19 pp.
17 Ghosh, S. S.; Musso, G. F. *Nucleic Acids Res.* **1987,** *15*, 5353-72.
18 Guo, Z.; Guilfoyle, R. A.; Thiel, A. J.; Wang, R.; Smith, L. M. *Nucleic Acids Res.* **1994,** *22*, 5456-65.
19 Henke, L.; Piunno, P. A. E.; McClure, A. C.; Krull, U. J. *Anal. Chim. Acta* **1997,** *344*, 201-213.
20 Ho, N. W. Y.; Gilham, P. T. *Biochemistry-USA* **1967,** *6*, 3632-9.
21 Ivanovskaya, M. G.; Gottikh, M. B.; Shabarova, Z. A. *Nucleos. Nucleot.* **1987,** *6*, 913-34.
22 Rasmussen, S. R.; Larsen, M. R.; Rasmussen, S. E. *Anal. Biochem.* **1991,** *198*, 138-42.
23 Sambrook, J.; Russell, D. *Molecular Cloning: A Laboratory Manual*, 3rd ed.; Cold Spring Harbor Laboratory Press: Cold Spring Harbor, 2001.
24 Ulman, A. *An introduction to ultrathin organic films: from Langmuir-Blodgett to self-assembly*; Academic Press: Boston, 1991.
25 Chu, B. C. F.; Wahl, G. M.; Orgel, L. E. *Nucleic Acids Res.* **1983,** *11*, 6513-29.
26 O'Donnell-Maloney, M. J.; Tang, K.; Koester, H.; Smith, C. L.; Cantor, C. R. *Anal. Chem.* **1997,** *69*, 2438-2443.
27 Jenison, R.; Yang, S.; Haeberli, A.; Polisky, B. *Nat. Biotechnol.* **2001,** *19*, 62-5.
28 Lin, Z.; Strother, T.; Cai, W.; Cao, X.; Smith, L. M.; Hamers, R. J. *Langmuir* **2002,** *18*, 788-796.
29 Kumar, A.; Larsson, O.; Parodi, D.; Liang, Z. *Nucleic Acids Res.* **2000,** *28*, e71, ii-vi.
30 Chrisey, L. A.; Lee, G. U.; O'Ferrall, C. E. *Nucleic Acids Res.* **1996,** *24*, 3031-3039.
31 Strother, T.; Hamers, R. J.; Smith, L. M. *Nucleic Acids Res.* **2000,** *28*, 3535-3541.
32 Rogers, Y.-H.; Jiang-Baucom, P.; Huang, Z.-J.; Bogdanov, V.; Anderson, S.; Boyce-Jacino, M. T. *Anal. Biochem.* **1999,** *266*, 23-30.
33 Clark, S. L.; Remcho, V. T. *Anal. Chem.* **2003,** *75*, 5692-5696.
34 Boncheva, M.; Scheibler, L.; Lincoln, P.; Vogel, H.; Aakerman, B. *Langmuir* **1999,** *15*, 4317-4320.
35 Sjodin, A.; Sjobom, H.; Karlsson, R.;; Biacore AB: Uppsala, Sweden, 2003.

36 Laird-Offinga, I.;; Biacore Corporation, 2002.
37 Bamdad, C. *Biophys. J.* **1998,** *75*, 1997-2003.
38 Johne, B.; Gadnell, M.; Hansen, K. *J. Immunol. Meth.* **1993,** *160*, 191-198.
39 Sepulveda, L.; Cortes, J. *J. Phys. Chem.- US* **1985,** *89*, 5322-4.
40 Huang, E.; Zhou, F.; Deng, L. *Langmuir* **2000,** *16*, 3272-3280.
41 Wood, S. J. *Microchem. J.* **1993,** *47*, 330-7.
42 Wang, K. Y.; McCurdy, S.; Shea, R. G.; Swaminathan, S.; Bolton, P. H. *Biochemistry USA* **1993,** *32*, 1899-1904.
43 Macaya, R. F.; Schultze, P.; Smith, F. W.; Roe, J. A.; Feigon, J. *Proc Nat Acad Sci USA* **1993,** *90*, 3745-3749.
44 Padmanabhan, K.; Padmanabhan, K. P.; Ferrara, J. D.; Sadler, J. E.; Tulinsky, A. *J. Biol. Chem.* **1993,** *268*, 17651-4.
45 Bock, L. C.; Griffin, L. C.; Latham, J. A.; Vermaas, E. H.; Toole, J. J. *Nature* **1992,** *355*, 564-566.
46 McFail-Isom, L.; Shui, X.; Williams, L. D. *Biochemistry-USA* **1998,** *37*, 17105-17111.
47 Kankia, B. I.; Marky, L. A. *J. Am. Chem. Soc.* **2001,** *123*, 10799-10804.
48 Huang, E.; Satjapipat, M.; Han, S.; Zhou, F. *Langmuir* **2001,** *17*, 1215-1224.
49 Levicky, R.; Herne, T. M.; Tarlov, M. J.; Satija, S. K. *J. Am. Chem. Soc.* **1998,** *120*, 9787-9792.
50 Peterlinz, K. A.; Georgiadis, R. M.; Herne, T. M.; Tarlov, M. J. *J. Am. Chem. Soc.* **1997,** *119*, 3401-3402.
51 Nelson, B. P.; Grimsrud, T. E.; Liles, M. R.; Goodman, R. M.; Corn, R. M. *Anal. Chem.* **2001,** *73*, 1-7.
52 Satjapipat, M.; Sanedrin, R.; Zhou, F. *Langmuir* **2001,** *17*, 7637-7644.
53 Sauthier, M. L.; Carroll, R. L.; Gorman, C. B.; Franzen, S. *Langmuir* **2002,** *18*, 1825-1830.
54 Benters, R.; Niemeyer, C. M.; Drutschmann, D.; Blohm, D.; Woehrle, D. *Nucleic Acids Res.* **2002,** *30*, e10/1-e10/7.
55 Zammatteo, N.; Jeanmart, L.; Hamels, S.; Courtois, S.; Louette, P.; Hevesi, L.; Remacle, J. *Anal. Biochem.* **2000,** *280*, 143-150.
56 Voss, U. B.; Malcolm, A. D. B. *Biochem. Soc. Trans.* **1988,** *16*, 367-8.
57 Beaucage, S. L. *Curr. Trends Med. Chem.* **2001,** *8*, 1213-44.
58 Zhang, G.; Zhou, Y.; Wu, X.; Yuan, J.; Ren, S. *J. Tongji Med. Univ.* **2000,** *20*, 89-91.
59 Lin, X. Q.; Miao, Q.; Jin, B. K. *Chin. Chem. Lett.* **1999,** *10*, 157-160.
60 Chrisey, L. A.; O'Ferrall, C. E.; Spargo, B. J.; Dulcey, C. S.; Calvert, J. M. *Nucleic Acids Res.* **1996,** *24*, 3040-3047.
61 Moss, L. G.; Moore, J. P.; Chan, L. *J. Biol. Chem.* **1981,** *256*, 12655-8.
62 Caruso, F.; Rodda, E.; Furlong, D. N.; Niikura, K.; Okahata, Y. *Anal. Chem.* **1997,** *69*, 2043-2049.
63 Lund, V.; Schmid, R.; Rickwood, D.; Hornes, E. *Nucleic Acids Res.* **1988,** *16*, 10861-80.
64 Herne, T. M.; Tarlov, M. J. *J. Am. Chem. Soc.* **1997,** *119*, 8916-8920.

Chapter 3: Anti-Thrombin Aptamer Optimal Packing Density

3.1 Introduction

The amount of molecular recognition element per unit area (i.e.- the packing density) can significantly impact the effectiveness of a heterogeneous assay. The optimal packing density is the maximum packing density of the molecular recognition element for which 100% activity is retained. Studies have been conducted to determine the optimal packing density for antibodies[1-3] and ssDNA used in hybridization assays.[4-11] There has been no report of a study regarding the optimal packing density for aptamers. In fact, very few studies involving immobilized aptamers have even attempted to measure the packing density of the attached aptamers.[12-14]

Aptamers have physico-chemical characteristics that should place their optimal packing density values somewhere between the optimal values for ssDNA and small proteins. Like ssDNA, aptamers are easily immobilized through a single attachment point, denaturing conditions during the attachment process should not be problematic to their future activity and they have a fairly low molecular weight (5-15 kD). Unlike ssDNA, but like proteins, aptamers have a 3D structure (especially when they are bound to their cognate ligand) that may have a larger hydrodynamic volume than that of dsDNA. And, like proteins, some aptamers must be able to change their conformation upon binding. A single attachment point and a low molecular weight for aptamers suggests that a packing density level close to non-aptamer ssDNA would be expected; however, the 3D structural constraints of aptamers will force the optimal packing density down towards values that are necessary for small proteins to be active.

A linear response over a wide range of analyte concentrations, high sensitivity to changes in analyte concentration and low non-specific binding interactions are desirable characteristics for a quantitative analytical assay. A high level of aptamer packing while

maintaining 100% of the immobilized aptamer function will allow for the greatest linear response, highest sensitivity and low non-specific binding.[2] A determination of the aptamer ability to bind thrombin (the measure of the aptamer 'activity') after being immobilized was the first step in this study. Immobilized aptamer activity analysis was performed for the aptamers attached to silica and the aptamers attached to gold (both covalent and affinity attachment). Due to activity analysis difficulties for the silica-appended aptamer and immobilization difficulties for the covalent attachment to gold, the optimal packing density determination for the anti-thrombin DNA aptamer was performed using the aptamer immobilized to the gold SPR chips via biotin-streptavidin interactions.

3.2 Materials And Methods

3.2.1 Materials

Binding studies for the aptamer attached to the silica beads were performed with beads that had DNA attached via a thioamide bond (PDC-mediated attachment). Binding studies for the aptamer attached to the gold substrate used either the CM3 chip with the DNA immobilized via an amide bond or the SA chip with DNA immobilized using affinity attachment. The Sunsphere NP-100 silica beads were from AGA Chemicals, Inc. (Charlotte, NC) and the gold substrate SPR sensor chips were from Biacore Corporation (Piscataway, NY). The Sypro-Ruby protein gel stain and the SDS-PAGE Protein M.W. Standards- Broad Range were purchased from Bio-Rad (Hercules, CA). All of the DNA was purchased from Integrated DNA Technologies, Inc. (Coralville, IA). DNA immobilization to the two different substrates is described in detail in chapter 2 of this work.

The binding buffer for the silica bead trials was 100 mM potassium phosphate, pH 7.4. The gold substrate trials used the same potassium phosphate buffer with 0.005% P20 surfactant (Biacore, Piscataway, NY) added. The surface regeneration solution for the SPR experiments was a 7 M urea aqueous solution. All of the solutions used in the gold

substrate experiments were filtered through a 0.22 μm filter and deaerated before injection into the SPR instrument.

Human α-thrombin (factor IIa) was purchased from Enzyme Research Laboratories (South Bend, IN). Porcine Pancreas Elastase, lyophilized type IV was purchased from Sigma (St. Louis, MO). Both of these reagents were aliquoted into single-use volumes and stored at -85°C until they were used.

3.2.2 Methods

The attachment level for the aptamer to the silica beads was determined by radio-labeling the DNA with ^{32}P (described in chapter 2). The attachment level for the aptamer to the SPR chips (gold substrate) was determined via hybridization assays (also described in chapter 2).

The activity of the immobilized anti-thrombin aptamer was evaluated by determining its ability to bind Human α-thrombin (factor IIa) (thrombin). The negative control for the analyte was Porcine Pancreas Elastase (elastase). Elastase was chosen as the negative control because it is a serine protease that has a similar molecular weight and isoelectric point (pI) to thrombin.

The method for determining the level of analyte binding was substrate dependent. For the silica beads, an incubate, wash, read-type format was used. In this scheme the aptamer-attached beads were slowly rotated at room temperature for 1 hour with a 10-fold excess of thrombin (with respect to the level of DNA on the beads) in binding buffer. After the incubation with thrombin, the reaction tube was centrifuged and the supernatant removed. The beads were washed 2 times with 50 μL of binding buffer and then analyzed for bound thrombin.

There were two methods attempted for the quantification of the level of thrombin bound to the aptamer immobilized on silica. The first method utilized the BCA assay (Pierce Biotechnology, Rockford, IL) using the 96-well plate protocol. The beads were incubated in

a microcentrifuge tube with the color-forming reagents to facilitate mixing. The absorbance reading at 562 nm was performed on a υ_{max} plate reader from Molecular Devices Corporation (Menlo Park, CA). The second method utilized a 12% discontinuous denaturing polyacrylamide gel (12% SDS-polyacrylamide gel). The washed beads were combined with 10 μL of SDS-loading buffer, heated for 10 minutes at 95°C, and then loaded onto a 12% SDS-polyacrylamide gel. Sypro-Ruby gel stain was used to visualize the protein on the gel and densitometry readings of the protein bands were performed using OptiQuant Image Analysis software (Packard Instruments Company, Meriden, CT). A standard curve of thrombin on a 12% SDS-polyacrylamide gel was used for quantification of the thrombin bound to the beads.

The Biacore 3000 SPR instrument was used to determine thrombin binding levels for the aptamer attached to the gold substrate. 60 microliters of thrombin in binding buffer was injected onto the SPR instrument at a flow rate of 30 μL/min using the Kinject mode. Binding buffer was used as the run buffer and a reference cell with scrambled sequence immobilized was used for a background subtraction. A 15 μL injection of 7 M urea was used to remove any remaining bound thrombin from the flow cell surface. The amount of thrombin bound by the immobilized aptamer was determined from a reference-subtracted plot.

The maximum response to an analyte expected for a flow cell (R_{max}) is based on the level of receptor molecule immobilized. The equation to determine R_{max} is: R_{max} = RU of immobilized receptor X $\frac{(analyte\ \ M.W.)}{(receptor\ \ M.W.)}$.[15] For this study's receptor/analyte combination, the molecular weight used for the aptamer was 5000 g/mol and the molecular weight used for thrombin was 37,000 g/mol. In other words, the maximum response to thrombin (reference cell subtracted) expected for an SPR chip that has 18 RU of aptamer immobilized would be 133 RU.

The optimal packing density for the immobilized anti-thrombin aptamer was determined using the aptamer attached to a gold substrate via affinity interactions. A range of aptamer packing densities were used to determine the packing density at which the activity of the immobilized aptamer dropped below 100%.

3.3 Results And Discussion

3.3.1 Activity Of Immobilized Aptamers

3.3.1.1 Silica

The BCA assay method for determining the amount of thrombin associated with the aptamer-attached silica beads was incompatible with the amine-modified silica beads. Calibration curves for thrombin and elastase free in solution were readily achieved. A thrombin calibration curve gave absorbance readings of 0.0064 to 0.1079 for thrombin levels between 1.64 and 21.3 picomoles, respectively. The range of thrombin values used in this calibration curve bracketed the expected thrombin binding level for the aptamer-immobilized beads. However, the absorbance readings for the silica beads were consistently between 0.2000 and 0.4500. It didn't matter if the beads were just ethanolamine-blocked (no DNA immobilized and not exposed to thrombin), ethanolamine-blocked beads exposed to thrombin, scramble-immobilized beads exposed to thrombin or aptamer-immobilized beads exposed to thrombin- the absorbance readings were always between 2 and 10 times as great as they should have been based on the aptamer packing density for a particular set of beads. These results indicate that primary amines present on the aminosiloxane-modified silica beads gave a color change with the BCA assay that overwhelmed any signal from bound thrombin. In light of these results a second technique for quantifying the thrombin binding level to the aptamer-modified silica beads was pursued.

Gel electrophoresis was the second technique used for detecting binding of thrombin to the DNA-attached silica beads. A gel of a standard curve of thrombin is shown in figure

3.1. Lanes 1 through 8 are incremental thrombin samples ranging from 0 to 70 picomoles, respectively. Lane 9 shows the molecular weight reference ladder produced by loading the SDS-PAGE Protein M.W. Standards- Broad Range sample onto the gel. The thrombin bands are located at the correct R_f value for a 37 kD protein.

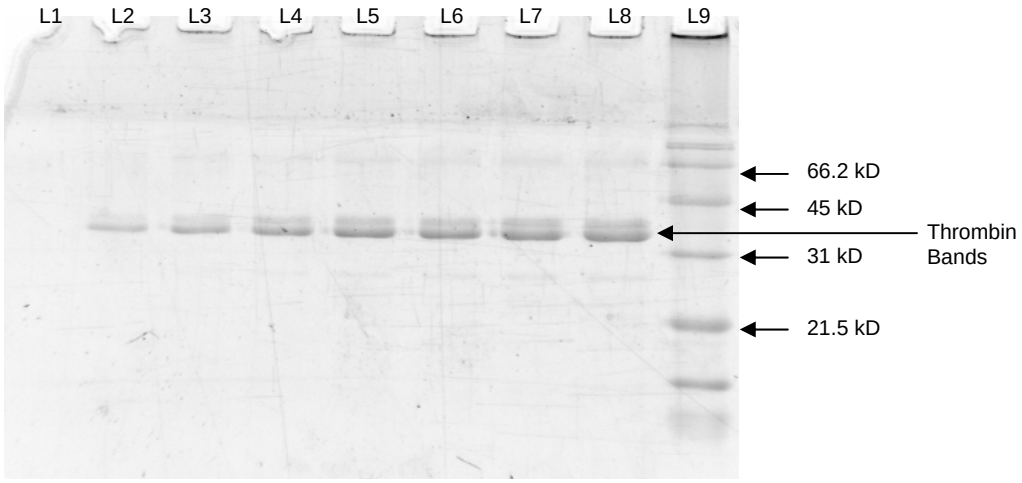

Figure 3.1: Standard curve for thrombin on a 12% SDS-polyacrylamide gel.

Initial experiments utilized beads that had a total of between 10 and 100 picomoles of DNA attached (aptamer or scrambled sequence). The gels for these experiments showed no bands for the lanes in which beads that had been exposed to thrombin were loaded- indicating that the immobilized aptamer was not binding the thrombin or too little thrombin was bound to the aptamer-immobilized beads to detect by this method. According to the vendor, Sypro-Ruby can detect as low as 1-10 ng of protein on a gel- this corresponds to between 0.03 and 0.3 picomoles for thrombin. Because the stain is sufficiently sensitive enough to detect the levels of thrombin expected to be associated with the aptamer-modified beads, an experiment was performed to determine if the unattached amine-appended aptamer could bind thrombin.

Figure 3.2 shows the results for a gel-shift assay designed to evaluate the binding ability of various forms of the scrambled and aptamer DNA used in these experiments. Under the electrophoresis conditions, thrombin should have no or limited mobility through

the gel (its pI and the gel pH will render it effectively uncharged) and the DNA should have a high level of mobility through the gel. Therefore, thrombin that was not associated with any DNA should not migrate into the gel but remain at the top. Thrombin that was associated with DNA should migrate into the gel because of its co-migration with the associated DNA. DNA that did not associate with thrombin should migrate to the bottom of the gel; whereas, DNA that was associated with thrombin would be retarded in its migration and would not get as far into the gel as the free DNA. The results of the experiment proved these predictions to be true.

The DNA was radio-labeled with ^{32}P as described in chapter 2 and the thrombin was detected with Sypro-Ruby stain. Table 3.1 gives the composition of each of the 9 samples used in the experiment. All samples were dissolved in binding buffer. Upon preparation of the samples, they were allowed to stand at room temperature for 30 minutes in order to allow for reaction with any thrombin that was present. The samples (except lane 5) were then combined with 2 μL of a 6X non-denaturing loading dye and loaded onto a 10% native (non-denaturing) polyacrylamide gel. Sample 5 (a.k.a.- lane 5) was combined with 4 μL of an SDS gel-loading buffer (denaturing), heated for 5 minutes at 95 °C and then loaded onto the above mentioned gel. The purpose of the native gel conditions was to allow any DNA-thrombin interactions to persist throughout the gel electrophoresis, thereby retarding the migration of the complex compared to the migration of the uncomplexed DNA. Sample 5 was treated with the denaturing loading buffer in order to confirm the effectiveness of the SDS for dissociating the aptamer-thrombin complex.

The results of staining the gel with Sypro-Ruby gel stain are shown in figure 3.2A. Sypro-Ruby is a stain that is specific for protein, in this case thrombin. Lane 1, which had no thrombin in the reaction tube, shows no band in the lane. Lanes 2-7 show bands corresponding to thrombin at the top of the gel. The thrombin bands in lanes 2-4, 6 and 7 extend into the gel and are somewhat disperse; this indicates that the thrombin interacted

with the DNA and were pulled into the gel by the DNA's migration. In contrast, the thrombin band in lane 5 is very compact and appears to be sitting on the bottom of the well (i.e.- the very top of the gel); this indicates that the thrombin was not interacting with the DNA and, therefore, it did not migrate into the gel during the electrophoresis. Lanes 8 and 9 did not contain thrombin in the sample so the lack of a band in each of these lanes is expected.

Figure 3.2B shows the results of the phospho-imaging scan of the gel by a Packard Cyclone Phosphor-imager (Packard Instruments Company, Meriden, CT). The spots in this gel image represent the location of radio-labeled DNA on the gel. In lane 1 all of the aptamer sequence is concentrated at the bottom of the gel- this is expected since there wasn't any thrombin present to retard its migration. Lanes 2, 3, 4 and 6 show aptamer near the top of the gel (mirroring the thrombin location in figure 3.2A), smearing throughout the middle of the gel, a band retarded about 1.5 cm from the bottom of the gel and then varying amounts of aptamer at the very bottom of the gel. The aptamer near the top of the gel is aptamer that remained bound to the thrombin during the electrophoresis. The aptamer that is above the bottom of the gel by about 1.5 cm was retarded because of interactions with the thrombin during the electrophoresis. Note that the intensity of these bands correlate to the ratio of thrombin to aptamer: the greater the thrombin (T) to aptamer (A) ratio, the less intense this band (lane 2: $T > A$; lane 4: $T < A$). The bottom bands on the gel for these lanes corresponds to aptamer that was free to migrate without interacting with the thrombin during the electrophoresis. The smearing in these lanes is possibly due to retarding interactions with thrombin in which the thrombin actually co-migrated with the aptamer further into the gel than the Sypro-Ruby stain indicates. It is quite possible that the thrombin level in this region was below the limit of detection for the Sypro-Ruby. The DNA in lanes 5, 7, 8 and 9 is all at the bottom of the gel- indicating no retardation in mobility due to interactions with thrombin during the electrophoresis. The result for lane 7 in figure B seems perplexing when compared with the lane 7 result in figure A: the thrombin appears to have co-migrated with the amine-appended scrambled sequence into the gel. Perhaps the

somewhat linear scrambled sequence (at least compared to the aptamer sequence) surrounded the thrombin (like SDS is reported to do) and aided its migration into the gel, but the scrambled sequence DNA's migration was not impeded by this phenomenon.

Lane #	DNA Type	Thrombin Added?	Thrombin to Aptamer Ratio
1	Apt	No	N/A
2	Apt	Yes	2:1
3	Apt	Yes	1:1
4	Apt	Yes	1:2
5	Apt	Yes	1:1
6	Apt-NH_2	Yes	1:1
7	Scram-NH_2	Yes	1:1
8	Apt-NH_2	No	N/A
9	Scram-NH_2	No	N/A

Table 3.1: Composition of each sample used in the gel-shift assay. Apt-NH_2 and Scram-NH_2 represent the 3' amine-modified aptamer sequence and the 3' amine-modified scrambled sequence, respectively.

3.2A

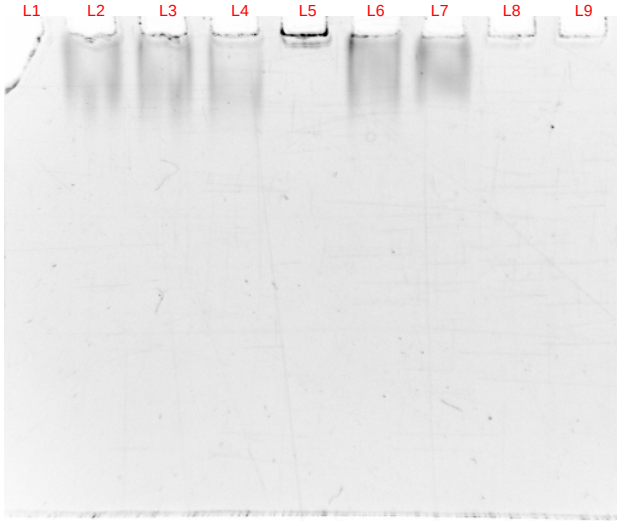

3.2B

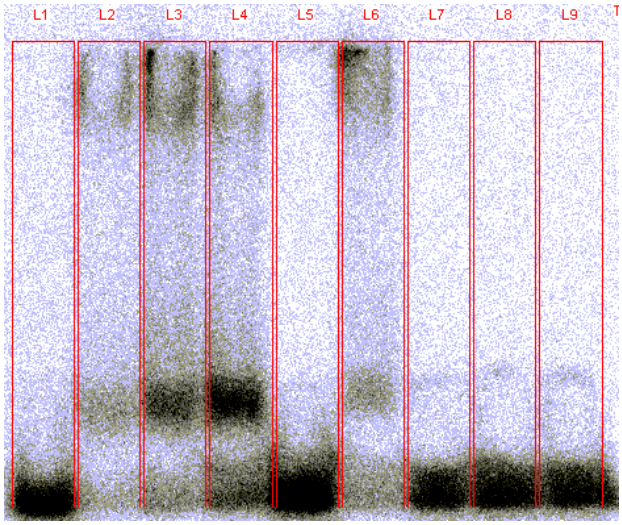

Figure 3.2: Gel pictures for the gel-shift assay. 3.4A: Gel stained with Sypro-Ruby (thrombin stained grey/black). 3.4B: Phosphor-image of gel. Radioactivity (corresponding to DNA) is represented by dark blue/black spots.

Taken together, the results shown in figures 3.2A and B indicate that the aptamer, when free in solution, is able to bind thrombin no matter whether there is an amine appended to the aptamer or not (lanes 2-4 and 6). In addition, SDS causes dissociation of the aptamer-thrombin complex (lane 5). The amine-appended scrambled DNA sequence may interact with thrombin, but it is a very weak interaction (lane 7).

Since it was verified that the amine-appended aptamer could bind thrombin (at least in a homogeneous assay), binding trials for thrombin to the DNA-immobilized beads were repeated. However, this time the DNA level was increased to see if the aptamer was binding thrombin in the previous trials, but at levels below the detection limit for Sypro-Ruby. It was necessary to increase the volume of the bead suspension in order to increase the amount of DNA available in the reaction mixture. This increase in bead volume meant that the surface area of the beads in the reaction mix was increased, too.

Figure 3.3 shows the 12% SDS-polyacrylamide gel (stained with Sypro-Ruby) results for a trial in which the amount of aptamer sequence and scrambled sequence immobilized to the beads was 415 and 422 picomoles, respectively. This DNA level represents a 9-fold increase in the bead surface area compared to previous experiments. Lane 1 is a 20 pmol thrombin standard. Lane 2 is the result for aptamer-immobilized beads and lane 3 is the result for scrambled-immobilized beads. Lane 4 is the protein M.W. standard. The thrombin bands are circled in red.

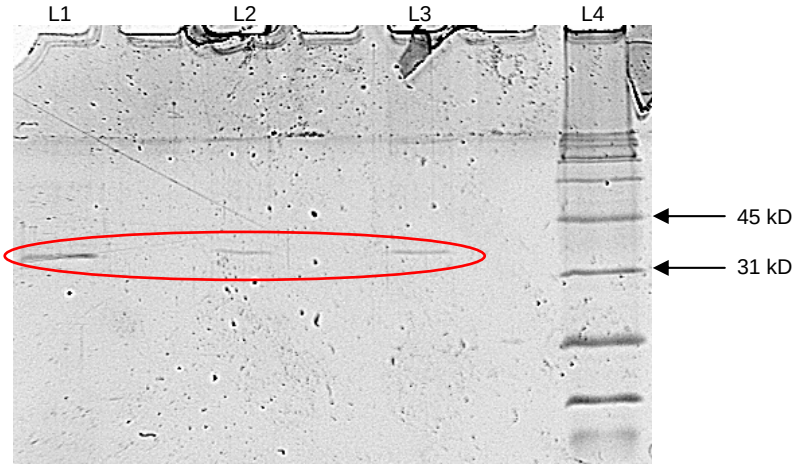

Figure 3.3: Gel results for thrombin binding to DNA-attached beads. The thrombin bands are circled in red.

The digital light units (DLU) for the thrombin band in lane 1 (corresponding to 20 picomoles of thrombin) was 11320 DLU. The level of thrombin for lanes 2 and 3 were 1150

and 1690 DLU, respectively. These numbers for lanes 2 and 3 correspond to approximately 2 and 3 picomoles of thrombin associated with the aptamer-attached beads and the scramble-attached beads, respectively. Other trials for thrombin binding produced results with no thrombin associated with the beads, thrombin associated with some of the beads but not with others (aptamer or scrambled sequence), or results similar to those represented by figure 3.3. In all of the cases, if thrombin was associated with beads, the thrombin levels on the gel were extremely low. These results indicated that thrombin was binding non-specifically to some entity.

Experiments showed that low amounts of ethanolamine-blocked PDC beads did not bind lower concentrations of thrombin; however, the experiments represented by figure 3.3 utilized substrate that had a total surface area 9 times as great and thrombin concentrations that were 10 to 20 times as high as previous. An experiment was performed to see if the larger bead surface area/higher concentrations of thrombin resulted in non-specific binding of thrombin to the beads.

The 12% SDS-polyacrylamide gel (stained with Sypro-Ruby) results shown in figure 3.4 indicate that thrombin was binding non-specifically to the modified beads- especially at large bead surface areas and high thrombin concentrations. Table 3.2 gives the sample composition for each lane. Nothing was loaded in lane 7 and lane 8 had the protein M.W. standard loaded on it. The beads were exposed to 328 picomoles of thrombin.

The results in lanes 1, 2, 4, 5 and 6 show a correlation between thrombin association and high bead surface area: the higher bead surface area lanes (1, 2 and 5) show a significantly greater amount of thrombin association than the lower bead surface area lanes (4 and 6). However, lane 3 shows an approximately equal level of thrombin association as lanes 1, 2 and 5, but with less than a third of the bead surface area. This is contrary to the theory that the greater bead surface area allows for an increase in non-specific interactions with thrombin, but there may be a reasonable explanation for this apparently divergent

result: the aptamer is binding thrombin but most of it is removed during the washing steps. Support for this hypothesis will be presented later in this chapter and in chapter 4.

Lane #	Bead Modification	Bead Surface Area (cm^2)	Total DNA On Beads (pmol)
1	Aptamer Immob.	5470	505
2	Scrambled Immob.	5470	481
3	Aptamer Immob.	1520	417
4	Scrambled Immob	1520	465
5	Ethanolamine Blocked (No DNA)	5470	N/A
6	Ethanolamine Blocked (No DNA)	1520	N/A

Table 3.2: Bead properties of samples loaded onto gel shown in figure 3.4.

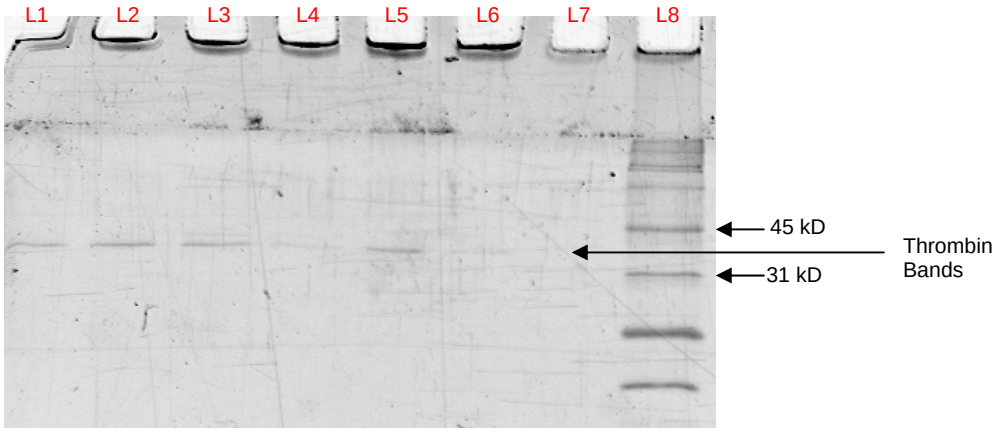

Figure 3.4: Thrombin association with beads at high bead surface area and high thrombin concentration.

3.3.1.2 Gold

Figure 3.5 shows typical SPR responses to an injection of thrombin over an SPR chip with aptamer sequence attached to flow cell 2 (trace B) and scrambled sequence attached to flow cell 1 (trace A). Figure 3.6 shows the reference-subtracted trace for the thrombin injection: flow cell 1 (reference cell) response subtracted from the response of flow cell 2 (sensor cell). Both flow cells shown in figure 3.5 exhibit a bulk response to the thrombin injection and a return to the pre-injection baseline at the end of the thrombin injection, but

there are minor differences in the flow cell's response that are indicative of binding to one flow cell and not the other. The signal trace for flow cell 2 shows a more gradual increase towards a signal plateau than for flow cell 1; this is due to the association process of the thrombin to the aptamer. The magnitude of the signal increase is greater for flow cell 2 than flow cell 1. And the decrease in the signal for flow cell 2 is slightly more gradual than for flow cell 1 at the end of the thrombin injection, due to the dissociation of the thrombin from the aptamer. The reference-subtracted trace (figure 3.6) reflects these differences.

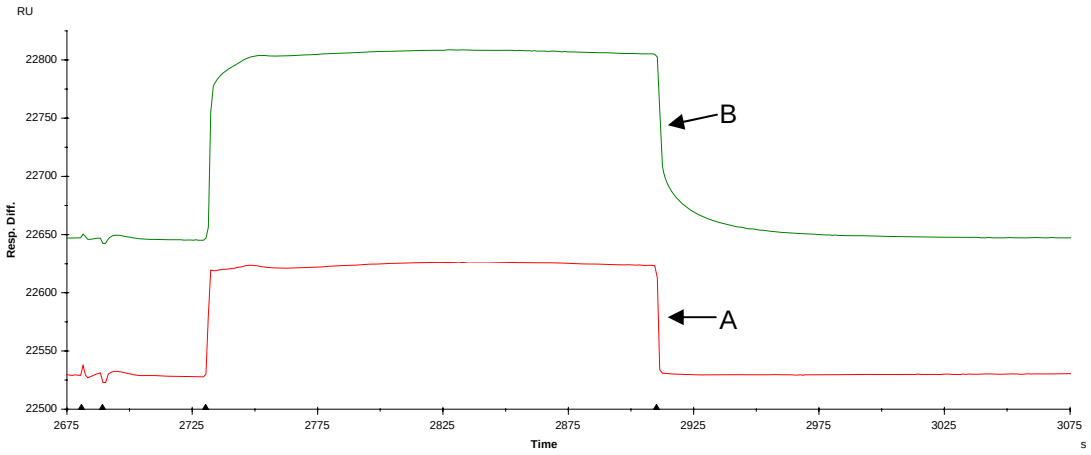

Figure 3.5: Response to a thrombin injection onto an SA chip with scrambled sequence immobilized to FC1 (trace A) and aptamer sequence immobilized to FC2 (trace B).

The level of thrombin binding to the sensor flow cell (FC2) was determined from figure 3.6. The baseline RU value prior to the thrombin injection is subtracted from the RU value of the plateau that occurs during the thrombin injection. A rapid RU increase followed by a plateau in signal during the thrombin injection indicates that the reaction has fast kinetics (discussed in chapter 4). All of the injections of thrombin in this study reached a steady-state within a short period of time after the injection. The signal noise seen in the traces (at about 2680, 2685, 2730 and 2905 s) is due to the injection process and the intensity can vary from flow cell to flow cell.

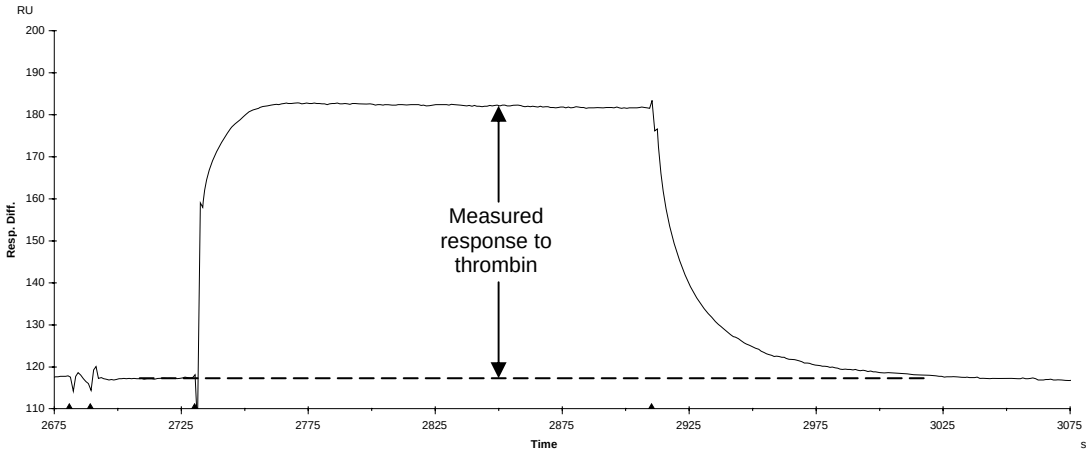

Figure 3.6: Reference-subtracted response to a thrombin injection. The trace is produced by subtracting the response for FC1 from the response for FC2 (figure 3.5).

The anti-thrombin aptamer bound thrombin specifically, with good precision and maintained high activity when it was immobilized both by covalent (CM3 chip) and affinity (SA chip) attachment methods. Figure 3.7 shows a typical reference-subtracted sensorgram trace for an injection of 11.7 μM elastase onto a sensor chip. The reference-subtracted trace shows a slight decrease in signal during the elastase injection; indicating that the reference flow cell had a slightly higher bulk response (11 RU) to the elastase injection than the signal flow cell. A hybridization assay showed that the reference flow cell had 1.31 pmol/cm^2 of scrambled sequence attached and the signal flow cell had 0.16 pmol/cm^2 of aptamer sequence attached. This discrepancy may have led to a greater bulk response on the reference flow cell than on the signal flow cell during the elastase injection. A similar phenomenon was observed for a dose response trial for aptamer immobilized to a CM3 chip. Those results will be presented later in this chapter.

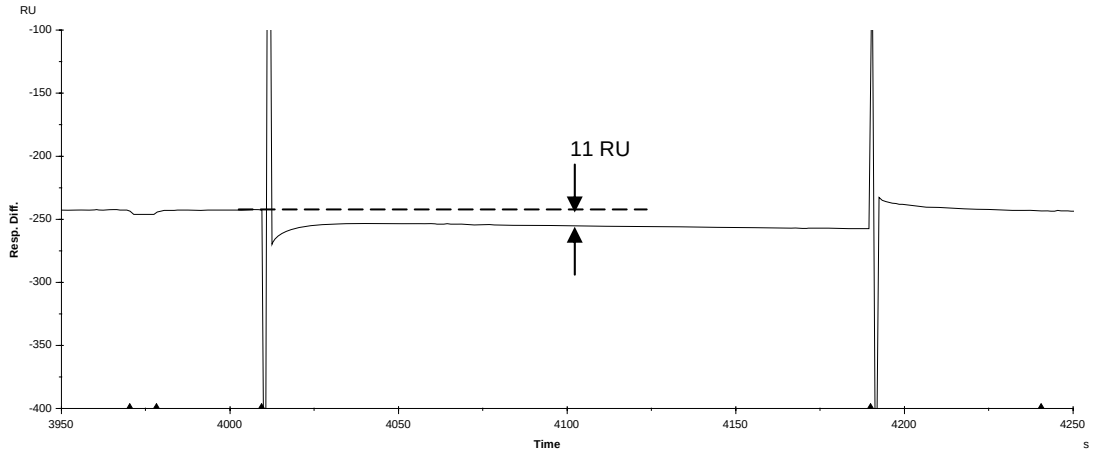

Figure 3.7: Reference-subtracted sensorgram for an elastase injection over a CM3 chip with aptamer sequence immobilized to the sensing flow cell and scrambled sequence immobilized to the reference flow cell.

Figure 3.8 shows a typical reference-subtracted sensorgram response to multiple injections of thrombin over the same sensor surface. The sensor flow cell had 9 RU (0.18 pmol/cm^2) of aptamer immobilized to an SA chip, which corresponds to an R_{max} of 67 RU for that flow cell. 90 μL injections of a 307 nM thrombin solution were made using Kinject mode at a flow rate of 30 μL/min. The responses to the injections of the regeneration solution are marked by a rapid drop in the baseline signal followed by a narrow spike in the positive RU direction: one is at 1178 seconds, a second at 2293 seconds and a third at 3187 seconds. The first injection of thrombin (721 – 901 seconds) produces a response of 66 RU. The next injection (1836 – 2016 seconds) is of buffer and produces no significant net change in the refractive index. The last two thrombin injections both produced a response of 65 RU. All three of the responses to injected thrombin were very close to the calculated R_{max} for the amount of aptamer immobilized to the sensor flow cell.

This type of precision and high level of activity was typical for the SA and CM3 flow cells immobilized with aptamer. In addition to these characteristics, sensor chips were stable to storage: sensor chips routinely gave a similar response to a thrombin injection after two or more weeks when properly stored (4°C in humid conditions).

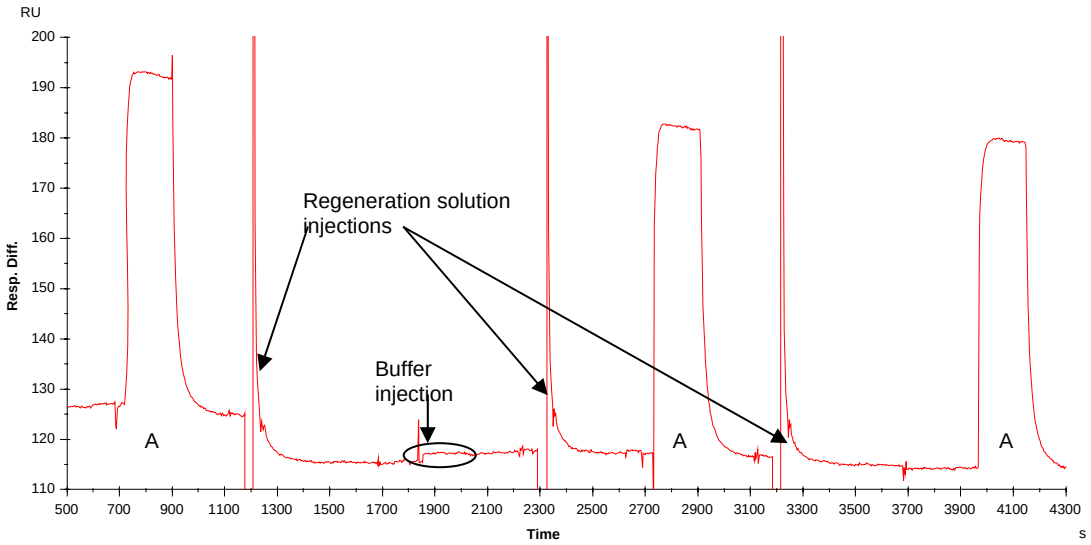

Figure 3.8: Reference-subtracted sensorgram for multiple injections of 307 nM thrombin over the same sensor surface. A: thrombin injections.

3.3.2 Dependence Of Aptamer Activity On Packing Density

The aptamer's activity was determined to be dependent on the packing density of the immobilized aptamer. Activity of the aptamer is defined as the attached aptamer's ability to detect the R_{max} level of thrombin for that flow cell's aptamer level. This study was conducted for the aptamer immobilized to the SA chip because it was possible to attach various levels of aptamer to the sensor surface- especially high levels that were not achieved by the covalent attachment techniques used in these studies.

An aptamer-immobilized flow cell's maximum response to thrombin was measured on the Biacore 3000 SPR instrument. Stepwise increases in thrombin solution concentration were injected over the sensor chip until the reference-subtracted response to thrombin reached a plateau. Regeneration solution was injected after the completion of every thrombin injection to remove any bound thrombin. Figure 3.9 shows two representative plots of the sensorgram response versus the injected thrombin concentration. The RU

value used to determine the percent activity was determined by extrapolating the binding response curve until it reached a plateau.

A

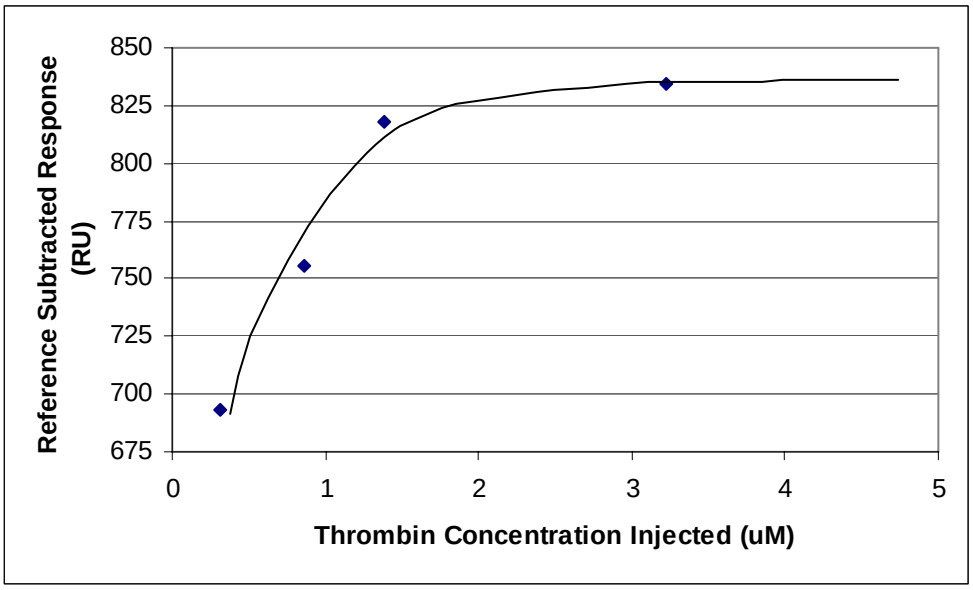

B

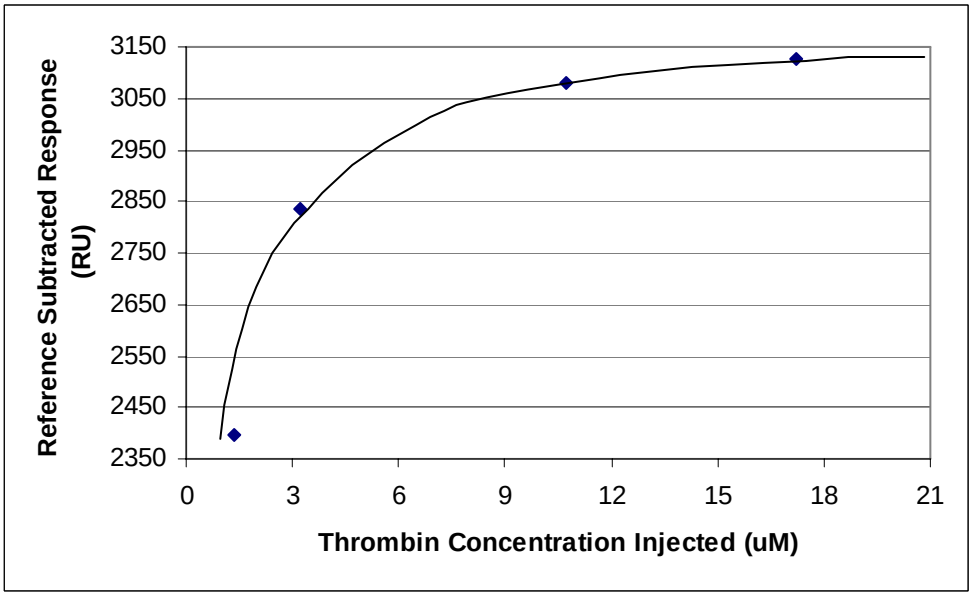

Figure 3.9: Reference subtracted response to thrombin for two flow cells with different aptamer packing densities. A: 2.00 pmol/cm^2 aptamer immobilized; B: 9.91 pmol/cm^2 aptamer immobilized.

Figure 3.10 compares the percentage of active immobilized aptamer molecules to the packing density of the aptamer molecules on the SA chip. The activity of the immobilized aptamer molecules was assessed by its response to thrombin injections- active aptamers bind thrombin, causing an increase in the reference-subtracted signal during injection. The percent activity for a flow cell was determined by comparing the maximum sensor response to thrombin with the R_{max} value calculated from the level of aptamer immobilized in that flow cell (determined by hybridization with complementary DNA). A flow cell that shows a maximum response to thrombin that is equal to its R_{max} value has an activity of 100% (100% of the immobilized aptamer molecules are active to binding thrombin).

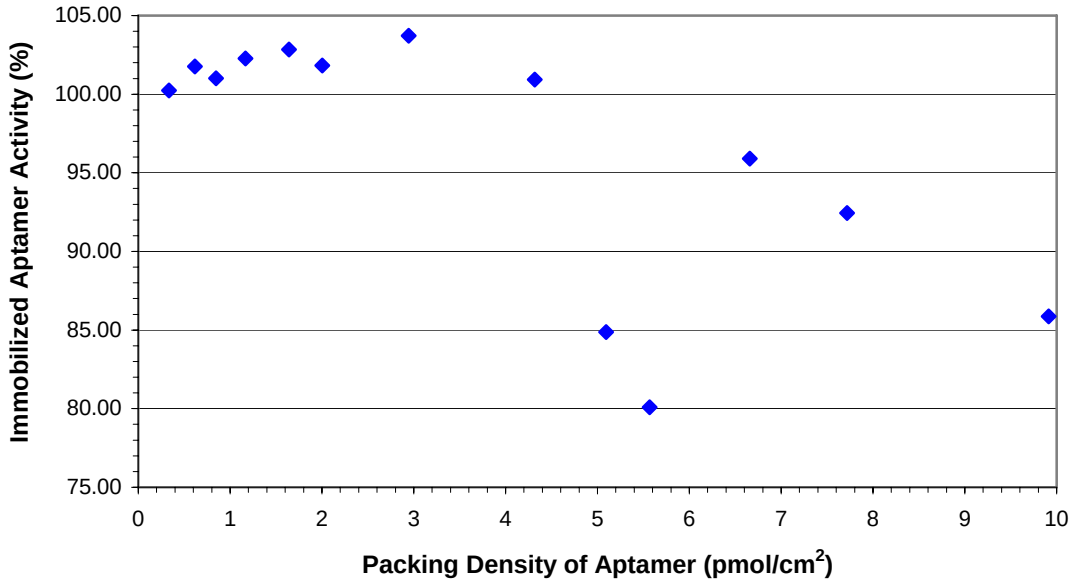

Figure 3.10: Percent activity of the immobilized anti-thrombin aptamer versus the packing density of the aptamer on the SA chip.

The first 8 aptamer packing density values (0.334 through 4.32 pmol/cm^2) show activity values for the immobilized aptamers of at least 100%. The values in excess of 100% are likely due to low values for R_{max}. The R_{max} value for a flow cell is based on the measured level of aptamer attached to that flow cell. The level of aptamer attached was determined with a hybridization assay. The sensitivity of the SPR instrument is 1 RU. This corresponds

to a sensitivity of 20 fmol/cm^2 for the DNA (M.W. = 5000 g/mol). However, for a 37 kD protein like thrombin, 1 RU change in refractive index on the SPR chip corresponds to a 2.7 fmol/cm^2 change in protein associated with the sensor surface. Therefore, the sensor surface is more sensitive to small changes in the level of thrombin associated with the surface than for the aptamer's complementary strand (which was used to determine the packing density of the aptamer on the surface). A small error in the packing density level is reasonable considering the sensitivity limit of the measuring system (SPR with low M.W. DNA strands).

The 5 highest packing density values show an activity level towards thrombin binding of less than 100%. There is an odd pattern to these last 5 data points: a rapid decrease in activity for the first two points (5.09 and 5.57 pmol/cm^2), a rise back to 95.9% activity and then a steady decline in activity for the last two packing densities. The trend displayed for the last three packing densities (a steady decline in activity as the packing density increases) is expected for packing densities exceeding the optimal packing density value. An explanation for the anomaly presented by the activity levels of the 5.09 and 5.57 pmol/cm^2 packing density flow cells is that these two flow cells were old. The aptamer had been immobilized to these flow cells over three months prior to the activity studies; whereas, the other packing density values are from flow cells that had aptamer immobilized within the week of activity testing.

The aptamers attached to the 'old' flow cells did not detach during this extended layaway (hybridization assays were done at the same time as the activity study), but may have become unable to bind thrombin for some reason. One possibility is that the solution-like dextran layer of the SA chip became less porous (due to dehydration) and, therefore, the thrombin molecules were not as able to penetrate into the dextran hydrogel as well as the AptComp DNA molecules. A more likely possibility is that the aptamer molecules were unable to form the correct 3D structure to bind thrombin (but were still available to hybridize to their complementary strands). This is quite possible if the aptamers were forming

intermolecular stacked, G-quartets[16] instead of the thrombin-binding 3D structure of **intra**molecular stacked, G-quartets. The length of time the aptamers have been immobilized should not be a factor in whether an intermolecular or an intramolecular configuration is preferred. However, the age of a sensor chip (especially with non-ideal storage conditions) may lead to a compacting of the dextran layer due to dehydration. A compacted dextran layer would force the immobilized aptamers closer together and possibly lead to the formation of intermolecular structures rather than intramolecular structures.

The optimal packing density for the affinity-immobilized anti-thrombin DNA aptamer is between 4.5 and 6 pmol/cm^2. Steel, *et. al.* found that a packing density of < 6.6 pmol/cm^2 was required for immobilized ssDNA probes to hybridize with 100% efficiency.[6] This value is in agreement with other studies that have determined hybridization efficiencies of 40% for 25 pmol/cm^2,[4] 90% for 5 pmol/cm^2,[9] and 16% for 50 pmol/cm^2[5] for immobilized ssDNA. Optimal packing density studies for IgG (160 kD antibody) and the Fab' fragment of IgG (46 kD) showed a maximum surface activity of ~38% and ~75%, respectively, for a packing density of 1 pmol/cm^2.[2] Dubrovsky, et. al. determined that 46% of the immobilized IgG molecules were active for a packing density of 2 pmol/cm^2.[3] As predicted, the optimal packing density for the anti-thrombin DNA aptamer is between the optimal packing densities for ssDNA and proteins- with the value lying closer to the optimal packing density for ssDNA used in hybridization assays.

3.3.3 Importance Of Reference Flow Cell Composition

In the SPR instrument, the reference flow cell is used as a bulk response subtraction for accurate determination of the level of binding of the analyte to the sensor surface. Therefore, the nature and level of any immobilized material can significantly influence the measured response to an analyte injection. Studies with the Biacore SPR system found that a high level of scrambled DNA sequence immobilized to the reference flow cell (relative

to the aptamer immobilization level) caused a dramatic decrease in the reference-subtracted signal at high thrombin concentrations for the CM3 chip only. In addition, it was determined that a blank reference flow cell (no scrambled DNA immobilized) worked just as well as a reference with scrambled sequence immobilized for both the CM3 and SA chips.

Figure 3.11 shows the plots of several subtracted responses to injections of thrombin over a CM3 sensor chip. All four of the flow cells used to create this plot were on the same CM3 chip. This allowed for all four of the flow cells' responses to each concentration of thrombin to be acquired with one injection of the thrombin solution.

The plot of FC4 – FC3 (green triangles) shows the response curve when there is too much scrambled sequence immobilized to the reference flow cell with respect to the sensor flow cell. The sensor flow cell (FC4) had 156 fmol/cm^2 of aptamer DNA immobilized. The reference flow cell (FC3) had 1.31 pmol/cm^2 of scrambled DNA immobilized (about 8.5 times as much DNA as the sensor flow cell). The expected reference-subtracted plot for a range of thrombin injections should either steadily increase (like the red circles and open squares) or plateau to a constant response value- not drop-off at the higher thrombin concentrations.

The indication from the FC4 – FC3 plot is that there is an increase in the non-specific interactions on the reference flow cell as the thrombin concentration increases. This theory is supported by the plot of FC3 – FC2 (blue diamonds): FC3 has 1.31 pmol/cm^2 of scrambled sequence immobilized and FC2 has no DNA immobilized. However, a plot of the response for FC2 (no DNA immobilized) subtracted from the response for FC1 (low amount of scrambled sequence immobilized) shows no increase in non-specific interactions as the thrombin concentration increases (FC1 – FC2 plot: pink squares). These results suggest that a high level of scrambled sequence immobilized to a flow cell allows for increasing non-specific interactions with thrombin as the thrombin concentration increases. This finding is contrary to a study of protein-protein interactions using SPR that found that the "immobilization levels for the active surface and the reference surface [can] differ by a few

thousand RU" without any detrimental consequences to the analysis.[17] Low levels of scrambled sequence immobilized to the reference flow cell do not result in an increase in non-specific interactions as the thrombin concentration increases. In fact, the response of the flow cell with a low level of scrambled sequence immobilized is essentially equivalent to a flow cell with no DNA immobilized. This result suggests that the reference flow cell does not need any non-aptamer DNA immobilized in order to acquire accurate reference-subtracted sensorgrams for thrombin injections.

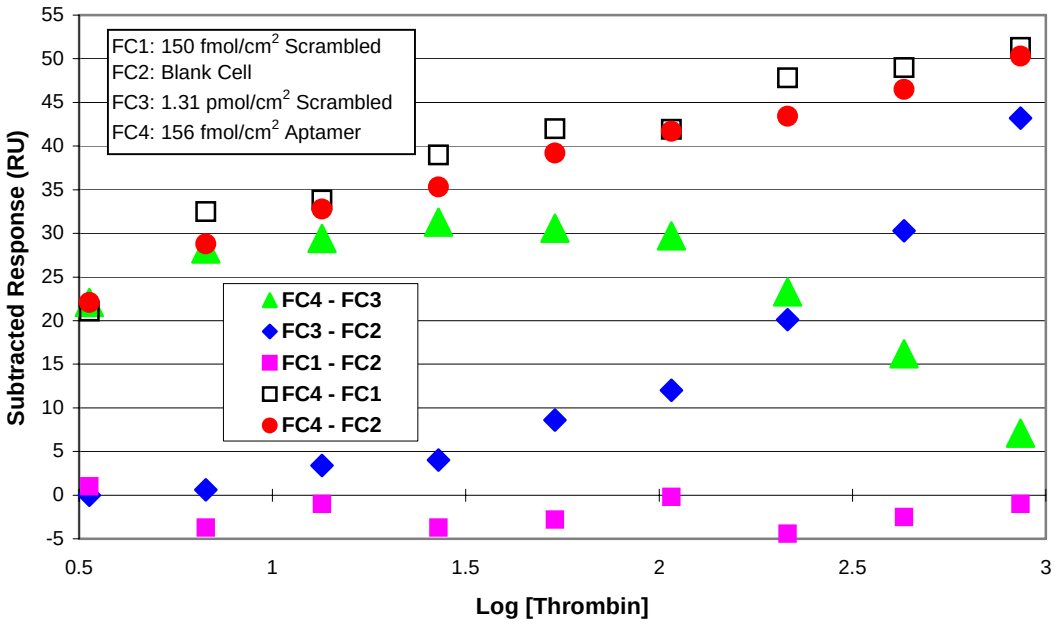

Figure 3.11: Importance of reference composition for CM3 chip.

The plot of FC4 – FC1 (open squares) shows the response curve when there is approximately equal packing densities between the sensor flow cell (FC4) and the reference flow cell (FC1): 156 and 150 fmol/cm^2, respectively. A similar result occurs for the FC4 – FC2 plot (red circles), where the reference flow cell (FC2) has no DNA immobilized. These comparable results indicate that a blank flow cell will work well as a reference for this analyte-receptor system with a CM3 chip. In fact, a blank flow cell may be

preferred over a scrambled-immobilized flow cell as a reference because there won't be any concern of increased non-specific interactions due to too high a level of immobilized DNA.

Contrary to the CM3 chip, the reference flow cell for the SA chip displayed no increase in non-specific interactions with high thrombin injections when the scrambled DNA level was about 8.5 times as much as the aptamer DNA level. For injections of 860 nM thrombin, the responses of the reference and sensor flow cells gave similar readings. In one trial the reference flow cell had 6 RU of scrambled sequence immobilized and gave a response of 38 RU to the thrombin injection; the sensor flow cell had 9 RU of aptamer sequence immobilized and gave a response of 108 RU. This corresponds to a reference-subtracted value of 70 RU for the injection of thrombin at a high concentration. When the level of scrambled DNA was increased to 78 RU on the reference flow cell (~8.5 times the aptamer level) but the aptamer level was left at 9 RU, the individual flow cell responses to the 860 nM thrombin injection were 44 and 115 RU, respectively. This corresponds to a reference-subtracted value of 71 RU- essentially no different from the results when there was a low level of scrambled sequence immobilized to the reference flow cell.

However, like the CM3 results, there appears to be no reason to use a flow cell with scrambled sequence immobilized as the reference for thrombin binding analysis. Kinetic runs for an aptamer-immobilized SA chip with a blank reference flow cell (no DNA immobilized) produced binding curves and kinetic data that mirrored the results for trials using a reference flow cell with scrambled sequence DNA immobilized. These results indicate that a scrambled DNA-immobilized reference flow cell is unnecessary for accurate binding characterization using the SA chip.

The difference between the two sensor chips in regard to non-specific interactions begs the question: what difference(s) between the two chips would cause this phenomenon? After the immobilization of the DNA onto the CM3 chip, an ethanolamine solution is injected to react with any remaining activated carboxyl groups on the surface. Even though it only extends a short distance into the solution, the immobilized

ethanolamine may act as support to extend the DNA out into the solution and/or minimize any DNA-substrate interactions. Herne and Tarlov found that the use of short 'spacer' molecules (molecules, like ethanolamine, that reacted with activated linking sites on the substrate to fill in between immobilized sensing molecules but were inert to analyte interactions) forced the immobilized 'probe' DNA to orient perpendicular to the substrate surface- resulting in greater hybridization efficiency.[18]

Non-specific interactions between thrombin and DNA are quite probably due to electrostatic attractions between the negatively-charged DNA phosphate backbone and the positively-charged lysine and arginine-rich exosite 1 on thrombin.[19] Hence, the more strands of negatively charged DNA, the more interactions that are possible with thrombin- especially if the DNA is sticking out into the solution. The streptavidin surface of the SA chip may allow the unstructured DNA molecules to have greater interactions with the surface than the carboxyl-modified surface of the CM3 chip. In addition, there was no 'blocking' molecule immobilized after the DNA, so the DNA molecules may not be forced to extend out into the solution either by support-like structures or by inhibition of DNA-substrate interactions.

3.4 Conclusions

The activity of the anti-thrombin DNA aptamer was evaluated for the aptamer immobilized to silica beads and to gold SPR sensor chips. Difficulties arose for the detection of thrombin associated with the silica beads, but the SPR technique provided activity analysis and some insight into practical considerations for aptamer use in heterogeneous assays.

A BCA assay for detection of thrombin associated with the silica beads resulted in an excessive background signal due to primary amines on the modified silica beads. Native polyacrylamide gel electrophoresis confirmed that the amine-appended aptamer bound to

thrombin in solution and that the thrombin-aptamer interaction was disrupted by the addition of SDS. Denaturing SDS-PAGE showed that ethanolamine-blocked PDC beads with a low surface area did not readily bind to thrombin but that a large bead surface area gave false positive results for thrombin binding. In addition, there was an indication that the immobilized aptamer was binding thrombin, but that a majority of the aptamer-bound thrombin was being removed by the washing steps.

The SPR curves for the binding of thrombin to gold-immobilized aptamer indicated that there are fast on and off rates for the aptamer-thrombin interaction- this supports the explanation for the results with the silica beads in which either no or very little thrombin was found to be associated with the aptamer-immobilized beads. The aptamer was specific, showed excellent precision towards thrombin injections and had very high activity when immobilized via covalent and affinity means (CM3 and SA chips, respectively). The aptamer remained attached to the substrate even after several months of storage for both attachment techniques; however, there may have been a problem with the dextran layer compacting (possibly due to dehydration) and allowing the aptamers to form intermolecular stacked, G-quartets (inactivating the aptamers) instead of the active intramolecular stacked, G-quartets. Aptamer-immobilized chips that had been stored for a few weeks retained their original activity.

SPR was used to determine the maximum packing density of the aptamer at which the aptamer retained 100% activity for binding thrombin. An optimal packing density for the DNA aptamer immobilized to an SA chip was found to be between 4.5 and 6 pmol/cm^2. This value is in excellent agreement with expectations based on the optimal values reported for ssDNA used for hybridization assays and for large and small proteins (IgG and its Fab' fragment, respectively).

The use of a so-called nonsense molecule on the reference flow cell (the scrambled DNA, in this case) may not be necessary for aptamer-based assays and may even interfere with accurate assays if immobilized at too high a level (compared to the aptamer

immobilization level). Results for the CM3 chip showed that too much scrambled sequence gave increased non-specific interactions at high thrombin concentrations. This may have been due to the ethanolamine blocker causing the DNA to extend farther out into the solution than it did when attached to the SA chip. A blank flow cell (nothing immobilized) worked as well as a reference flow cell that had a small amount of scrambled sequence immobilized. Karlsson and Fält found that a blank reference flow cell worked fine for measuring protein-protein interactions with an SPR instrument.[17] This was also found to be true for RNA-protein interactions where the RNA was immobilized to an SA chip via affinity interactions.[15] The use of a nonsense molecule immobilized to the reference is no longer a given and may even be a detriment to an effective analysis.

3.5 References

1 Baszkin, A.; Boissonnade, M. M.; Kamyshny, A.; Magdassi, S. *J. Coll. Interface Sci.* **2001,** *244*, 18-23.
2 Herron, J. N.; Wang, H.-k.; Janatova, V.; Durtschi, J. D.; Caldwell, K. D.; Christensen, D. A.; Chang, I. N.; Huang, S.-C. *Surfactant Science Series* **1998,** *75*, 221-280.
3 Dubrovsky, T. B.; Demcheva, M. V.; Savitsky, A. P.; Mantrova, E. Y.; Savransky, V. V.; Belovolova, L. V. *Biosens. Bioelectron.* **1993,** *8*, 377-85.
4 O'Donnell-Maloney, M. J.; Tang, K.; Koester, H.; Smith, C. L.; Cantor, C. R. *Anal. Chem.* **1997,** *69*, 2438-2443.
5 Rogers, Y.-H.; Jiang-Baucom, P.; Huang, Z.-J.; Bogdanov, V.; Anderson, S.; Boyce-Jacino, M. T. *Anal. Biochem.* **1999,** *266*, 23-30.
6 Steel, A. B.; Herne, T. M.; Tarlov, M. J. *Anal. Chem.* **1998,** *70*, 4670-4677.
7 Steel, A. B.; Levicky, R.; Herne, T. M.; Tarlov, M. J. *Proc.- Electrochem. Soc.* **1999,** *99-5*, 132-143.
8 Huang, E.; Satjapipat, M.; Han, S.; Zhou, F. *Langmuir* **2001,** *17*, 1215-1224.
9 Boncheva, M.; Scheibler, L.; Lincoln, P.; Vogel, H.; Aakerman, B. *Langmuir* **1999,** *15*, 4317-4320.
10 Satjapipat, M.; Sanedrin, R.; Zhou, F. *Langmuir* **2001,** *17*, 7637-7644.
11 Peterson, A. W.; Heaton, R. J.; Georgiadis, R. M. *Nucleic Acids Res.* **2001,** *29*, 5163-8.
12 Deng, Q.; German, I.; Buchanan, D.; Kennedy, R. T. *Anal. Chem.* **2001,** *73*, 5415-5421.
13 Liss, M.; Petersen, B.; Wolf, H.; Prohaska, E. *Anal. Chem.* **2002,** *74*, 4488-4495.
14 Clark, S. L.; Remcho, V. T. *Anal. Chem.* **2003,** *75*, 5692-5696.
15 Laird-Offinga, I.;; Biacore Corporation, 2002.
16 Cheng, A.; Van Dyke, M. W. *International Journal on Genes and Genomes* **1997,** *197*, 253-260.
17 Karlsson, R.; Falt, A. *J. Immunol. Methods* **1997,** *200*, 121-133.
18 Herne, T. M.; Tarlov, M. J. *J. Am. Chem. Soc.* **1997,** *119*, 8916-8920.
19 Tsiang, M.; Jain, A. K.; Dunn, K. E.; Rojas, M. E.; Leung, L. L. K.; Gibbs, C. S. *J. Biol. Chem.* **1995,** *270*, 16854-16863.

Chapter 4: Kinetics Of The Immobilized Anti-Thrombin Aptamer

4.1 Introduction

The kinetics of an analyte-receptor interaction determines the feasibility of utilizing a particular assay methodology in a diagnostic test for that analyte. Numerous factors can influence the interaction kinetics, including solution composition (pH, etc.), the conformation of the molecule, any modification to the binding elements (fluorophors, etc.), and any attachment methodologies. Even though the attachment of aptamers should lead to fully active molecules with homogenous binding characteristics (due to the ease of controlling the number and points of attachment), the aptamer's binding kinetics may be altered due to the immobilization itself or the binding kinetics may even vary according to the method of attachment. Potyrailo, *et. al.* found that homogeneous assay conditions resulted in a higher dissociation constant (K_D) than heterogeneous assay conditions for the anti-thrombin aptamer;[1] while Liss, *et. al.* reported that covalent attachment of the anti-IgE DNA aptamer led to a faster dissociation rate (k_d) for the complex than did affinity attachment of the aptamer.[2] In contrast, Kleinjung, *et. al.* found that the affinity immobilized RNA aptamer to L-adenosine had a K_D similar to the value determined via equilibrium microdialysis.[3] Therefore, a study was performed using the gold-immobilized anti-thrombin DNA aptamer to determine the kinetic parameters for thrombin binding to a covalently and affinity-attached aptamer.

The kinetics of a binding reaction are often expressed in terms of two different, but related constants: the binding (or association) constant (K_A) and the dissociation constant (K_D). These two measures of the analyte-receptor affinity are derived from the actual kinetic parameters: the association (or on-) rate (k_a) and the dissociation (or off-) rate (k_d). K_A is equal to the ratio of k_a to k_d; while K_D is equal to the ratio k_d to k_a. K_D values (the common

measure of an aptamer's affinity for the analyte) in the nM range represent high affinity between the aptamer and the analyte, but say very little about the magnitude of the association and dissociation reaction rates.

The kinetic reaction rates (k_a and k_d) of a binding reaction impose specific requirements on an analytical assay in order to obtain any meaningful data from the assay. High affinity (large K_A or small K_D) is necessary to effect a separation that is often an integral component of a molecular recognition element-based assay, but the actual on- and off-rates determine the type of assay that is applicable for that particular ligand-analyte system. A binding reaction with a fast on-rate followed by a slow off-rate (common for antibodies) is best suited to an incubate, wash, and read style assay (e.g.- ELISA) because this format allows sufficient time for the association reaction and the wash step will not cause a significant loss of signal due to dissociation of the ligand-analyte complex. In contrast, a binding reaction with a fast on-rate and a fast off-rate is best suited for use in a real-time, continuous-monitoring biosensor.

4.2 Materials And Methods

4.2.1 Materials

The kinetic studies were performed on a Biacore 3000 SPR instrument and analyzed using BIAevaluation software, version 3. The DNA (aptamer and scrambled sequence) was immobilized to CM3 and SA sensor chips as described in chapter 2. The thrombin solutions were made up in 100 mM potassium phosphate, pH 7.4. The binding buffer was 100 mM potassium phosphate, pH 7.4 and the regeneration solution was 7 M urea.

4.2.2 Methods

The experimental data that was used in the kinetic evaluation of the immobilized anti-thrombin aptamer was generated by injecting a series of thrombin solutions with different

concentrations through a reference and sensing flow cell that had very low quantities (2-13 RU) of scrambled and aptamer DNA immobilized, respectively. The thrombin concentration series spanned a range of 100-fold: the lowest being 1.5 nM and the highest being 108 nM. A blank injection (0 nM thrombin) was also included in the series. Each cycle represents the injection of one concentration of thrombin followed by a dissociation period and then a regeneration injection. Thrombin concentrations were injected in random order and at least one concentration of thrombin was injected in duplicate to verify the precision of the measurements. A cycle consisted of an initial 10 minute equilibration phase (binding buffer flowing through the flow cells), a thrombin injection for 150 seconds (to ensure signal plateau), a 10 minute dissociation period and then an injection of 7M urea (regeneration). The flow rate of the buffer solution was 75 μL/min and the temperature during the experiments was maintained at 25°C.

The experimental data were evaluated using BIAevaluation software, version 3, according to the global fitting model. The response curves for various analyte concentrations were globally fit to several binding models provided with the above software. The program determines the best fit for the model based on a least squares calculation. Apparent rate constants (k_a and k_d values) were calculated based on the best fitted model: heterogeneous ligand. Reference-subtracted data curves were used in the evaluations. All of the curves in the data set were normalized to a pre-injection baseline level of 0 RU and the thrombin injection start-time synchronized prior to performing the evaluation.

The kinetic fit results were evaluated according to 1) the level of similarity between the model-generated sensorgram curves and the experimental sensorgram curves and 2) a comparison of the accuracy of the model-generated maximum response value (R_{max}) to the experimental R_{max} value. The closeness of the model fit to the experimental data was based on visual inspection of the overlaid curves (model-generated and experimental), the residuals plot for these overlays and the X^2 value. The comparison of the maximum

response to thrombin is based on the highest concentration of thrombin injected for the data set that is being evaluated.

4.3 Results And Discussion

4.3.1 Kinetic Analysis

4.3.1.1 Best Fit

The best kinetic fit using BIAevaluation software was a heterogeneous ligand-binding model. This model corresponds to the analyte molecule binding either to two different binding sites on the ligand or to two different ligands immobilized on the substrate ($A + L \underset{k_{d1}}{\overset{k_{a1}}{\rightleftharpoons}} AL$; $A + L^{*} \underset{k_{d2}}{\overset{k_{a2}}{\rightleftharpoons}} AL^{*}$). Figure 4.1A shows a typical heterogeneous ligand binding fit for a kinetics experiment on an SA chip with aptamer immobilized. The experimental, reference-subtracted sensorgrams are colored, while the kinetically fit curves are shown as black traces. The residuals plot for this fit is shown below the sensorgram traces (figure 4.1B). Visual inspection of the plot overlays (figure 4.1A) and the residuals plot provide an indication of the deviation of the fitted traces from the experimental sensorgrams; hence, an appropriateness of the fit to the data.

During the association phase of binding (starting at 0 seconds), the fitted traces (black traces) mirror the experimental traces except at the lowest thrombin concentration (lowest response curve) and the two highest thrombin concentrations (two highest response curves). The disparity occurs within the first 25 seconds of thrombin injection and is reflected in the residuals plot. After the initial part of the thrombin injection, the fitted curves mirror the experimental curves with good accuracy all the way through the dissociation phase of the sensorgrams (dissociation starts at 150 seconds). There is a slight deviation after about 250 seconds, which is likely due to baseline drift for a couple of the trials.

Besides the visual similarity of the fitted curves to the experimental sensorgram traces, several other factors indicate a good fit for the heterogeneous ligand kinetic model. The

maximum experimental response to thrombin ($R_{max\ exp}$) for this kinetic trial was 51 RU. The heterogeneous ligand kinetic model predicted an $R_{max}1$ = 42 RU and an $R_{max}2$ = 15 RU; these sum to 57 RU which is slightly higher than the experimental value. In addition, the X^2 value for this fit is very low: 0.88.

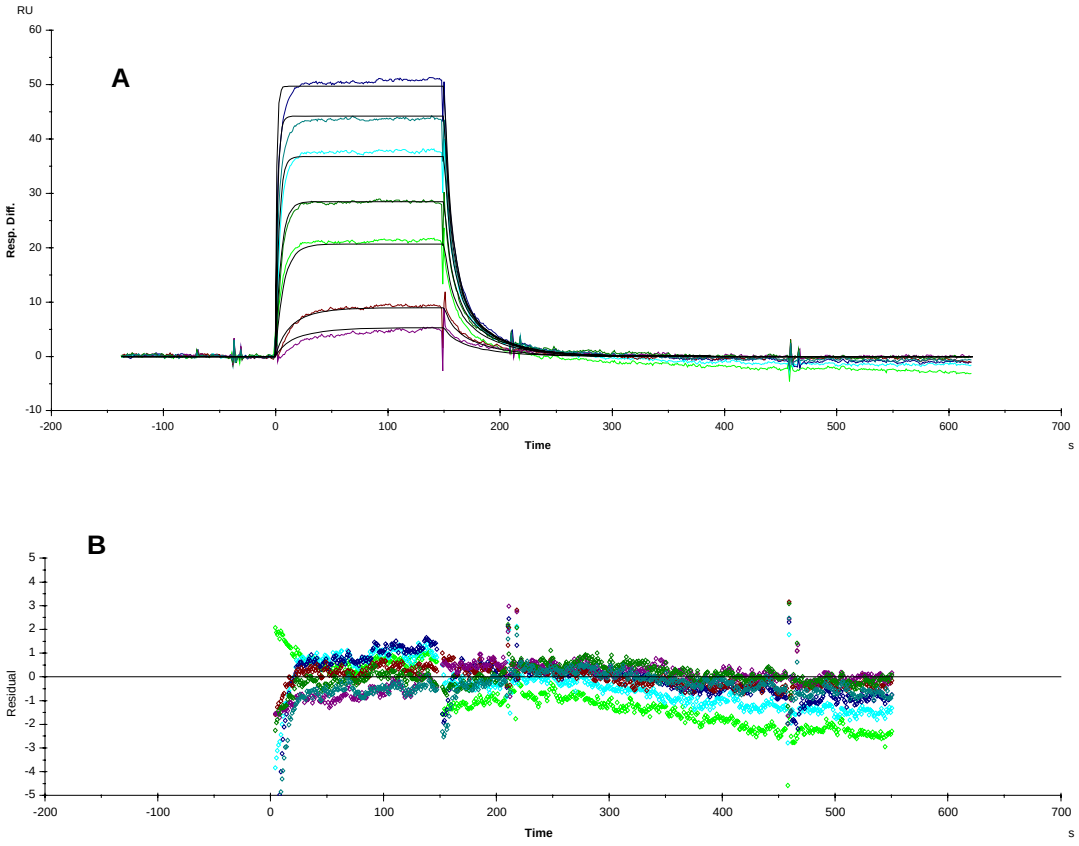

Figure 4.1: Plot of fitted and experimental sensorgrams (A) and corresponding residual plot (B) for a heterogeneous ligand kinetic binding model.

The experimental data were fit using several other kinetic models. Among these were a Langmuir 1:1 model, a bivalent analyte model and a two-state reaction (conformation change). The Langmuir 1:1 model is the simplest binding model (analyte A binds to ligand L: A + L $\underset{k_d}{\overset{k_a}{\rightleftharpoons}}$ AL) and was the expected fit for this system. The bivalent analyte model represents thrombin binding to the aptamer via its two different exosites: I and II

(A + L $\underset{k_{d1}}{\overset{k_{a1}}{\rightleftharpoons}}$ AL; AL + L $\underset{k_{d2}}{\overset{k_{a2}}{\rightleftharpoons}}$ AL_2). The two-state reaction model accounts for a conformational change in the complex that must be reversed in order for dissociation of the complex to occur (A + L $\underset{k_{d1}}{\overset{k_{a1}}{\rightleftharpoons}}$ AL; AL $\underset{k_{d2}}{\overset{k_{a2}}{\rightleftharpoons}}$ AL^*).

Figure 4.2 shows the results of a Langmuir 1:1 kinetic fit for the same kinetic data that was used for the heterogeneous ligand kinetic fit (figure 4.1). Visual inspection of the trace overlays (figure 4.2A) and the residuals plot (figure 4.2B) clearly shows that this is a worse fit than the heterogeneous ligand kinetic fit (figure 4.1). Only the three middle fitted traces come close to matching the experimental traces during the association phase of the binding. The dissociation phase shows an even greater disparity between the fitted and experimental curves: all of the fitted traces show a faster dissociation process than realized by the experimental data. This is clearly illustrated by the overlap of the residual plots between about 170 seconds and 230 seconds. The calculated R_{max} from the fitted data is very close to the experimental R_{max} (53 versus 51, respectively). However, the X^2 value (1.63) for this fit is twice that of the heterogeneous ligand fit.

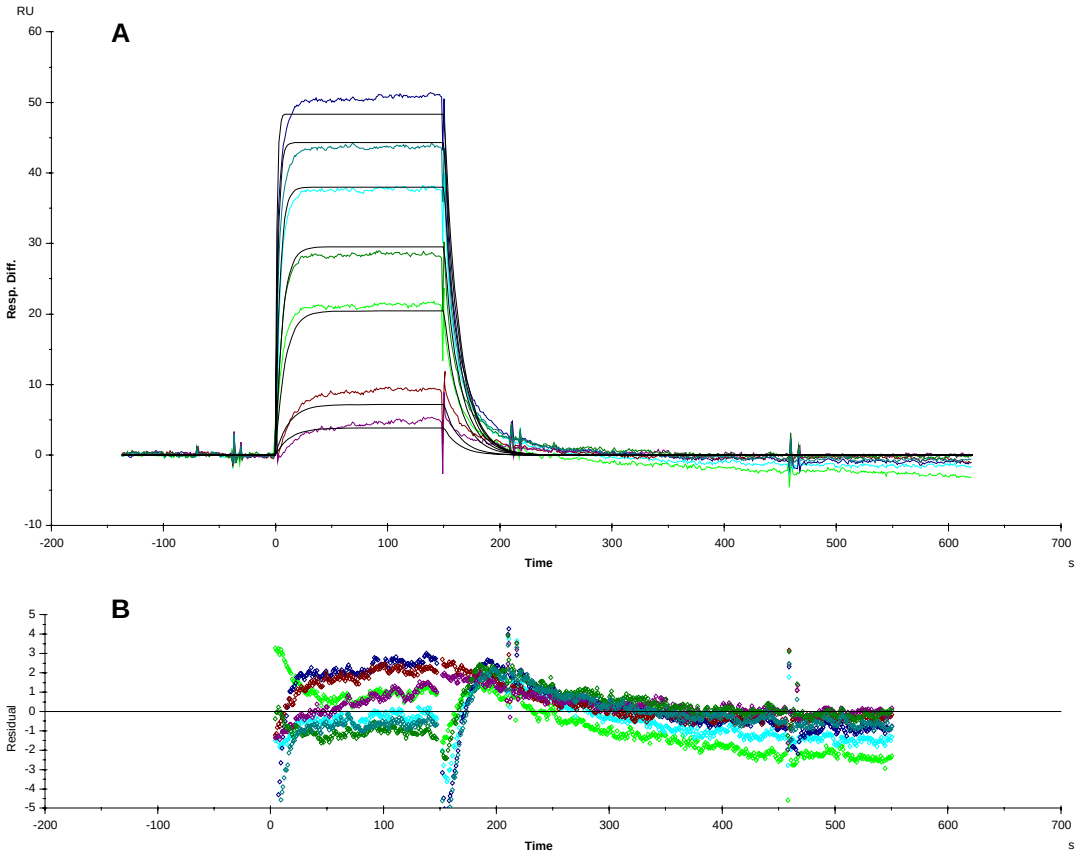

Figure 4.2: Langmuir 1:1 kinetic fit. A: Fitted traces with experimental sensorgrams. B: Residuals for figure 4.2A.

Figure 4.3 shows the results for a kinetic fit using a bivalent analyte kinetic model for the same kinetic data as the previous two fits. This model shows a reasonably good fit to the data. There is a slight discrepancy for the two lowest and two highest thrombin concentration curves at the beginning of the injection (~ 0 – 20 seconds), but the remainder of the association and all of the dissociation fit is good. The closeness of the fit is reflected in a low X^2 value: 0.76. Despite the closeness of the fitted traces to the experimental sensorgrams, this model was deemed an inappropriate fit because the R_{max} value determined from the model (72 RU) was significantly higher than the experimental R_{max} value (51 RU).

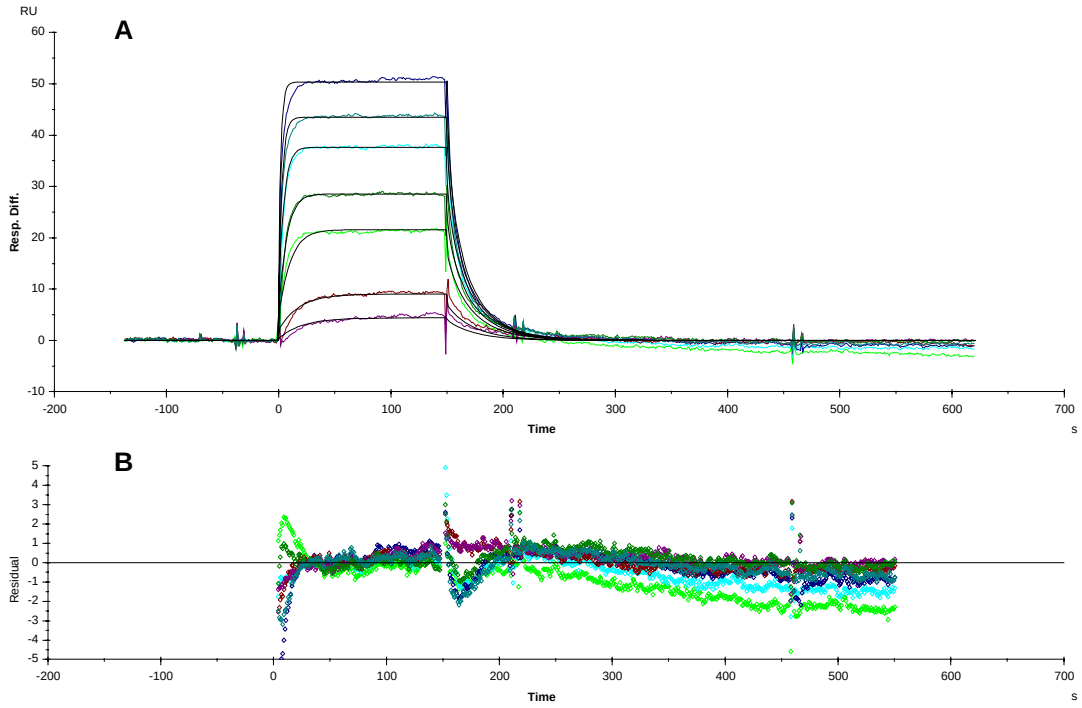

Figure 4.3: Bivalent analyte kinetic fit plots. A: kinetic model fits with experimental sensorgrams. B: residuals plot for the kinetic/experimental traces shown in A.

Figure 4.4 shows the results of a kinetic fit for the data using the two-state reaction (conformation change) kinetic model. This fit shows considerable discrepancies between the fitted traces and the experimental sensorgrams, especially during the association phase of binding. The dissociation phase fit is slightly better with the main discrepancies at the beginning of the dissociation phase (150 – 170 seconds). The R_{max} value calculated by the model (54 RU) is very close to the experimental R_{max} (51 RU). However, as visualized by the plots in figure 4.4, this fit is unacceptable with a X^2 value of 1.23.

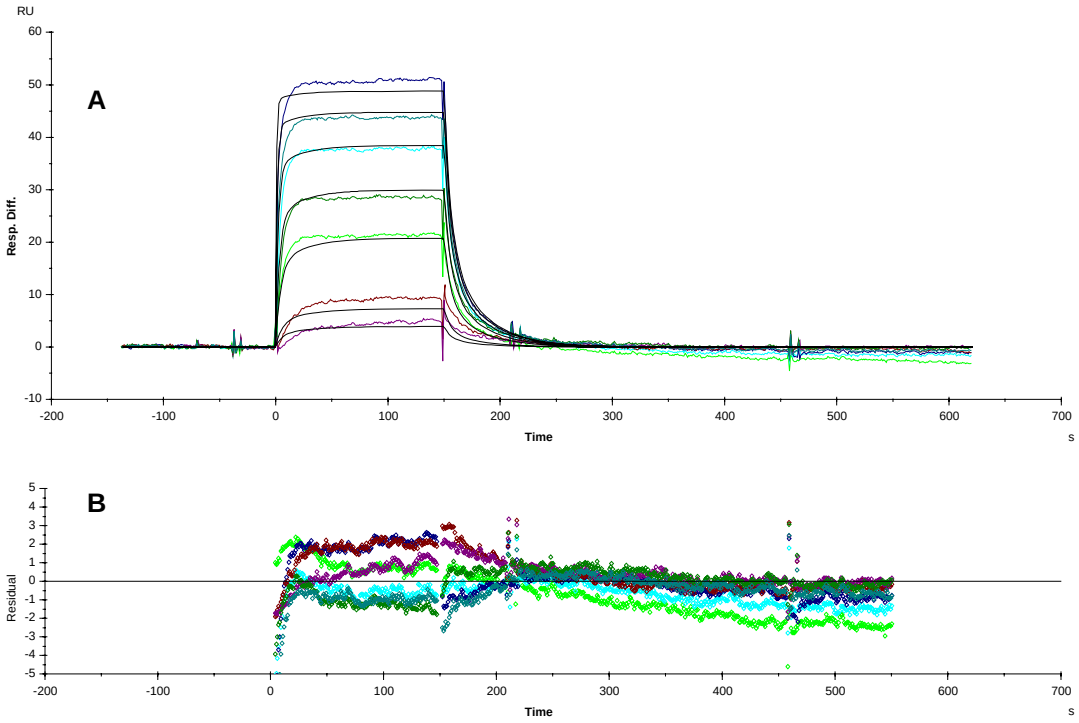

Figure 4.4: Kinetic fit using the two-state reaction (conformation change) kinetic model. A: kinetically generated traces and the experimental sensorgrams. B: residuals plot for the plots in figure 4.4A.

Table 4.1 shows the kinetic parameters determined by the heterogeneous ligand model fit to the data displayed above. These values signify a fast association rate (6.3 X 10^6 $M^{-1}s^{-1}$ and 1.2 X 10^7 $M^{-1}s^{-1}$), a fast dissociation rate (0.14 s^{-1} and 0.03 s^{-1}) and high affinity (K_D1 and 2: 0.23 nM and 2.6 nM, respectively).

k_{a1} ($M^{-1}s^{-1}$)	Stand. Error	k_{d1} (s^{-1})	Stand. Error	k_{a2} ($M^{-1}s^{-1}$)	Stand. Error	k_{d2} (s^{-1})	Stand. Error
6.3 E+6	1.1 E+5	0.14	3.8 E-3	1.2 E+7	3.2 E+5	3.0 E-2	8.0 E-4

$R_{max}1$ (RU)	Stand. Error	$R_{max}2$ (RU)	Stand. Error	K_{A1} (M^{-1})	K_{D1} (nM)	K_{A2} (M^{-1})	K_{D2} (nM)
42	0.55	15	0.62	4.4 E+7	0.23	3.9 E+8	2.6

Table 4.1: Kinetic data for heterogeneous ligand fit shown in figure 4.1. The standard error for each calculated value is displayed in the adjacent cell to the right.

The results from this kinetic trial are representative of results from additional kinetic trials with the SA sensor chip and trials using the CM3 sensor chip: the heterogeneous ligand kinetic model gave the best fit for the experimental data. Table 4.2 shows a summary of the average kinetic data from the heterogeneous ligand fits for the trials using aptamer immobilized to the SA chip and trials using aptamer immobilized to the CM3 chip. These average results indicate that the affinity of the thrombin aptamer is slightly higher when it is immobilized to the CM3 chip than the SA chip: K_D1 for the CM3 equals 12 ± 5.5 nM versus 24 ± 2.1 nM for the SA chip; K_D2 for the CM3 chip equals 0.64 ± 0.37 nM versus 1.7 ± 0.92 nM for the SA chip.

Chip	k_{a1} ($M^{-1}s^{-1}$)	Stand. Error	k_{d1} (s^{-1})	Stand. Error	k_{a2} ($M^{-1}s^{-1}$)	Stand. Error	k_{d2} (s^{-1})	Stand. Error
SA	6.0 E+6	4.5 E+5	0.15	3.5 E-3	1.7 E+7	7.3 E+6	3.0 E-2	7.1 E-4
CM3	1.9 E+7	7.6 E+6	0.20	0.011	4.1 E+7	2.4 E+7	2.2 E-2	2.1 E-4

Chip	K_{A1} (M^{-1})	Stand. Error	K_{D1} (nM)	Stand. Error	K_{A2} (M^{-1})	Stand. Error	K_{D2} (nM)	Stand. Error
SA	4.1 E+7	4.1 E+6	24	2.1	5.7 E+8	2.6 E+8	1.7	0.92
CM3	9.2 E+7	4.2 E+7	12	5.5	1.9 E+9	1.1 E+9	0.64	0.37

Table 4.2: Average kinetic values (with associated standard error) for aptamer immobilized to the SA sensor chip (N = 5) and the CM3 sensor chip (N = 3).

4.3.1.2 Rationale For Heterogeneous Ligand Fit

The result of the heterogeneous ligand-binding model as the best kinetic fit for the thrombin – DNA aptamer interaction was unexpected. This indicates that there is some heterogeneity in the DNA bound to the sensing flow cell surface. Capillary electrophoresis (CE) and matrix-assisted laser desorption ionization time-of-flight mass spectrometry (MALDI-TOF) analysis of the synthesized DNA by the vendor showed no truncated or mis-synthesized sequences. Therefore, any heterogeneity must be due to a difference in affinity between individual aptamer molecules within the immobilized population. An affinity

difference could be caused by improperly folded or partially folded aptamer, but this is unlikely because it has been shown that the thrombin aptamer readily forms only one structure in the presence of K^+ ions (a stacked, G-quartet) and this structure is very stable.[4-6]

One possibility for heterogeneity in the attached aptamer is if some of the immobilized aptamers are forming **inter**molecular G-quartets instead of **intra**molecular G-quartets. However, this would only explain heterogeneity in the association phase (the aptamer molecules would need to reform into intramolecular G-quadraplexes in order to bind thrombin) and not the dissociation phase- unless the G-quartets formed by intermolecular interactions can bind thrombin. It is unlikely that intermolecularly-formed G-quartets can bind thrombin because they would not form the same TT loops which are implicated in the specific binding of the aptamer to thrombin.[7]

A second possible cause for the heterogeneity in the immobilized aptamer is in the way that the stacked, G-quartet is formed. It has been shown that the two TT loops of the aptamer structure can either cross over the narrow grooves of the G-quadraplex (NMR structure) or cross over the wide grooves of the G-quadraplex (x-ray crystal structure).[7] Figure 4.5 shows the schematics of the two possible special arrangements for the anti-thrombin aptamer based on the NMR and x-ray crystal data. There is no indication that one structure is preferred over the other (thermodynamically, kinetically or in binding thrombin) so it is entirely possible that the sensor surface has some aptamers immobilized in one conformation and the other aptamers immobilized in the other conformation. Both of these immobilized aptamers should bind thrombin, but the difference in the spatial arrangement of the moieties involved in the specific binding of the aptamer to thrombin (the two TT loops) could be the cause of heterogeneity in the system.

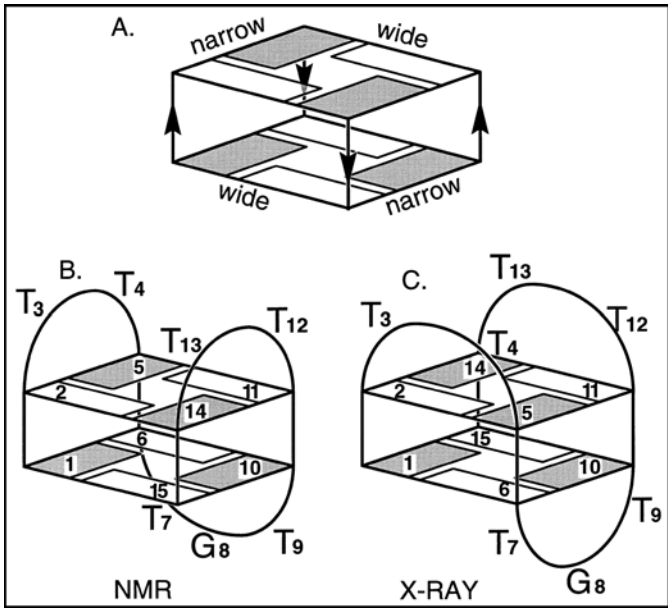

Figure 4.5: Cartoon depictions of the anti-thrombin DNA aptamer tertiary structure. A: Diagram of stacked, G-quartet structure showing narrow and wide grooves. Both the NMR and x-ray structures are in agreement at this level. B: The NMR-based structure- the two TT loops cross the narrow grooves of the G-quadraplex. C: The x-ray crystallography-based structure- the two TT loops cross the wide grooves of the G-quadraplex. Adapted from Kelly, *et. al.*[7]

A final possible cause for the heterogeneity in the ligand is the possibility that the immobilized aptamers were able to bind thrombin either through the two TT loops (T_3T_4 and $T_{12}T_{13}$ in figure 2) or through the TGT loop ($T_7G_8T_9$ in figure 2) at the other end of the stacked, G-quartet. Both Wang, *et. al.* and Macaya, *et. al.* reported binding interactions between the two TT loops of the aptamer with thrombin; [5] [4] while Padmanabhan *et. al.* reported binding interactions both between the TT loops of the aptamer and the TGT loop of the aptamer with thrombin. [6] Even though the aptamers were attached through the 5' end (G_1 in figure 2), the 12 carbon linker that was used for both the affinity and covalent attachment may have allowed for exposure of either thrombin-binding ends of the aptamer.

4.3.1.3 Control Experiments: Mass Transfer And Linked Reaction

As part of the kinetic analysis experiments, control experiments were implemented to analyze for mass transfer limitations during the kinetic experiment and linked reaction (conformational change, etc.) complications. Figures 4.6 and 4.7 show the results from a mass transfer limited experiment and a linked reaction experiment, respectively. The sensorgram's slope during the association step for the three flow rates appears identical (figure 4.6- 0 to 125 seconds). This implies that the rate of the analyte binding to the ligand is constant at these three flow rates; therefore, the binding reaction is not mass transport-limited for this system. The results displayed in figure 4.7 indicate that the reaction involves no linked reactions. This is illustrated by the same dissociation rate for the three different lengths of injection (0 to 800 seconds). The results of these experiments show that the kinetic evaluation experiments are not complicated by any mass transfer or linked reaction phenomena.

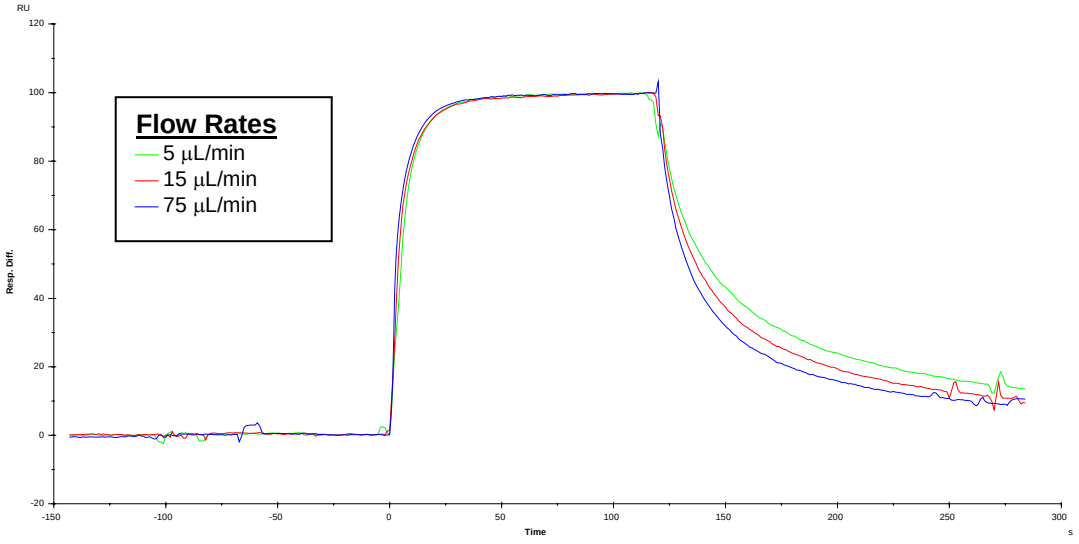

Figure 4.6: Plot overlay for the mass transfer limited experiment.

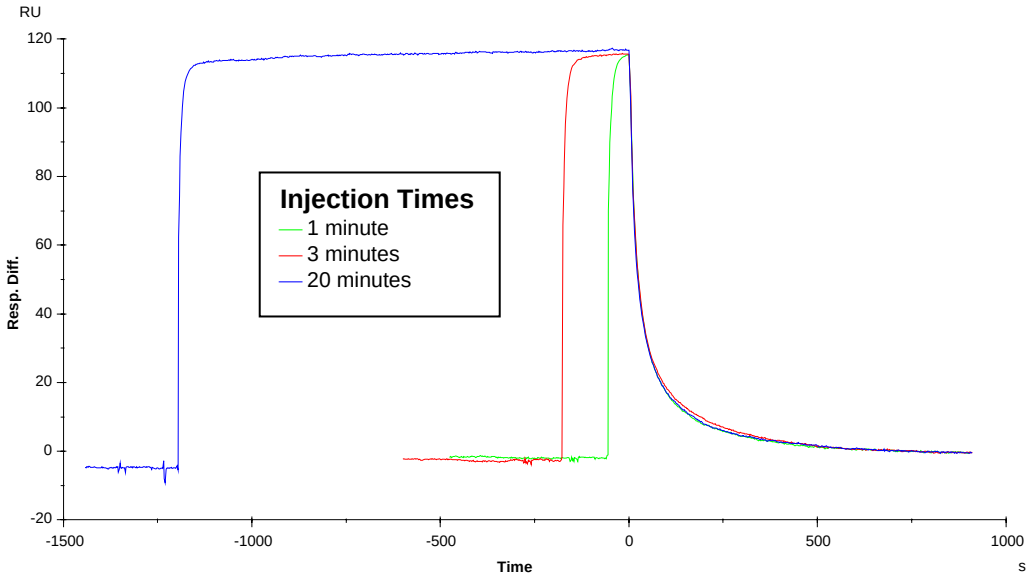

Figure 4.7: Plot overlay for the linked reaction experiment.

4.3.1.4 Association Rate Limitation

Determination of the limitation on the association rate for a heterogeneous binding interaction can help in assessing if there would be an advantage to employing a microfluidic-based assay system for the analyte-ligand pair. A diffusion-limited association phase for an analyte-ligand system will benefit from the inherently small diffusion distances realized with microfluidic devices.[8] An analysis to determine the limitation on the association rate (diffusion or analyte-ligand interaction limited) was performed for the thrombin-aptamer system.

A comparison between the actual surface concentration of thrombin ($\Gamma_{A\ actual}$) and the calculated surface concentration of thrombin ($\Gamma_{A\ calc}$) gives an indication as to the limitation on the association rate. For a diffusion-limited reaction, $\Gamma_{A\ calc}$ will be less than $\Gamma_{A\ actual}$.[9] The actual surface concentration of thrombin was determined from the plateau in the experimental reference-subtracted sensorgram signal during the thrombin injection. The calculated surface concentration of thrombin was determined according to the formula

$\Gamma_{A\ calc} = \frac{2}{\sqrt{\Pi}} C_0 \sqrt{Dt}$; where C_0 is the bulk concentration of thrombin in the flow cell, D is the diffusion coefficient for thrombin, and t is the time period between the start of the injection of the thrombin solution and the point at which the actual surface concentration was measured (the beginning of the signal plateau). The diffusion coefficient used for thrombin was that determined for bovine thrombin: 8.76 X 10^{-7} cm^2/s.[10] Bovine thrombin has a molecular weight (33.7 kD) similar to the human analog (37 kD).

Figure 4.8 shows the ratio of $\Gamma_{A\ actual}$ to $\Gamma_{A\ calc}$ plotted against the base-10 logarithm of the thrombin concentration for three flow cells that had different amounts of aptamer attached via affinity immobilization (SA chip). A ratio of $\Gamma_{A\ actual}$ to $\Gamma_{A\ calc}$ greater than one is indicative of a diffusion-limited association reaction. The two flow cells with the higher amounts of aptamer immobilized (91 and 69 RU max.) show $\Gamma_{A\ actual}$ to $\Gamma_{A\ calc}$ ratios greater than one at the lower concentrations of thrombin- indicating diffusion-limited association at these lower thrombin concentrations. When the thrombin concentration gets high enough the ratio falls below one- indicating a reaction-limited association process. This break point occurs at lower thrombin concentrations for the 69 RU max. flow cell than for the 91 RU max. flow cell. The flow cell with the lowest amount of aptamer immobilized (11 RU max.) shows reaction-limited association at all of the thrombin concentrations sampled.

Even though there appears to be contradictory evidence, this plot shows that the association reaction rate is diffusion-limited. The change that occurs from apparent diffusion-limited association to reaction-limited association is easily explained by the fact that at higher thrombin concentrations the reaction becomes limited by the number of aptamer receptor sites.[9] The flow cell with the lowest amount of aptamer immobilized (11 RU max.) never shows diffusion-limited characteristics because the association reaction is always limited by the number of aptamer receptor sites for the thrombin concentrations sampled.

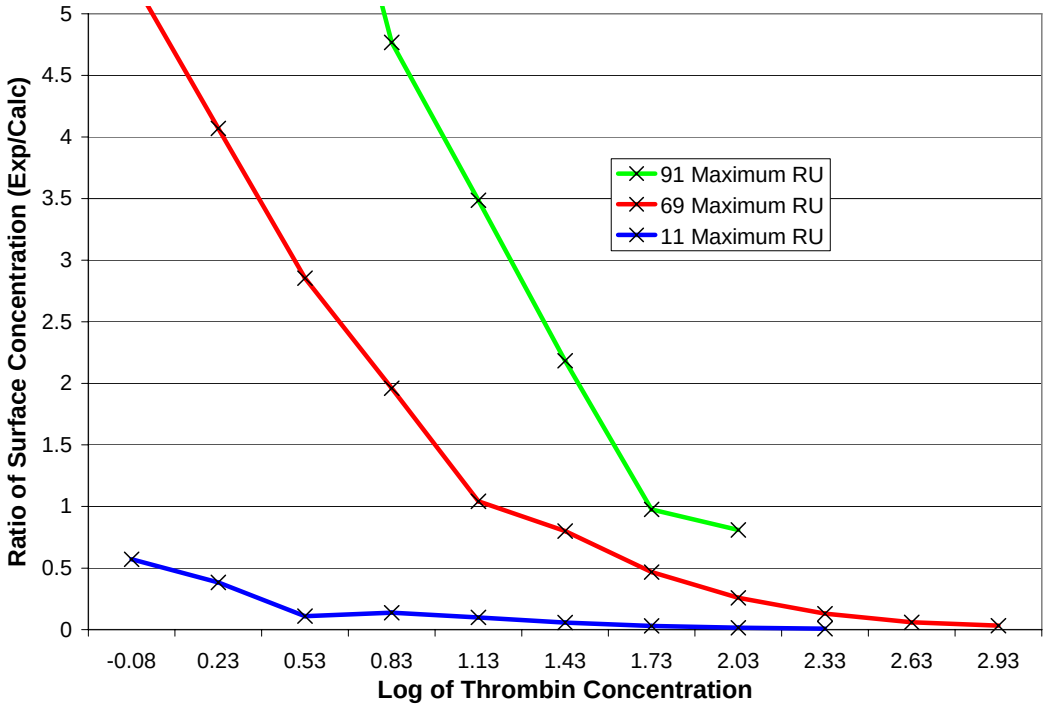

Figure 4.8: Plot of the ratio $\Gamma_{A\ actual}$: $\Gamma_{A\ calc}$ versus the $\log_{10}$ of the thrombin concentration for three flow cells with different amounts of aptamer immobilized.

4.3.2 Kinetic Comparisons

4.3.2.1 Covalent Versus Affinity Attachment

One of the goals of these experiments was to determine if the binding kinetics of the anti-thrombin aptamer changed with the immobilization strategy: covalent versus affinity attachment. One study of an attached aptamer (the anti-IgE DNA aptamer) found that the covalent attachment of the aptamer via a 3' or 5' amine resulted in faster dissociation of the aptamer-IgE complex than the affinity attachment via a 3' or 5' biotin (0.0034 s^{-1} versus 0.0005 s^{-1}, respectively).[2] There have been no other reports concerning investigations into any difference in kinetic values for aptamers immobilized via one strategy versus another. The present study produced results that indicate that there is very little difference between a covalently attached and an affinity-attached aptamer (see table 4.2). The biggest difference

is between the k_a1 values: 6.0 E+6 $M^{-1}s^{-1}$ for the affinity immobilized aptamer (SA chip) and 1.9 E+7 $M^{-1}s^{-1}$ for the covalently immobilized aptamer (CM3 chip). This difference is significantly smaller than the difference reported for the anti-IgE DNA aptamer. These results indicate that there is no significant difference in the binding kinetics of the anti-thrombin DNA aptamer due to the immobilization technique.

4.3.2.2 Heterogeneous Versus Homogeneous Systems

Another goal of these experiments was to determine if the binding kinetics varied between homogeneous aptamer assays (solution-based assays) and heterogeneous aptamer assays (immobilized aptamer assays). In work with the anti-thrombin DNA aptamer, Potyrailo and coworkers found a significant difference between the K_D value of the immobilized aptamer (47 nM) and the solution-phase aptamer (1.1 μM).[1] Determination of the K_D value for the solution-based aptamer was beyond the scope of this study; however, the values obtained from this study for the K_D of the immobilized aptamer (0.64 to 24 nM) match fairly well to the value obtained for a study that immobilized thrombin to a bottom of a microtitre plate and introduced the solution phase aptamer (1.4 to 6.2 nM).[11] Other studies of the anti-thrombin aptamer have determined the K_D to be 2.7 nM via a competitive equilibrium binding study,[12] 25 nM by clotting time analysis[13] and 100 nM via a filter binding assay.[14] Kinetic studies of other immobilized aptamers have shown that the K_D value is unaffected by immobilization;[2, 15-17] in fact, a slight improvement in the affinity was often realized for the attached aptamer. This may be because the solution-based affinity assays are compromised by the fast dissociation rates of the aptamer-analyte complex compared to the separation process.[18]

4.4 Conclusions

4.4.1 Binding With Heterogeneous Ligand

The best kinetic fit to the experimental data for thrombin's association with surface-immobilized anti-thrombin DNA aptamer was a heterogeneous ligand model. Several kinetic models were compared for the best fit, including a heterogeneous ligand, a Langmuir 1:1, a bivalent analyte, and a two-state reaction model. Both the Langmuir 1:1 and the two-state models produced results that gave excellent R_{max} values compared to the experimental values; however, the visual inspection of the plot overlays and residuals, and the calculated X^2 values indicated some deviations from a good fit. The bivalent analyte model results mirrored the experimental results closely except that the R_{max} value based on the model was significantly higher than the experimental value. The heterogeneous ligand model produced the best fit to the experimental data: both in its ability to mirror the sensorgram traces and to calculate the correct R_{max} value.

There are two plausible explanations for the heterogeneity in the immobilized aptamer: 1) that the DNA can fold in two different manners but still present the same basic tertiary conformation for specific binding to thrombin and 2) there are two different sites on the aptamer available for thrombin binding. The NMR-determined aptamer structure places the two TT loops crossing over the narrow grooves of the stacked, G-quartet; while the x-ray crystallography-based structure shows the two TT loops crossing over the wide grooves. This small difference in the folding between individual anti-thrombin aptamer molecules may provide enough of a difference in the kinetic rates of association and dissociation to cause the surface to 'appear' heterogeneous to kinetic models. In addition, the x-ray crystallography-based structure shows binding of two different thrombin molecules to either end of an aptamer molecule: one through the TT loops and the other through the TGT loop. Even though the aptamer was attached to the substrate via the same end of the molecule as the location of the TGT loop, the linker length (12 carbons) may have allowed for

thrombin access to this end. These two binding sites may have contributed to the heterogeneity seen in the kinetic analysis.

Even though there appears to be some heterogeneity in the immobilized aptamer population, the kinetics of its binding to thrombin occurs at fast rates and with high affinity. The kinetics of the association are not attachment methodology dependent (covalent versus affinity) and the association phase appears to be limited by diffusion of the thrombin molecules to the sensor surface. The association rate (k_a) is on the order of 10^7 $M^{-1}s^{-1}$, the dissociation rate (k_d) is on the order of 10^{-1} to 10^{-2} s^{-1}, and the binding consant (K_D) is in the nM range for both of the attachment strategies. The response time for changes in thrombin concentration should be shortened by utilizing microfluidic devices in conjunction with the anti-thrombin aptamer because the association phase is diffusion limited.

4.4.2 Aptamers Versus Antibodies

The affinity of aptamers rivals that of antibodies- making them a viable complement to antibodies as diagnostic agents. Aptamers may be able to fill a niche that it has been difficult for antibodies to fill: detection of small, toxic and endogenous molecules. However, the optimal assay format and appropriate application may be different between aptamers and antibodies because of the differences in the two recognition elements kinetic rates.

An anti-p24 monoclonal antibody (mAb) was determined to have a dissociation constant (K_D) of 29 nM with a relatively slow on-rate (k_a) of 2.5 X 10^5 $M^{-1}s^{-1}$ and a slow off-rate (k_d) of 8.3 X 10^{-3} s^{-1}.[19] These slow on- and off-rates for antibodies make them amenable to assay formats that utilize an incubate, wash and read process (e.g.- ELISA) because there is usually enough time allotted for full binding between the analyte and the antibody and the dissociation is slow enough that a washing step will not remove a significant amount of the bound analyte. On the other hand, the slow kinetics make antibody use in continuous-monitoring, real-time biosensors impractical- the slow on- and off-rates of antibodies will result in sluggish responses.

In contrast to antibodies, aptamers appear to have fast association and dissociation kinetics (and high affinities) that will make them well-suited to biosensors that can give a rapid and continuous analysis. The results for the binding of thrombin to the aptamer-immobilized beads (unable to detect thrombin specifically bound to the aptamer-modified beads) are easily explained by the fast on- and off-rates: the thrombin may have been binding to the aptamer-coated beads, but the wash cycle of the analysis removed most of the bound thrombin molecules because of their fast dissociation rate. Even though this characteristic may be disadvantageous for one assay format (ELAA: an ELISA-style aptamer-based assay format), it gives aptamers an advantage over antibodies in their suitability for use in real-time, continuous-monitoring biosensors.

4.5 References

1 Potyrailo, R. A.; Conrad, R. C.; Ellington, A. D.; Hieftje, G. M. *Anal. Chem.* **1998,** *70*, 3419-3425.
2 Liss, M.; Petersen, B.; Wolf, H.; Prohaska, E. *Anal. Chem.* **2002,** *74*, 4488-4495.
3 Kleinjung, F.; Klussmann, S.; Erdmann, V. A.; Scheller, F. W.; Furste, J. P.; Bier, F. F. *Anal. Chem.* **1998,** *70*, 328-331.
4 Macaya, R. F.; Schultze, P.; Smith, F. W.; Roe, J. A.; Feigon, J. *Proc Nat Acad Sci USA* **1993,** *90*, 3745-3749.
5 Wang, K. Y.; McCurdy, S.; Shea, R. G.; Swaminathan, S.; Bolton, P. H. *Biochemistry USA* **1993,** *32*, 1899-1904.
6 Padmanabhan, K.; Padmanabhan, K. P.; Ferrara, J. D.; Sadler, J. E.; Tulinsky, A. *J. Biol. Chem.* **1993,** *268*, 17651-4.
7 Kelly, J. A.; Feigon, J.; Yeates, T. O. *J. Mol. Biol.* **1996,** *256*, 417-22.
8 Rossier, J. S.; Gokulrangan, G.; Girault, H. H.; Svojanovsky, S.; Wilson, G. S. *Langmuir* **2000,** *16*, 8489-8494.
9 Stenberg, M.; Nygren, H. *J. Immunol. Meth.* **1988,** *113*, 3-15.
10 Harmison, C. R.; Landaburu, R. H.; Seegers, W. H. *J. Biol. Chem.* **1961,** *236*, 1693-6.
11 Tsiang, M.; Gibbs, C. S.; Griffin, L. C.; Dunn, K. E.; Leung, L. L. *J Biol Chem* **1995,** *270*, 19370-6.
12 Wu, Q.; Tsiang, M.; Sadler, J. E. *J. Biol. Chem.* **1992,** *267*, 24408-12.
13 Bock, L. C.; Griffin, L. C.; Latham, J. A.; Vermaas, E. H.; Toole, J. J. *Nature* **1992,** *355*, 564-566.
14 Macaya, R. F.; Waldron, J. A.; Beutel, B. A.; Gao, H.; Joesten, M. E.; Yang, M.; Patel, R.; Bertelsen, A. H.; Cook, A. F. *Biochemistry-USA* **1995,** *34*, 4478-92.
15 Deng, Q.; German, I.; Buchanan, D.; Kennedy, R. T. *Anal. Chem.* **2001,** *73*, 5415-5421.
16 McCauley, T. G.; Hamaguchi, N.; Stanton, M. *Anal. Biochem.* **2003,** *319*, 244-250.
17 Clark, S. L.; Remcho, V. T. *Anal. Chem.* **2003,** *75*, 5692-5696.
18 Neri, D.; Montigiani, S.; Kirkham, P. *Trends Biotechnol.* **1996,** *14*, 465-70.
19 Karlsson, R. *Anal. Biochem.* **1994,** *221*, 142-51.

Chapter 5: Conclusions

5.1 Aptamer Immobilization

The tertiary structure of aptamers distinguishes them from other ssRNA and ssDNA. This is evidenced in the difference in the attachment levels between the scrambled sequence and the aptamer sequence for the CM3 chip. Not all aptamers appear to require cations for structure stabilization and/or binding, but those that do warrant special precautions when attempting covalent attachment- especially if the reactive moiety is an amine appended to the aptamer. This may have been a contributing factor for the low sensitivity of the covalently linked anti-IgE aptamer described by Liss, *et. al.*[1]

Besides the above mentioned concern, aptamers appear to be relatively easy to immobilize. They are amenable to many different attachment strategies as long as any reactive moieties are spaced a little bit away from the substrate and aptamer structure. Affinity attachment (use of the strong biotin/streptavidin interaction) is also a viable option; however, it may not be applicable to attachment of the biotin-binding ssRNA aptamer.[2]

Additional experiments could be performed to support the theory that attachment levels may be limited by interaction between the aptamer structure and an appended moiety. For the thrombin aptamer, addition of K^+ to the immobilization buffer and NMR studies are appropriate. Studies with other aptamer structures (those known to require cations for structure stabilization and those that do not require cations) using various attachment techniques would contribute to our knowledge base.

5.2 Activity And Optimal Packing Density

The anti-thrombin DNA aptamer displayed no difference in its ability to selectively bind thrombin due to the attachment strategy. In addition, the immobilized aptamer was stable to repeated analysis, showed excellent precision and retained activity upon storage. Due to

aptamers' chemical stability (especially ssDNA) and ability to reform its active tertiary structure, it is expected that all ssDNA aptamers should have the same characteristics as the thrombin aptamer when immobilized.

The optimal packing density for the anti-thrombin DNA aptamer was determined to be between 4.5 and 6 pmol/cm^2 – a value slightly below the optimal packing density for ssDNA used in hybridization assays.[3] It is expected that the optimal packing density for aptamers will not be dependant upon the aptamer (since they all have a relatively small footprint-even with their tertiary structure), but will be determined by the size its cognate ligand. A very small ligand will not require additional space because they normally fit into the aptamer's structure;[4] whereas larger ligands (like IgE and polysaccharides) will require a lower packing density because they need to fit around the aptamer's tertiary structure.[5]

The requirements of a reference flow cell for use in SPR-based analysis were also investigated. It was determined that a low level of immobilized non-sense DNA (scrambled sequence) or no DNA immobilized worked well for a reference. The affinity-immobilized aptamer system showed no sensitivity to the level of non-sense DNA immobilized to the reference, but the covalently-attached aptamer system had a significantly increased level of non-specific binding of thrombin to the reference cell at high concentrations of thrombin. This was potentially due to the use of a blocking molecule (ethanolamine) which may have forced the non-sense DNA strands to extend out into the solution, increasing their availability for non-specific interactions with the thrombin molecules. It is likely that similar results would occur for other aptamers (especially those with positively charged ligands).

5.3 Immobilized Aptamer Kinetics

Kinetic analysis of the immobilized anti-thrombin DNA aptamer indicated that there was heterogeneity in the immobilized aptamers. This heterogeneity is likely due either to a difference in the folding of the aptamer or binding of thrombin to both ends of the aptamer.

The rate of association and the rate of dissociation for the immobilized aptamer are very fast, which indicates that this aptamer — analyte pair is best suited to a continuous, real-time monitoring system. This characteristic may be unique to the anti-thrombin aptamer; the anti-IgE DNA aptamer has much slower kinetics (k_d = 10^{-3} – 5 X 10^{-4} s^{-1})[1] and is therefore better suited to an incubate, wash and read format. Each aptamer will need to be evaluated to determine the assay format that best suits its binding kinetics.

The association reaction rate for the anti-thrombin DNA aptamer binding to thrombin is diffusion-limited. This means that miniaturization will decrease the analysis time because the rate of delivery of the analyte to the surface will be increased. The advantage of rapid analysis time that is effected by microfluidic devices may be extended to aptamer-based assays- dependant upon the individual aptamer – analyte kinetics.

5.4 Influence Of SELEX

The selection process used for the isolation of aptamers determines the binding characteristics of the aptamer. Binders with medium to strong affinity are isolated because the weak binders are washed away during the selection process and the very strong binders are not regenerated and amplified because they are not dissociated from the target. In addition, the selection routine may determine the kinetics of the aptamer – ligand interaction: the more extensive the wash regimen during the selection process, the more likely the isolated aptamer(s) will have slow dissociation kinetics. Modification of the SELEX protocol may be a viable technique for manipulating the aptamer's binding kinetics to fit the desired assay format.

5.5 References

1 Liss, M.; Petersen, B.; Wolf, H.; Prohaska, E. *Anal Chem* 2002, 74, 4488-4495.
2 Nix, J.; Sussman, D.; Wilson, C. *J Mol Biol* 2000, 296, 1235-1244.
3 Steel, A. B.; Herne, T. M.; Tarlov, M. J. *Anal Chem* 1998, 70, 4670-4677.
4 Feigon, J.; Dieckmann, T.; Smith, F. W. *Chem Biol* 1996, 3, 611-617.
5 Hermann, T.; Patel, D. J. *Science (Washington, D. C.)* 2000, 287, 820-827.